



BioFSI Lab



# Squid-Inspired Nozzles for Enhanced Thrust in Rotary Propulsors

Daehyun Choi<sup>1</sup>, Joao Pedro D. Fonseca<sup>1</sup>, Halley J. Wallace<sup>1</sup>,  
**Paras Singh<sup>2</sup>**, William F. Gilly<sup>3</sup>, and Saad M. Bhamla<sup>1</sup>

<sup>1</sup>School of Chemical and Biomolecular Engineering, Georgia Institute of Technology

<sup>2</sup>School of Aerospace Engineering, Georgia Institute of Technology

<sup>3</sup>Hopkins Marine Station, Stanford University

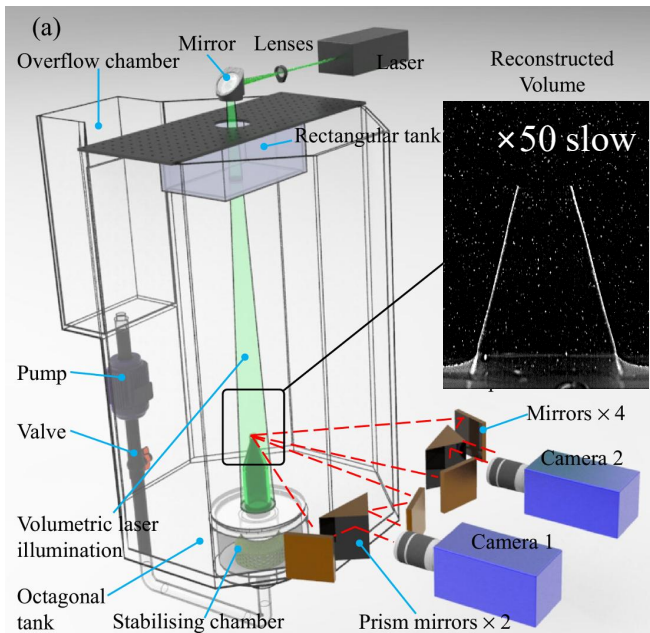
<sup>4</sup>Aerospace Engineering, University of Birmingham

DARPA YFA Monthly Meeting  
16 June 2025



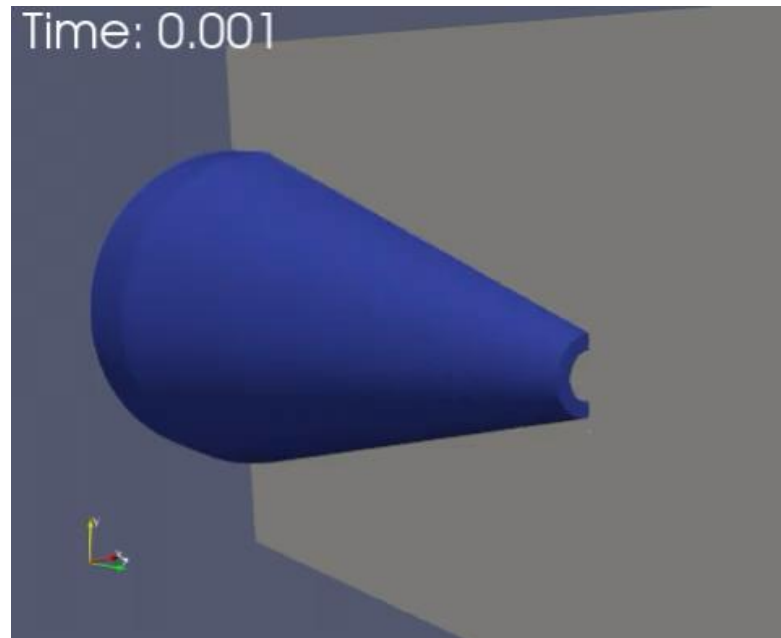
# Project overview

**Task 1.** Develop and validate soft nozzle shape for  $\eta_{p,\max} = 0.8$  and  $C_{T,\max} = 0.7$  across  $Re = 10^3-10^8$



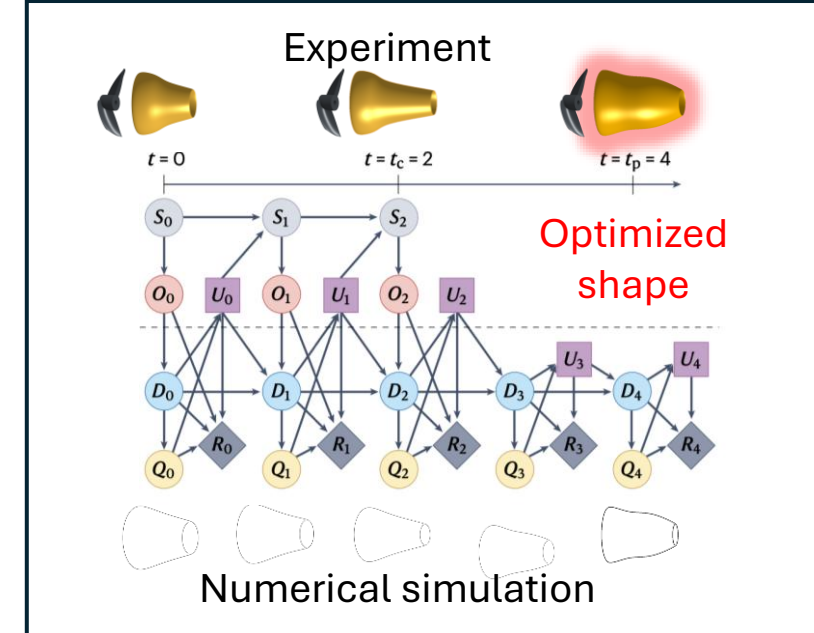
**Experiment**

**Task 2.** FSI modeling for dense nozzle performance predictions across diverse parameters



**Computation**

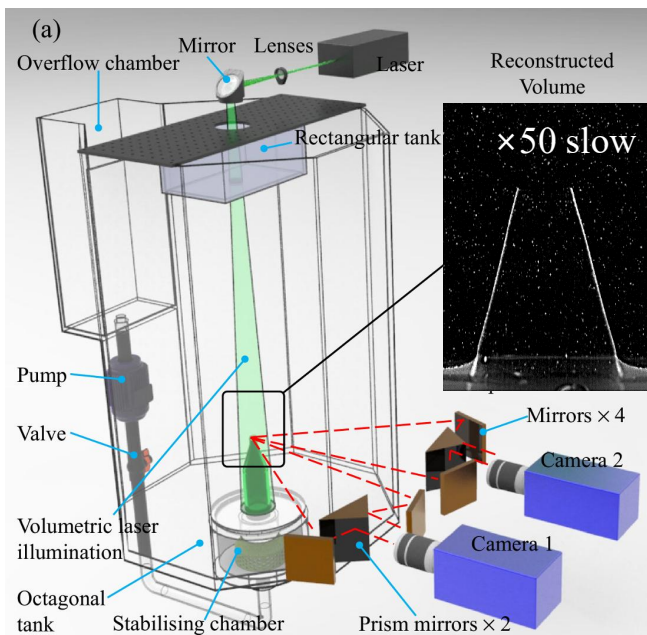
**Task 3.** Optimize soft nozzle design for enhanced propulsion using a PINN across  $Re = 10^3-10^8$



**Data-driven modeling**

# Project overview

**Task 1.** Develop and validate soft nozzle shape for  $\eta_{p,max} = 0.8$  and  $C_{T,max} = 0.7$  across  $Re = 10^3-10^8$

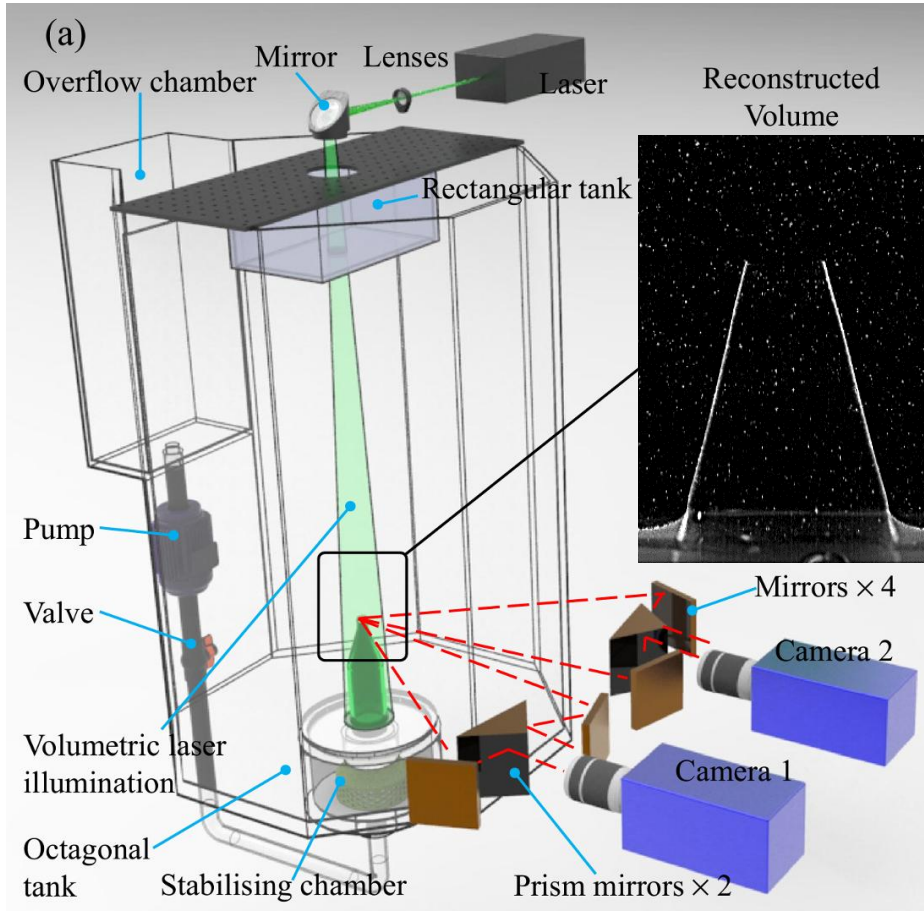


**Experiment**

## Key goals:

- To understand the Fluid structure interaction using controlled set and 3D measurement on both solid/fluid
- to provide reliable data for validation of CFD
- the validation of flow stabilizer, simultaneous measurement of solid/flow, parameter test with various nozzle shapes

# Initial PTV Setup

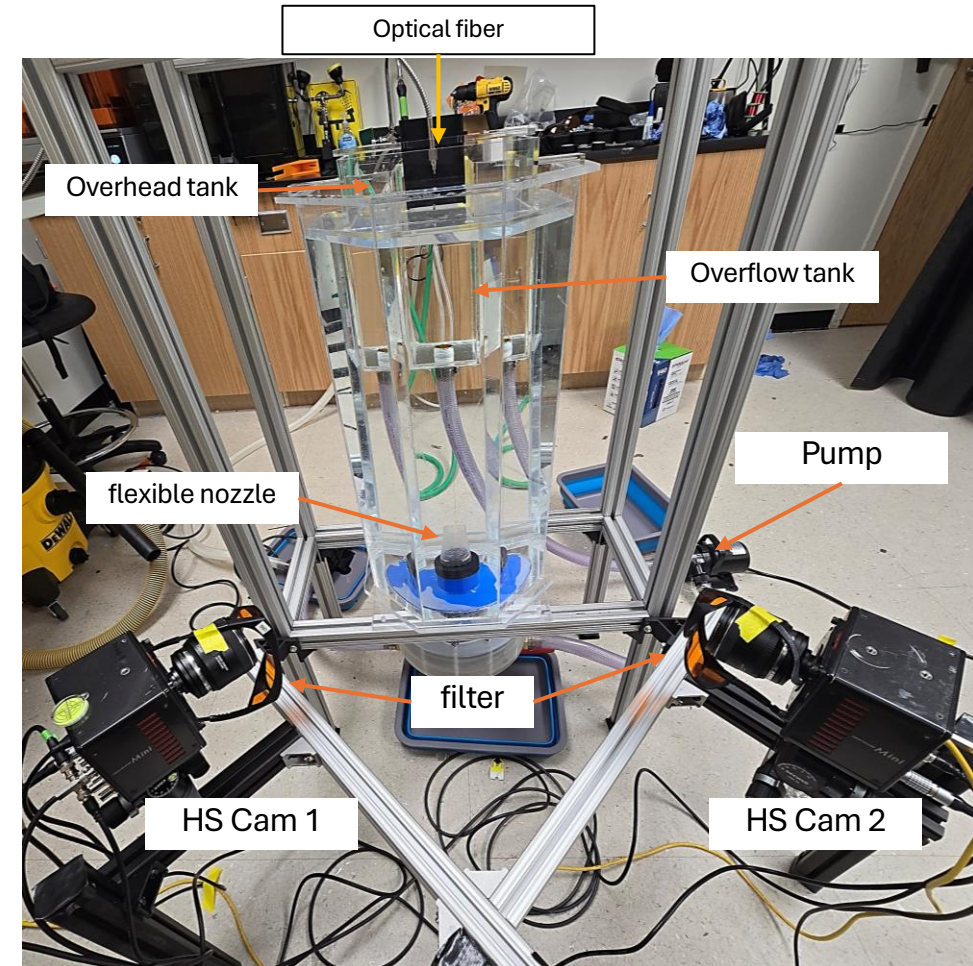


3D-DIC & 2D-PIV measurement plan

Zeng et al. 2023 EIF

## Key tasks :

1. Measure the deformation of the nozzle
2. Map the trajectories of seed particles to track fluid flow



Initial PTV and nozzle deformation measurement setup

# Calibration models

## 1. Tsai Model

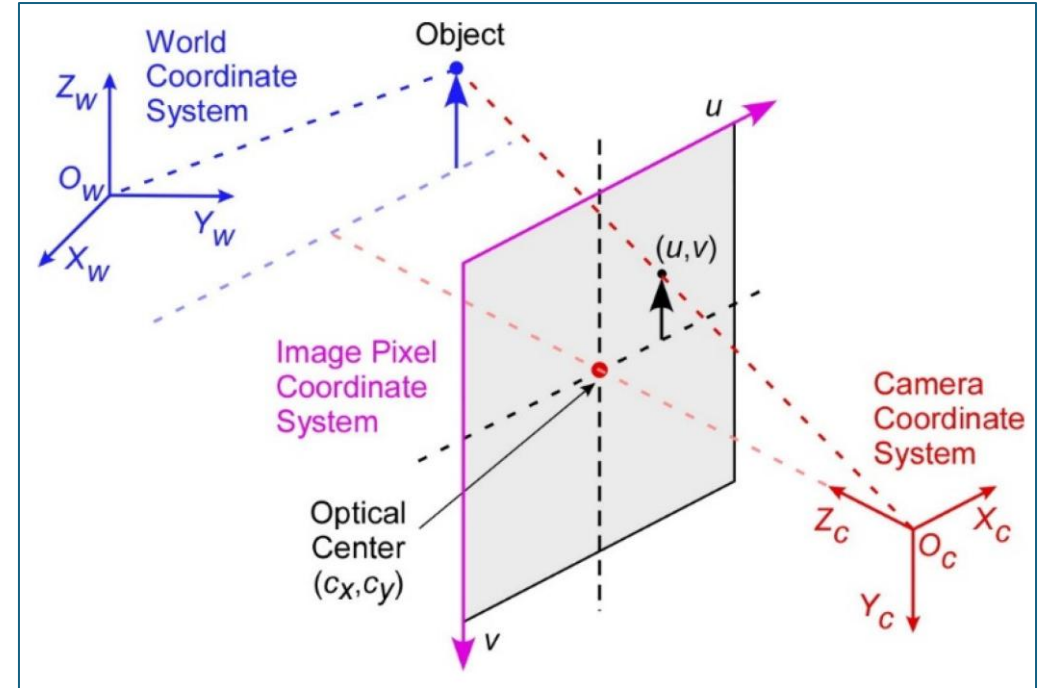
$$\vec{r} - \vec{O} = \left( \begin{bmatrix} \eta + x_h \\ \zeta + y_h \\ f \end{bmatrix} + \vec{e}(\eta, \zeta) \right) \cdot [R]$$

$$\vec{e}(\eta, \zeta) = [E] \cdot P(\eta, \zeta) = \begin{bmatrix} E_{11} & E_{12} & E_{13} & E_{14} & E_{15} \\ E_{21} & E_{22} & E_{23} & E_{24} & E_{25} \\ 0 & 0 & 0 & 0 & 0 \end{bmatrix} \cdot \begin{bmatrix} \eta \\ \zeta \\ \eta^2 \\ \zeta^2 \\ \eta \zeta \end{bmatrix}$$

Symbol	Description
$\vec{r}$	Particle position in the lab space coordinates
$\vec{O}$	Position of a camera's imaging center
$\eta, \zeta$	image space coordinates (pixels) of a particle
$x_h, y_h$	Correction to the camera's imaging center (in pixels)
$f$	The camera's principle distance divided by the pixel size
$\vec{e}(\eta, \zeta)$	A nonlinear correction term to compensate for image distortion and multimedia problems.
$[R]$	The rotation matrix which corresponds to the camera orientation vector.

## Key takeaways :

1. Calibration is difficult due to requirement of initial guess for pinhole model



2D image, 3D camera, and 3D world coordinate systems used in the camera calibration.

- The basic model uses the physical pin-hole camera model concepts to project 3D points onto an imaging plane
- employs a non-convex optimization, making it **difficult to converge to the optimal solution**.
- requires **an initial guess, a major difficulty in calibration process**
- performs better in extrapolations beyond the calibration region

# Calibration models

## 2. Extended Zolof Model

$$\begin{bmatrix} \eta \\ \zeta \end{bmatrix} = \begin{bmatrix} P_\eta(\vec{r}) \\ P_\zeta(\vec{r}) \end{bmatrix}$$

$$\begin{bmatrix} P_\eta(\vec{r}) \\ P_\zeta(\vec{r}) \end{bmatrix} = S A^\top$$

$P_\eta$  and  $P_\zeta$  are polynomial functions of the  $\vec{r} = (x, y, z)$  coordinates

$$A = \begin{bmatrix} a_0^\eta, a_0^\eta, \dots, a_{18}^\eta \\ a_0^\zeta, a_1^\zeta, \dots, a_{18}^\zeta \end{bmatrix}$$

$A$  is the polynomial coefficients matrix

$$S(x, y, z) = [1, x, y, z, x^2, y^2, z^2, xy, yz, xz, x^3, y^3, xyz, x^2y, x^2z, xy^2, y^2z, xz^2, yz^2]$$

$S$  is the 19 polynomial components

### Key takeaways :

1. easier to calibrate than the Tsai model
2. does not require an initial guess

- For the transformation from image-space to lab-space a we use a **pinhole model** in which the direction vector is obtained for each 2D image point via a polynomial of degree 3.
- We assume that each 2D camera position  $(\eta, \zeta)$  is associated with a (straight) **line of sight** and that **all the lines of sight cross at some points in the 3D physical world at the camera position  $O_i$**

- the transformation can be formalized as a linear least squares problem s.t. its globally optimal parameters can be found exactly.
- **Disadvantage of the extended Zolof model** is that it **does not comply with a physical principle**.
- **extrapolation** of the model to regions **beyond the region of the calibration**, or careless use of high-degree polynomials could **lead to errors**.

# Calibration models

## 3. MLOS (Multiplicative Line-of-Sight) approach (Future implementation)

### Key challenge in tomographic reconstruction:

- standard algorithms assume a **uniform mapping function** (the rule for how a 3D voxel projects to 2D camera pixels) across the entire volume and for all cameras.
- Factors like lens distortions or depth-of-field effects mean that the same particle can appear differently shaped on different cameras or in different locations.
- Uniform mapping function struggles with this, leading to inaccuracies like deformed particles, incorrect intensities, and ghost particles.

### Approach

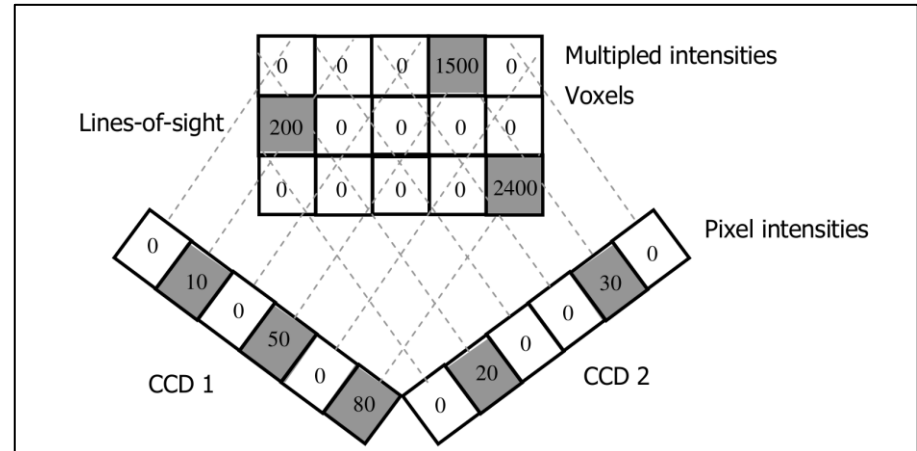
- Assigns an initial intensity to each voxel in the 3D space. This is done by multiplying the intensities of all camera pixels that view that particular voxel.

$$P_i = \int_{-\infty}^{\infty} I(x, y, z) ds_i$$

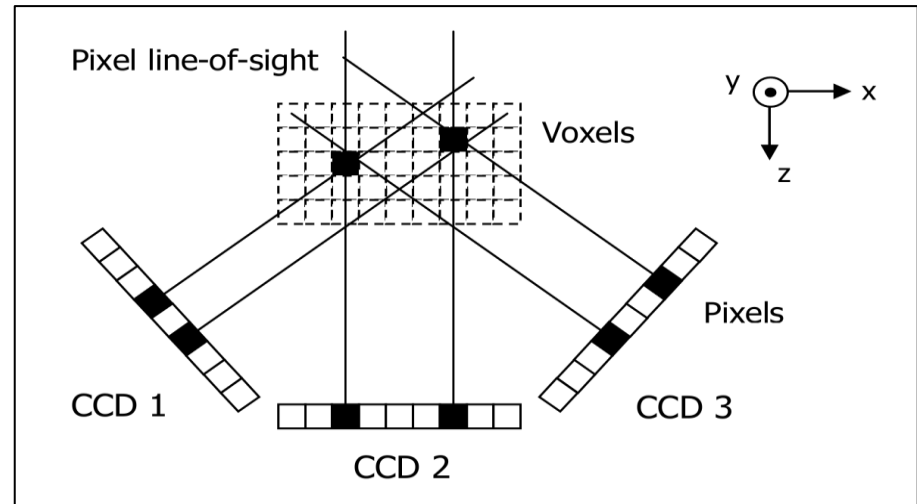
$$P_i = \sum_j W_{ij} I_j$$

$P_i$ : Recorded intensity of pixel i on a camera.

- $I(x, y, z)$  represents the intensity source function of the illuminated particle field
- Weighting factor representing the influence of pixel i on voxel j (or vice-versa)

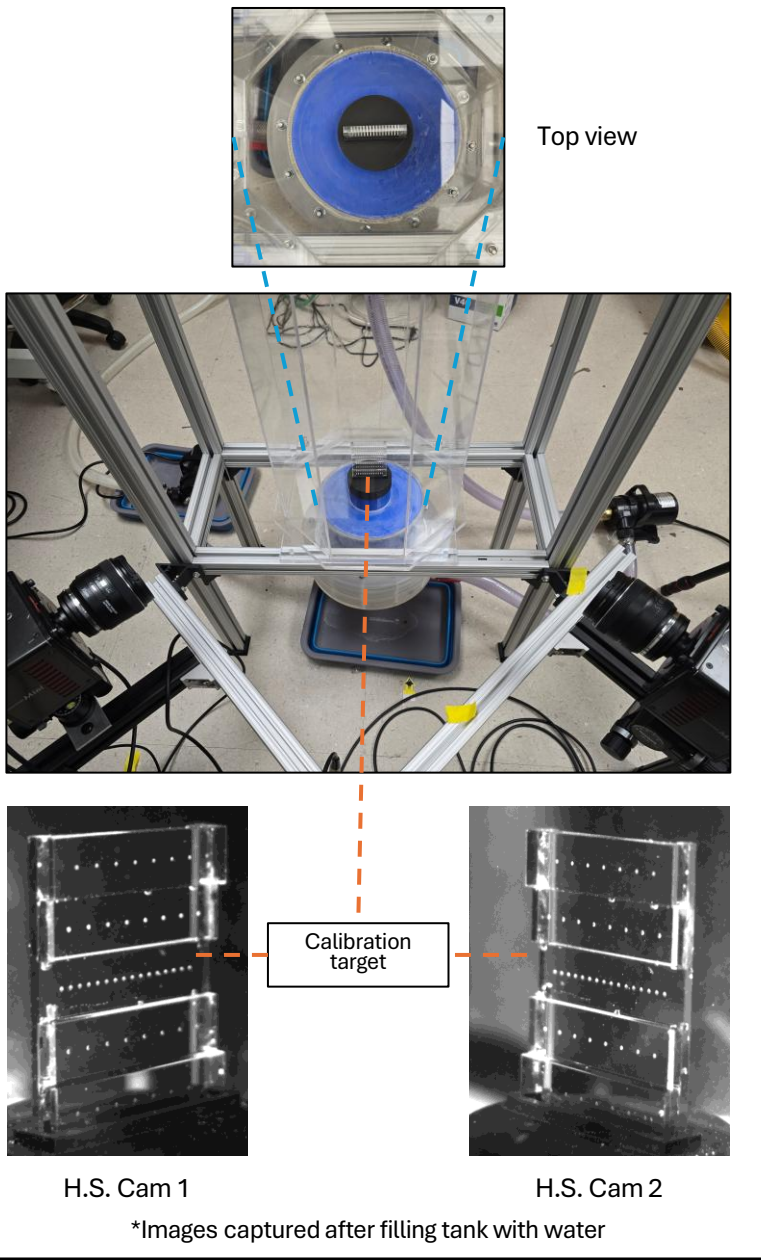


Schematic of the multiplied line-of-sight (MLOS) approach to determining non-zero voxels

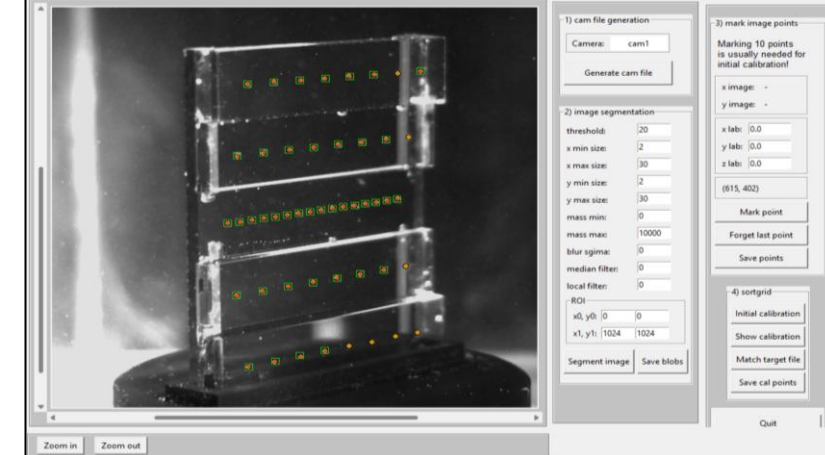


Multi-camera algebraic reconstruction technique. Filled voxels represent particle locations required to satisfy the filled pixels in each CCD or camera projection

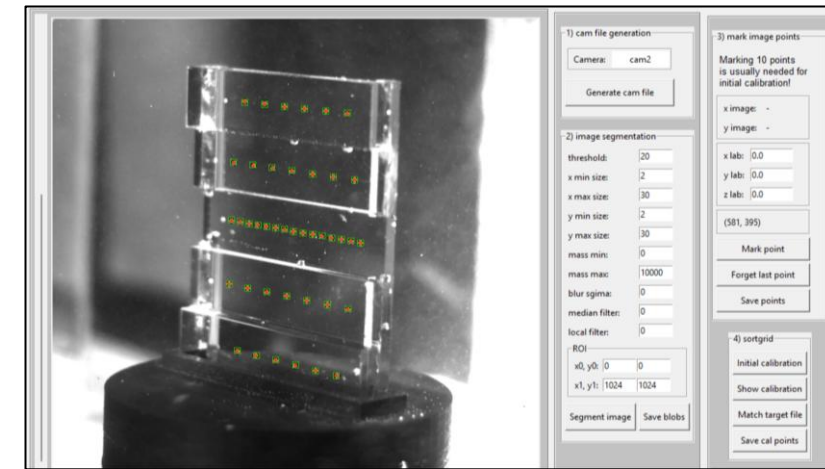
# Multi Step Calibration Target setup



Automated calibration point/blob detection  
and manual calibration setup

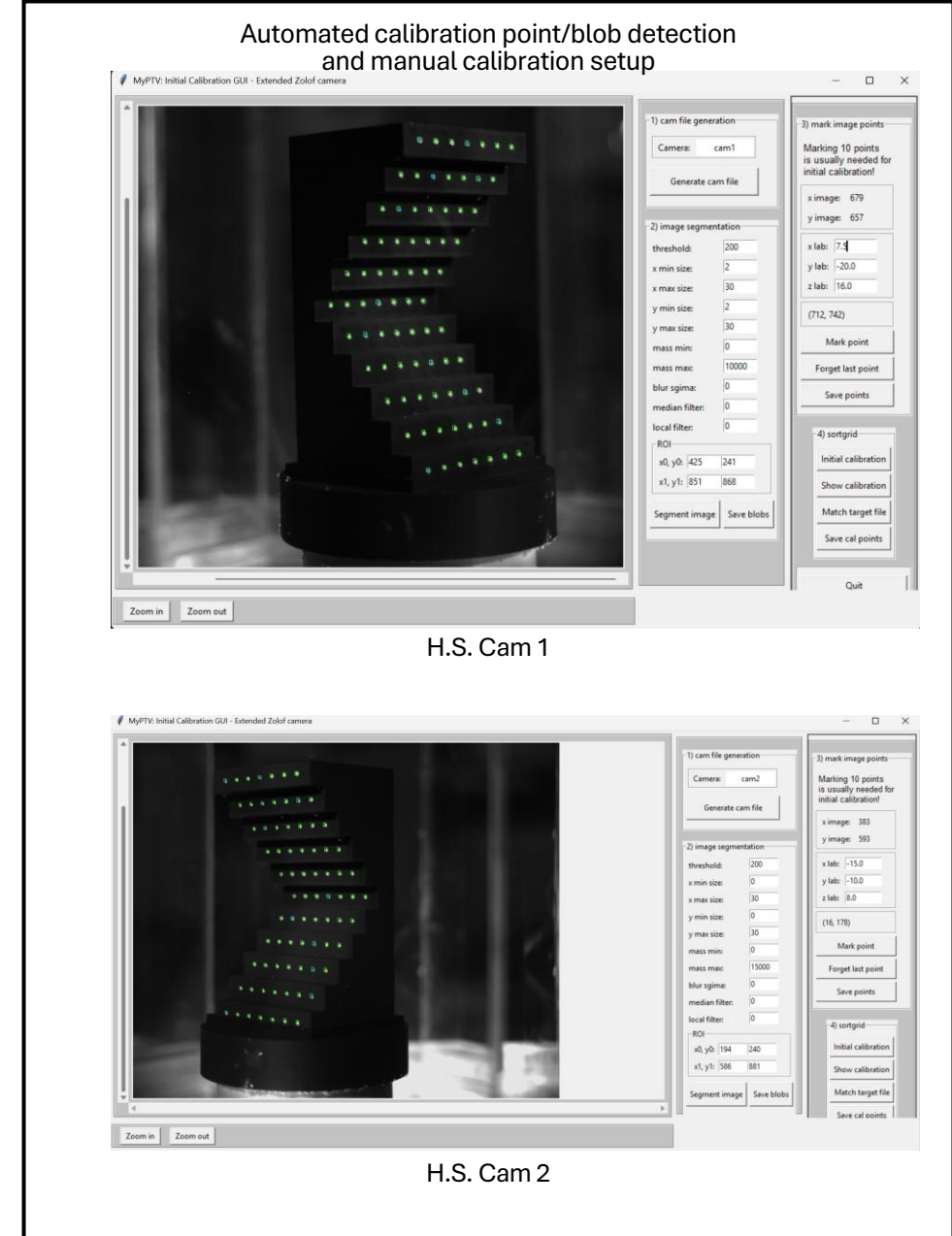
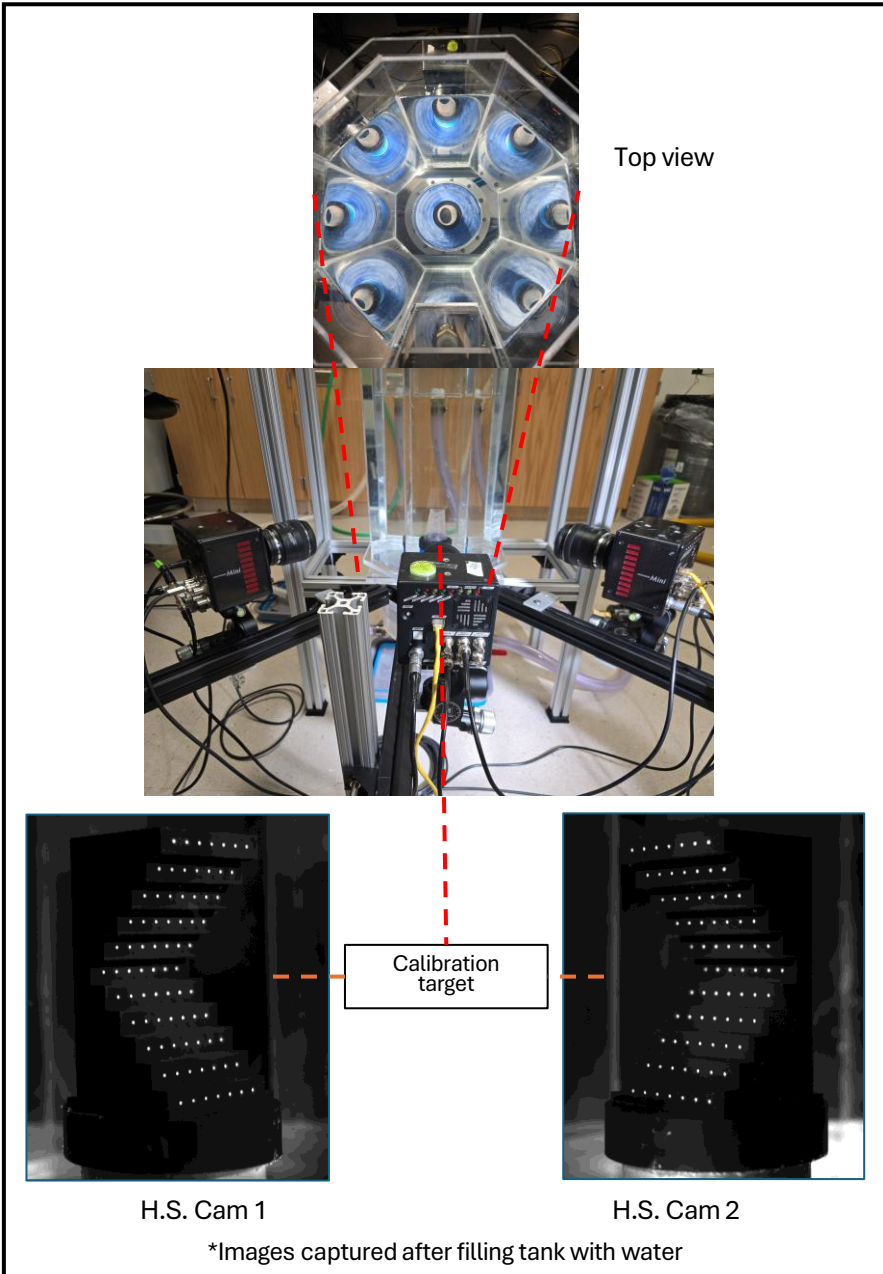


H.S. Cam 1

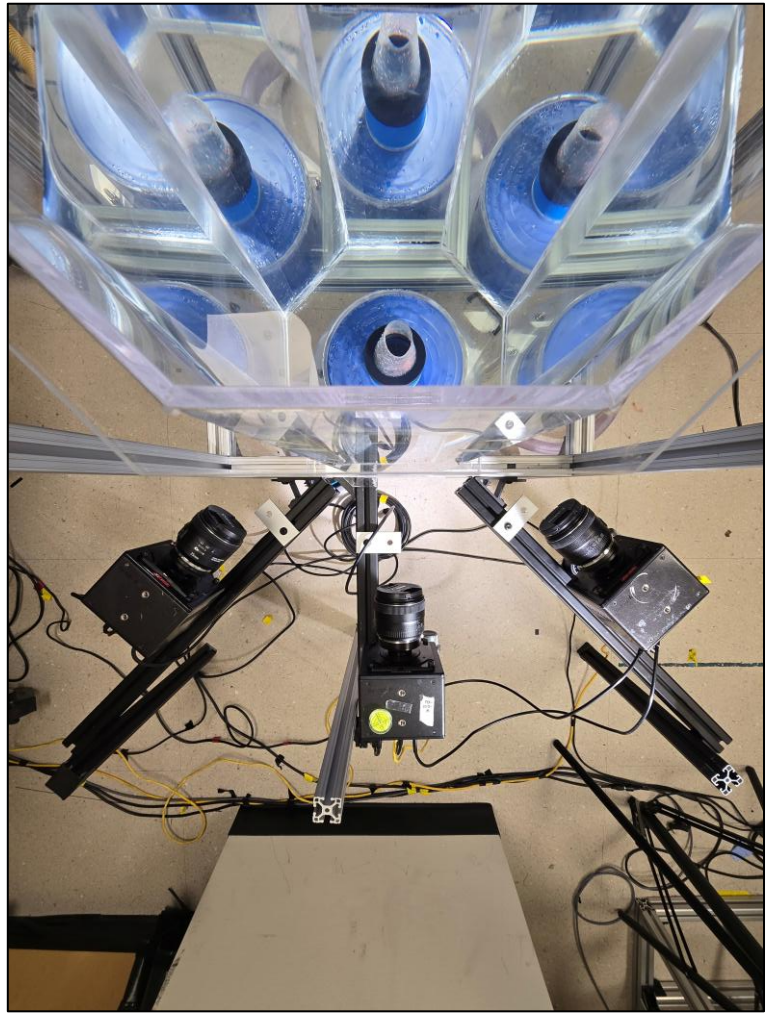


H.S. Cam 2

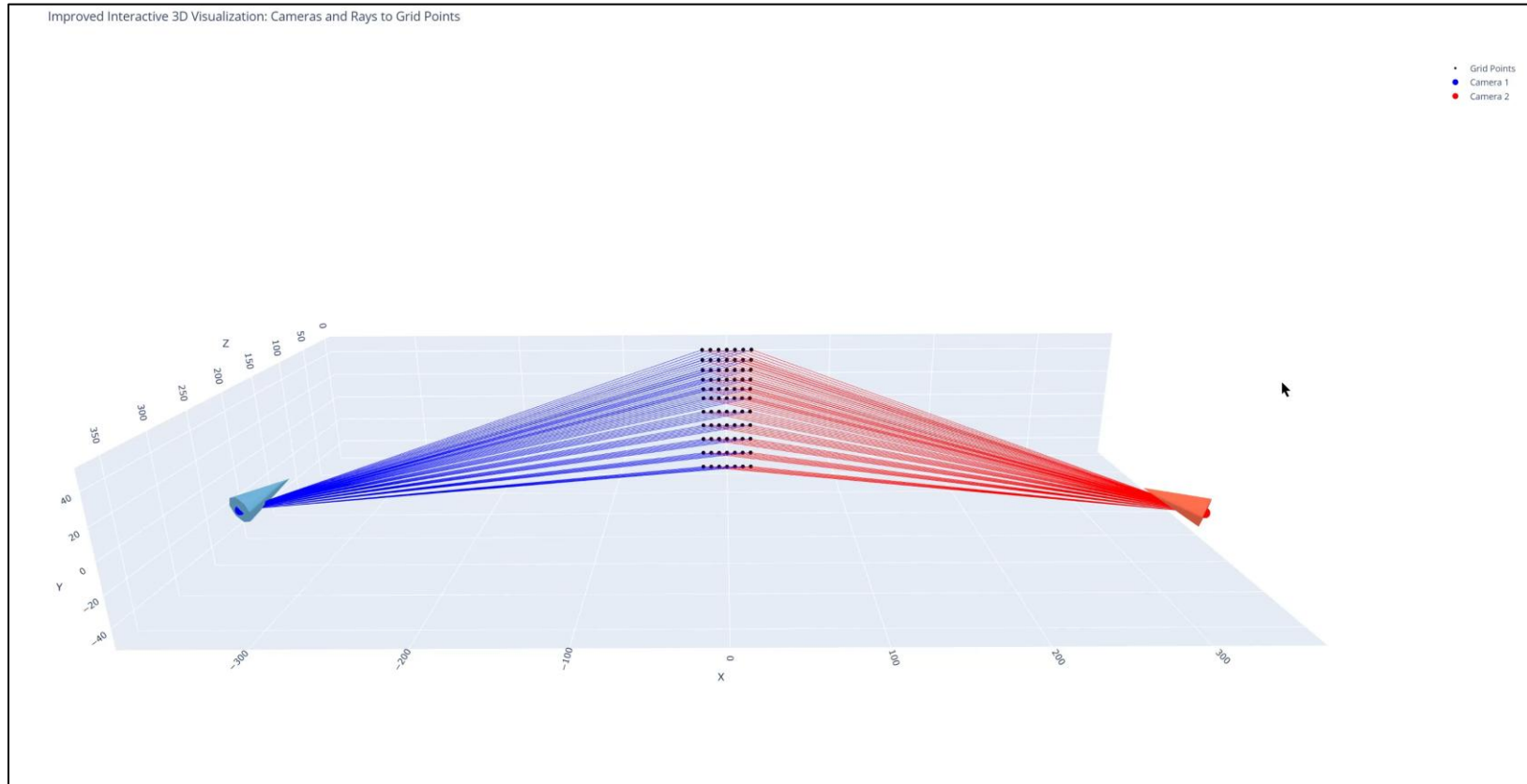
# Revised Multi Step Calibration Target setup



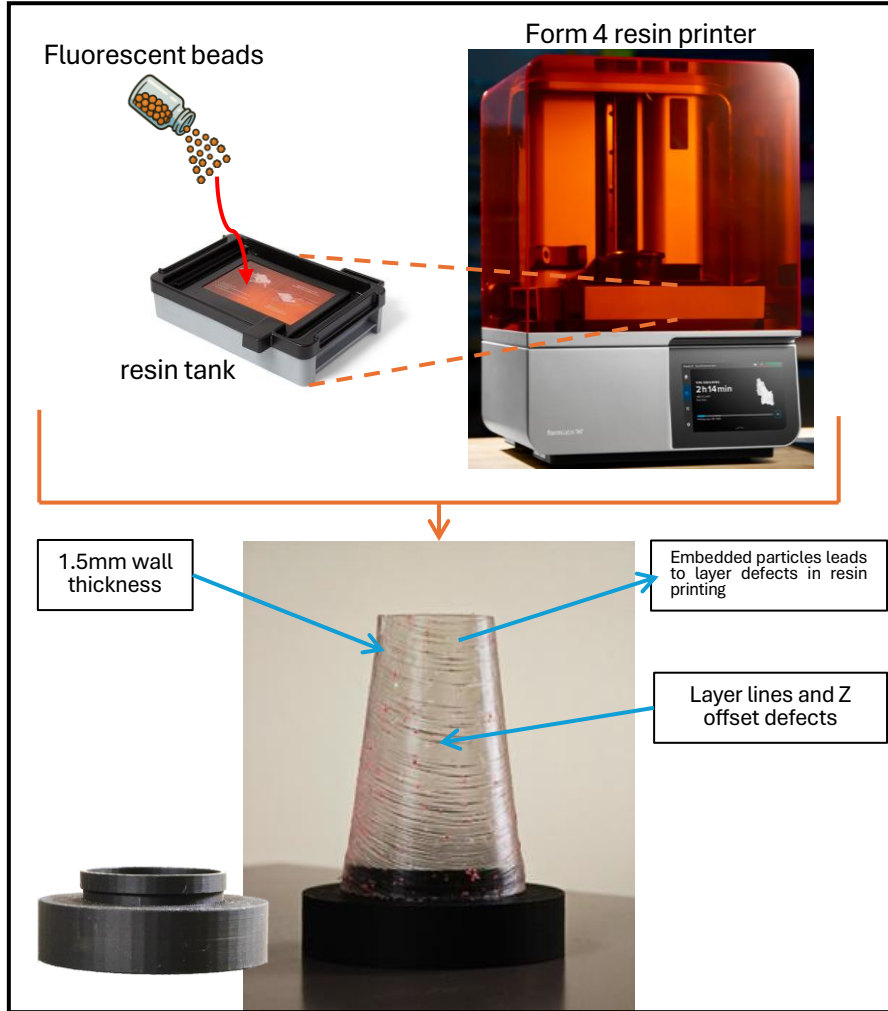
# Camera position and orientation estimation using Extended Zolof model



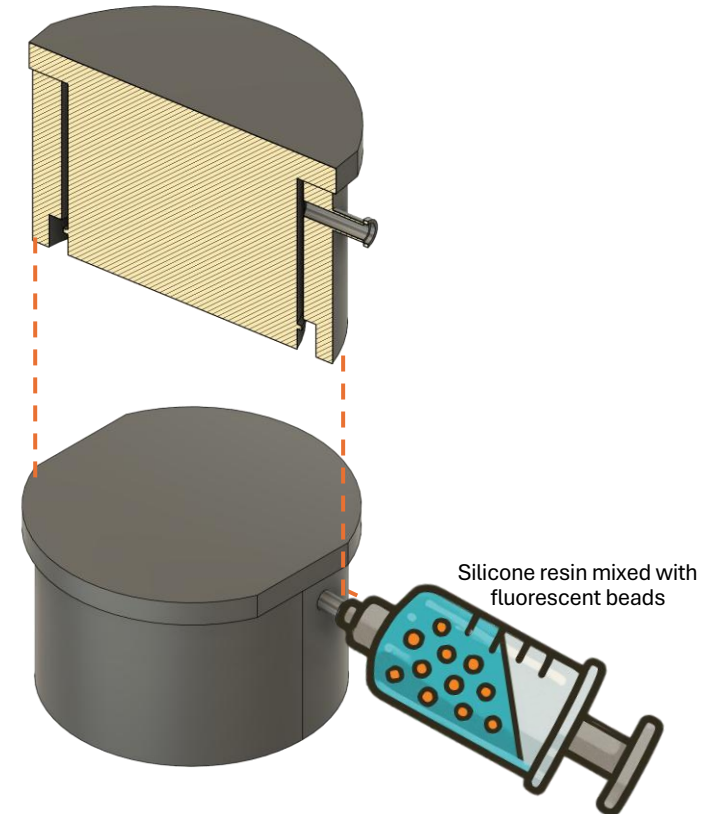
\*Middle camera was not used  
for current calibration



# Nozzle fabrication for deformation measurement



- Transparent Mold for flexible nozzle
- Silicone + binder + fluorescent beads combination to control stiffness as well as control the density of beads in the flexible nozzle ( hard to control using Form 4 resin printer)
- Better surface finish will help reduce optical defects and structural defects



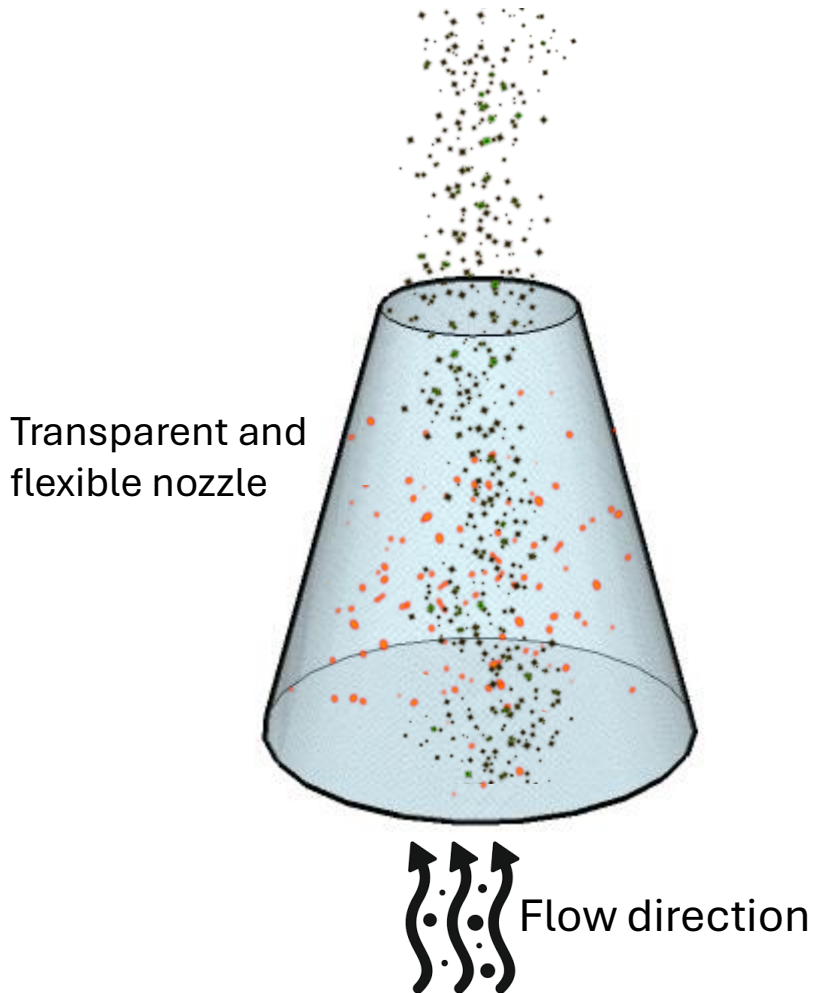
# Transparent nozzle fabrication



## Next Steps:

- Flexible and transparent nozzle fabrication with embedded fluorescent beads.

# Simultaneous Deformation and flow measurement

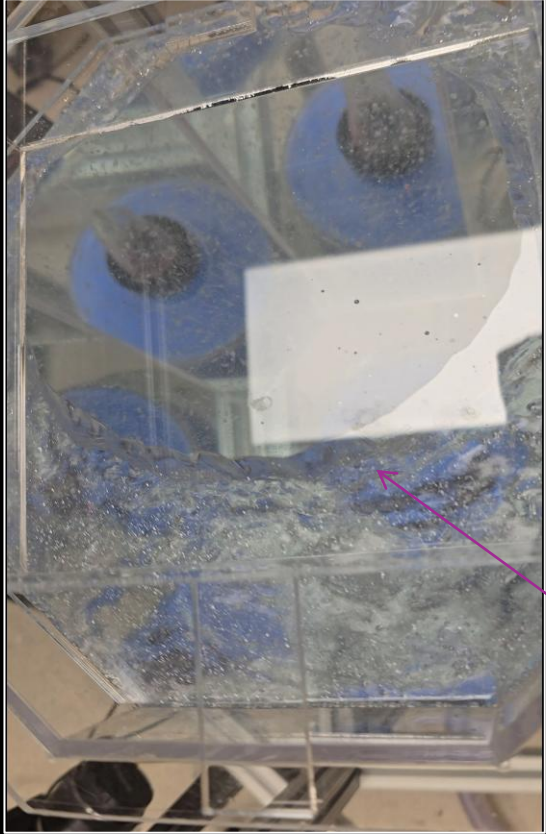


Orange fluorescent beads (e.g., 1–5  $\mu\text{m}$ ) are stuck onto the nozzle surface.

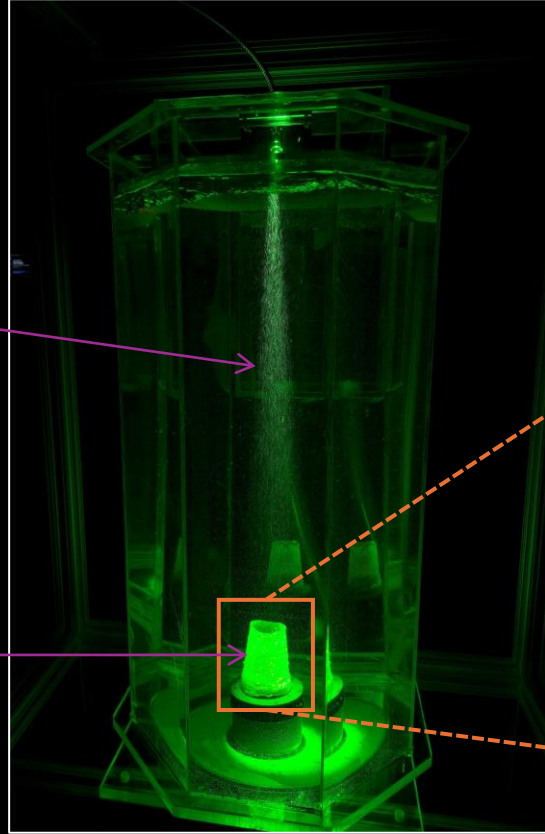
- Serve as **static reference markers** for detecting nozzle deformation.
  - Easily distinguishable via **fluorescence filtering** (e.g., long-pass or band-pass filters).
- White polyamide beads/hollow glass spheres are seeded in the flowing fluid.
- Act as **Lagrangian tracers** to track fluid motion.
  - Non-fluorescent or different spectral profile → distinguishable from orange beads.

- Polyamide particles in water
- Orange fluorescent beads embedded inside the nozzle

# Green Laser(525nm) Setup

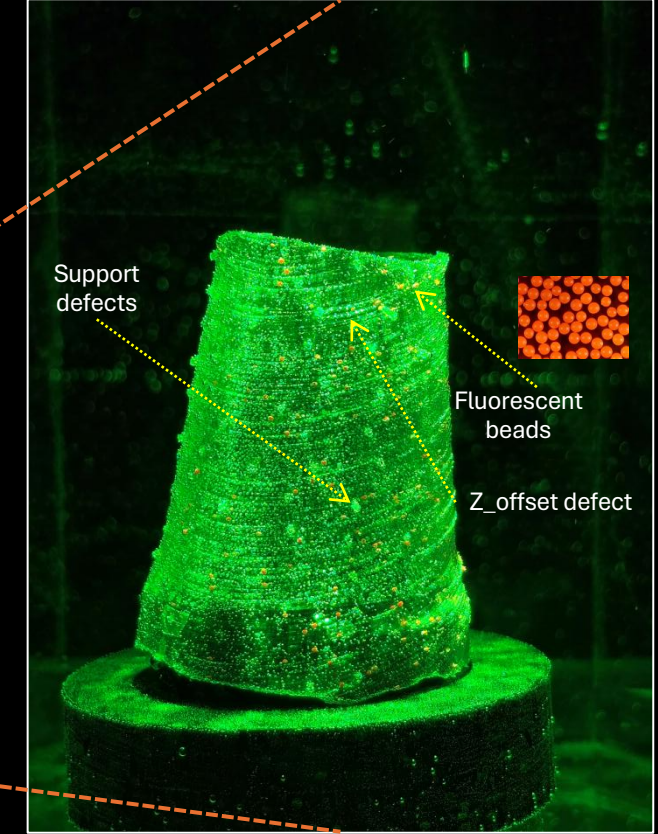


Laser window

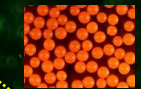


Volumetric laser  
illumination cone

Flexible  
cone



Support  
defects

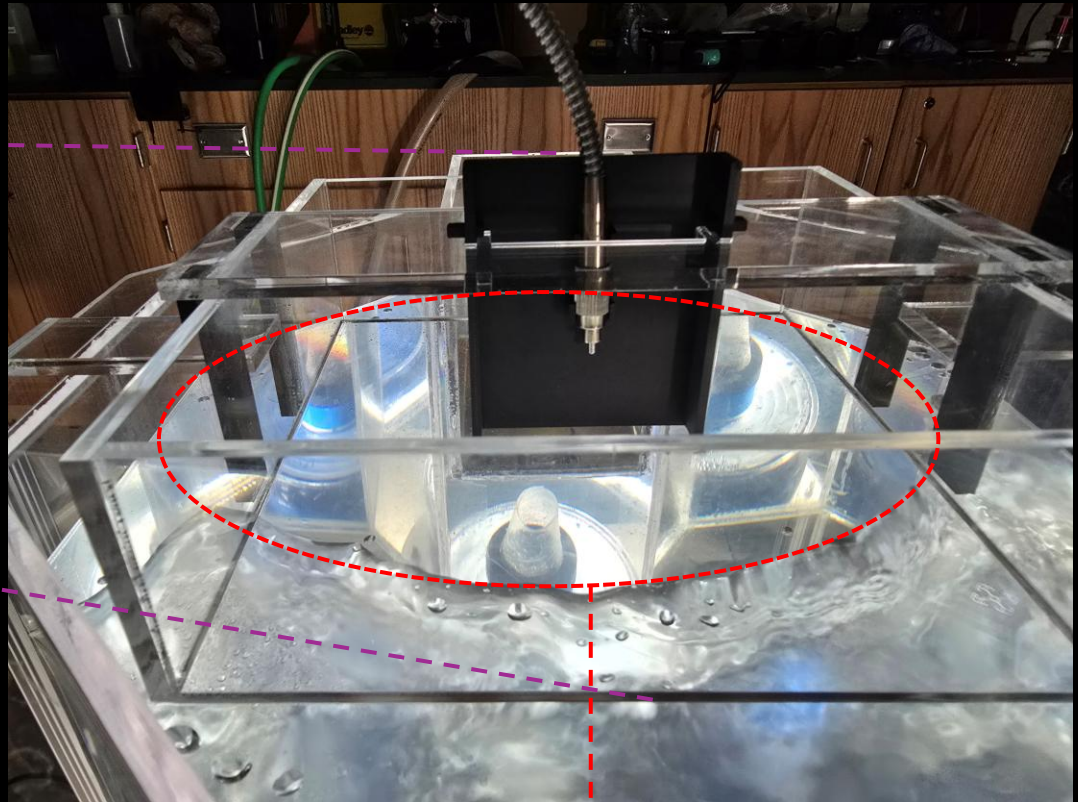
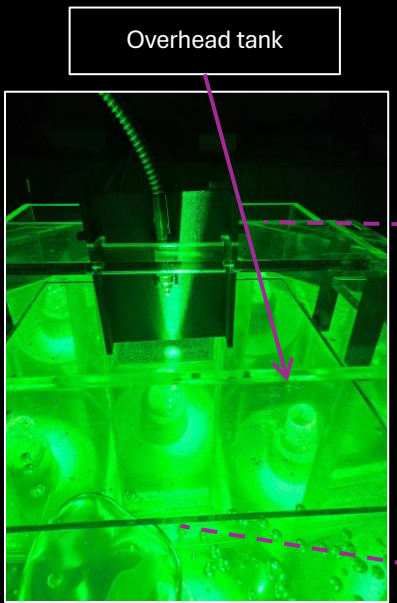


Fluorescent  
beads

Z\_offset defect

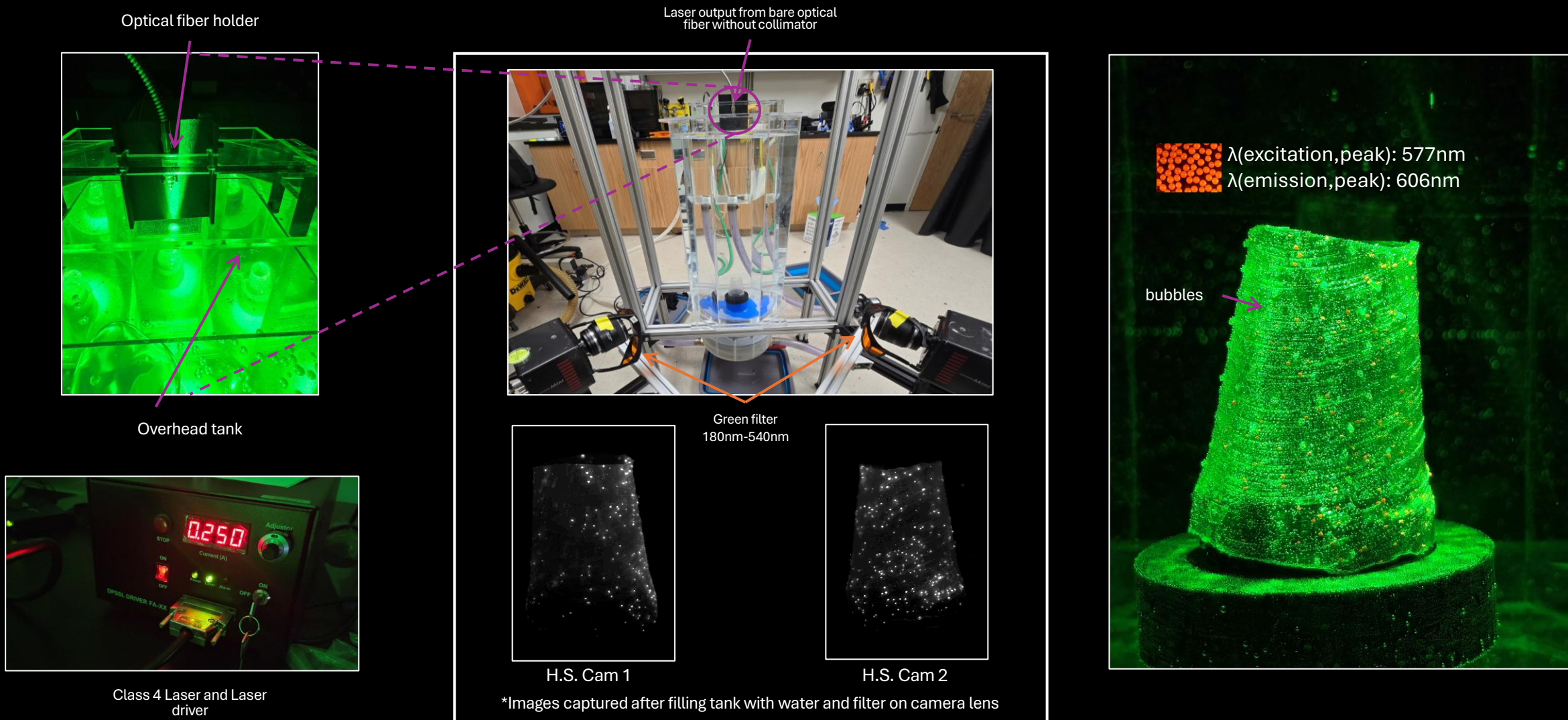
- Partial filling helps in stopping bubble formation in the bottom of the overhead tank
- Bubble accumulation blocks laser considerably
- Overhead tank stops laser light **shimmering effects**

# Overhead Tank

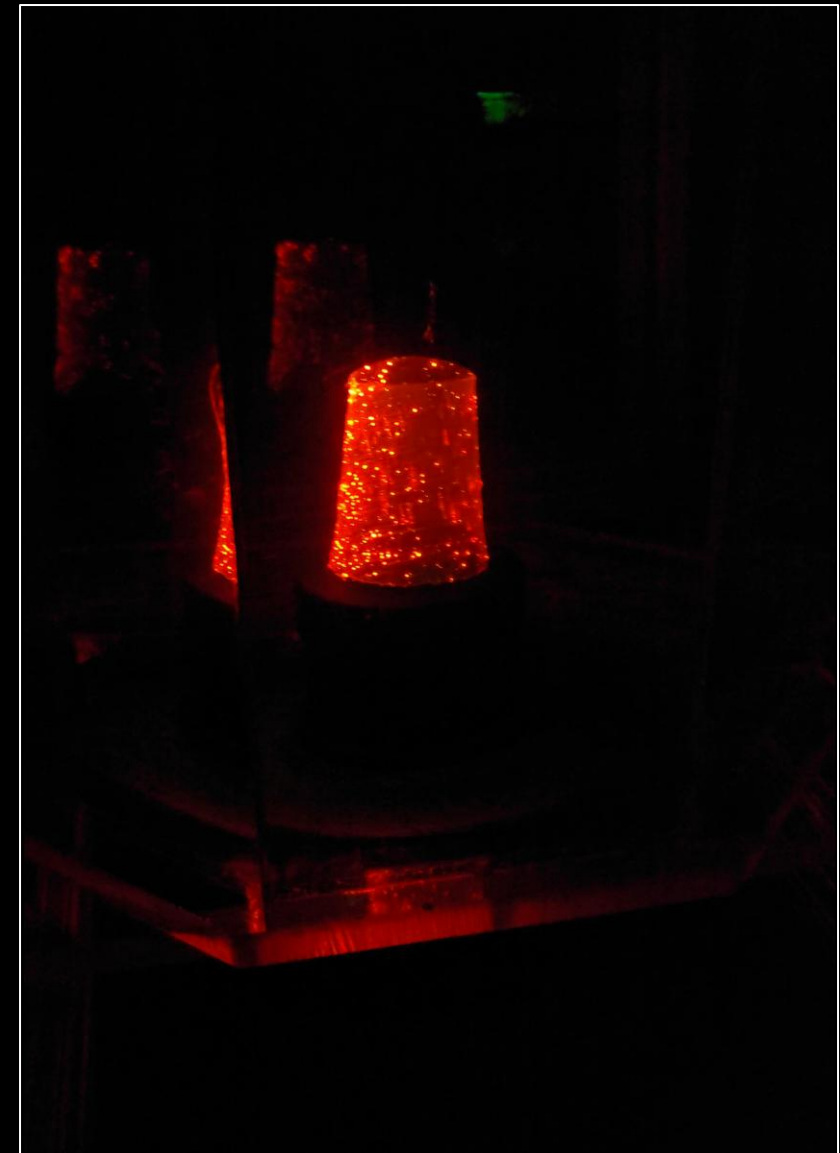
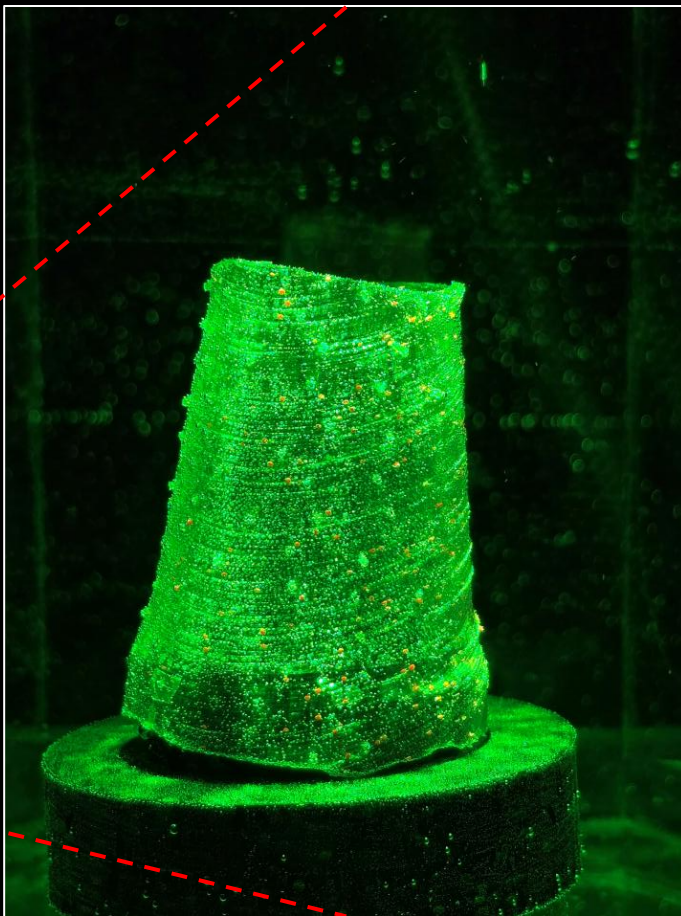
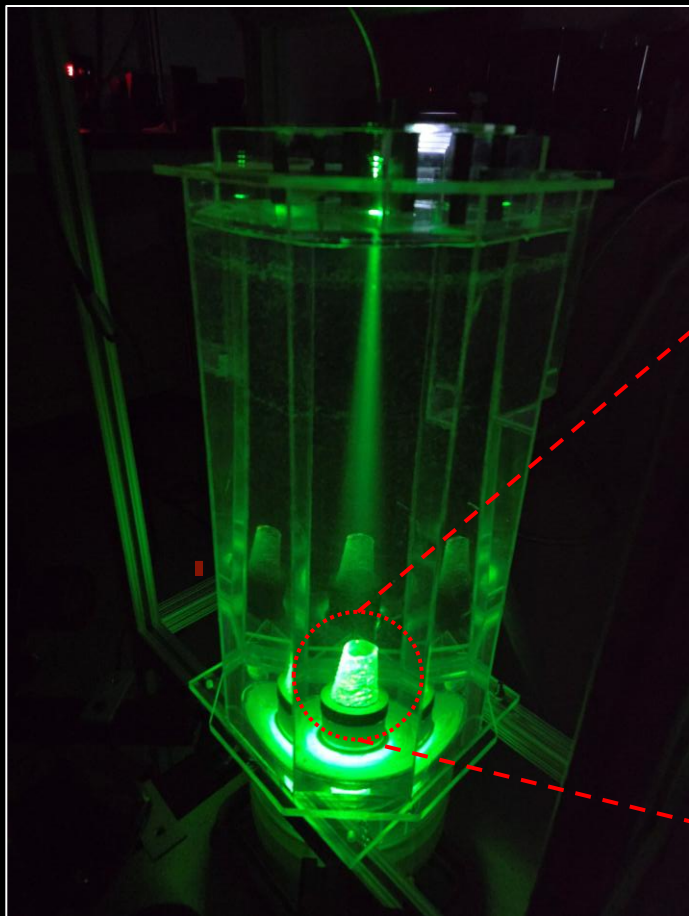


Overhead tank makes a contact window so that laser can travel directly through the acrylic and water interface without shimmering

# Orange Fluorescent particles detection setup

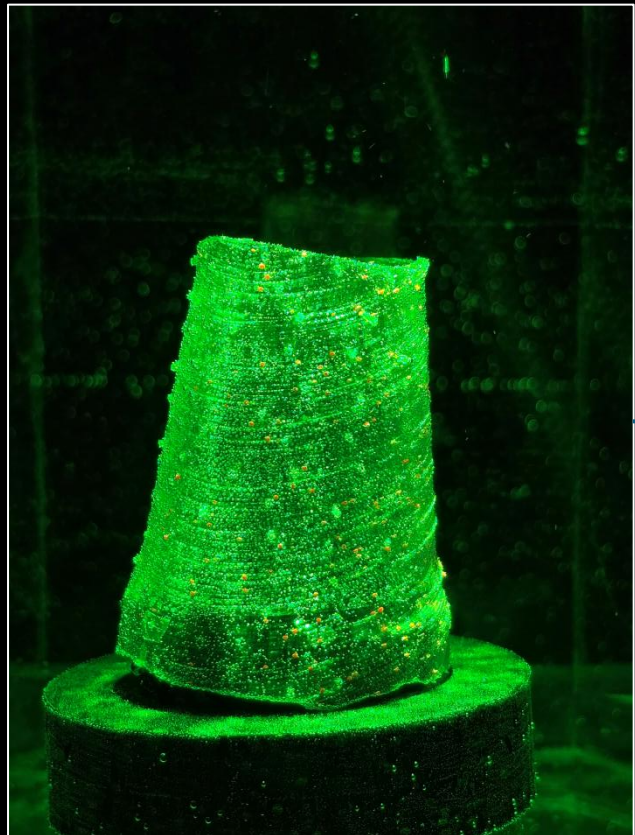


# Laser Setup



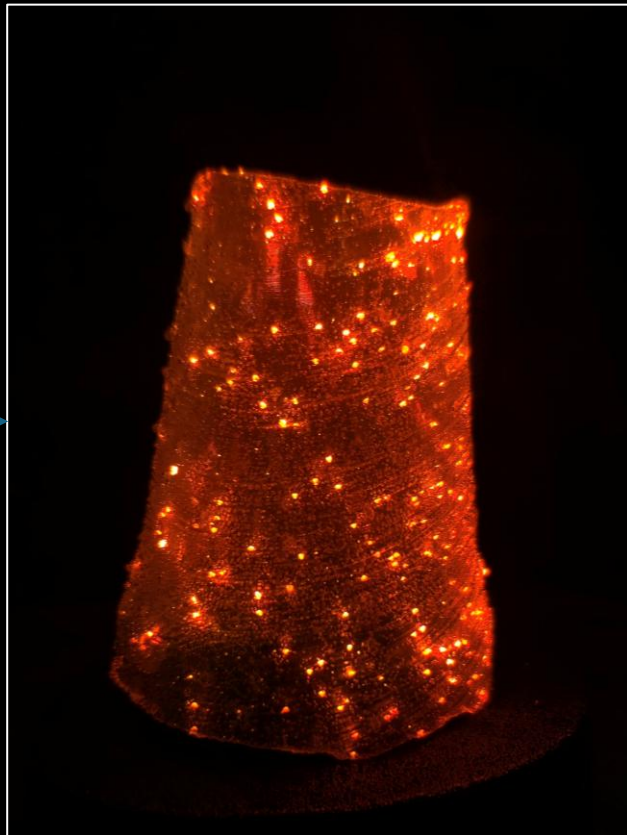
\*Smartphone camera with green filter

# Laser Setup



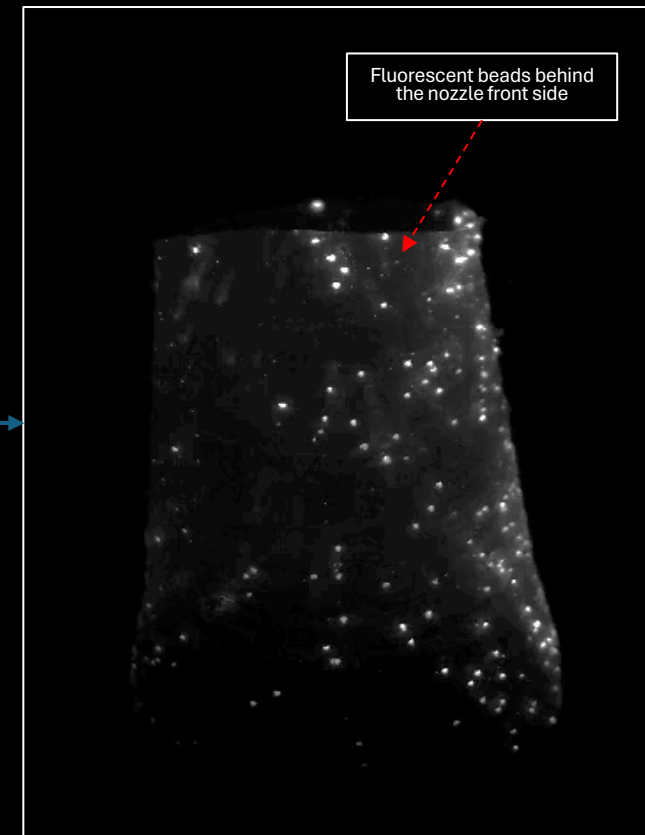
- Bubble accumulation on the nozzle leads to loss of transparency
- Resin printing defects like layer line defects leads to higher accumulation of bubbles on the nozzle.

\*Smartphone camera



- A green(180nm-540nm) filter improves contrast and better visibility of fluorescent particles and removes most reflections from layer defects and bubbles.

\*Smartphone camera with green filter

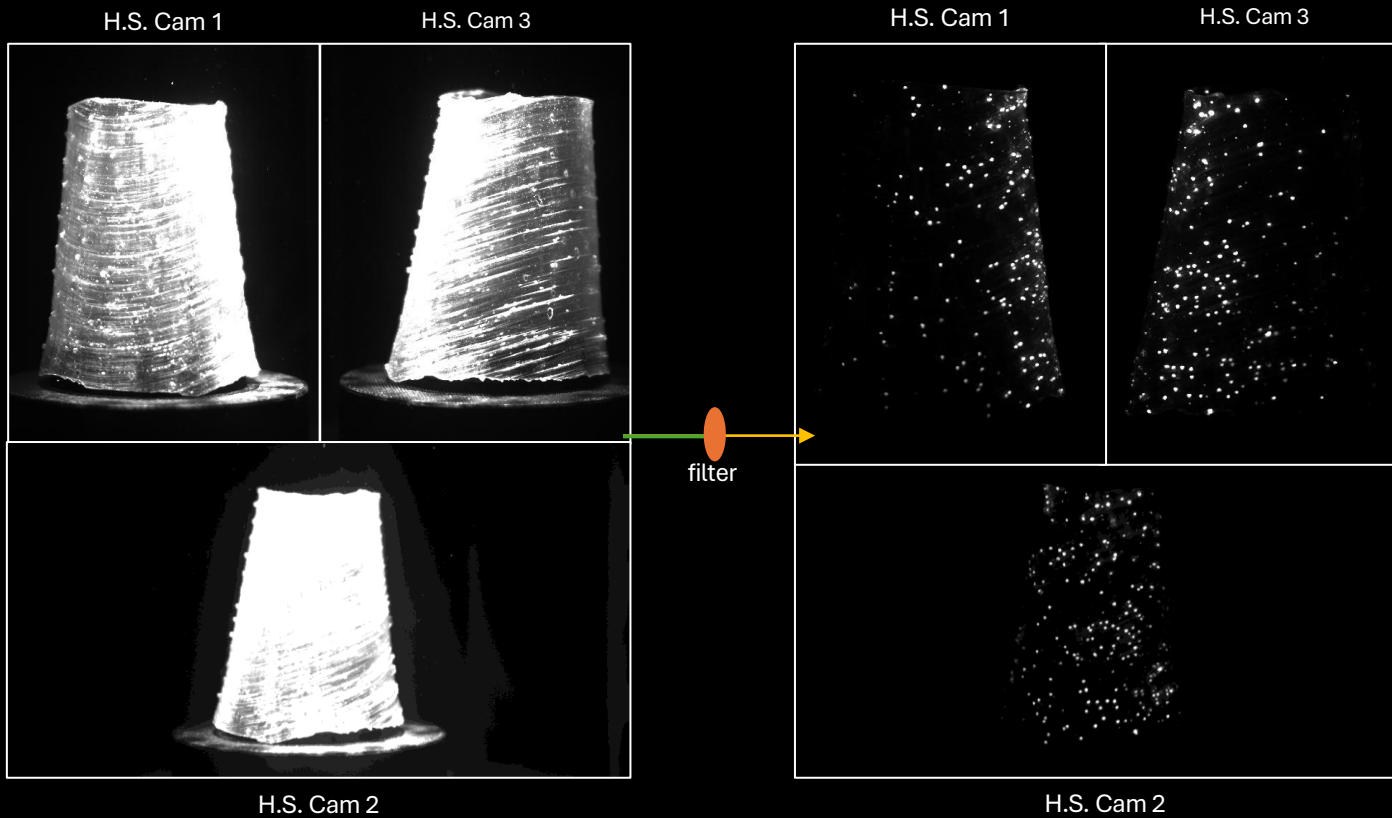


- Using green filter and High Speed camera removes most of the noise/reflections from printing defects.

\*Photron Fastcam Mini AX 200.

with green filter

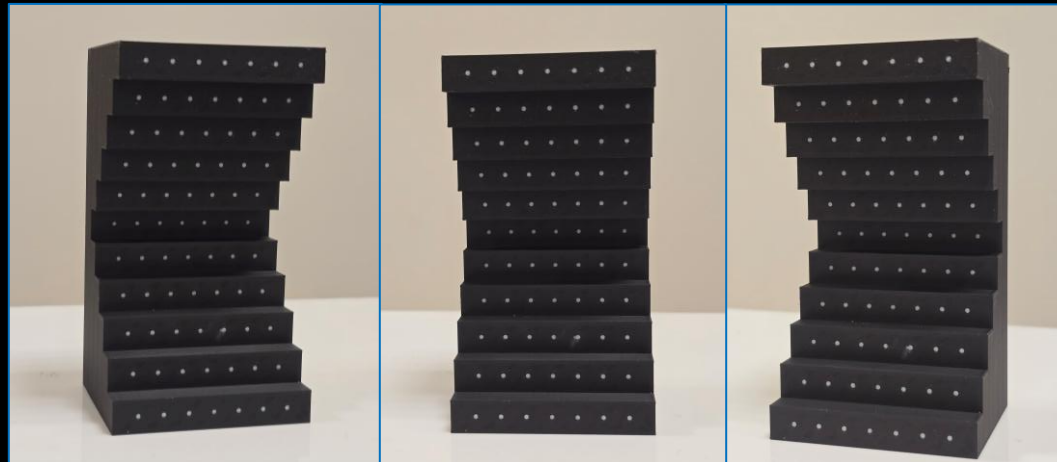
# Laser Setup with Green filter(180-532 nm)



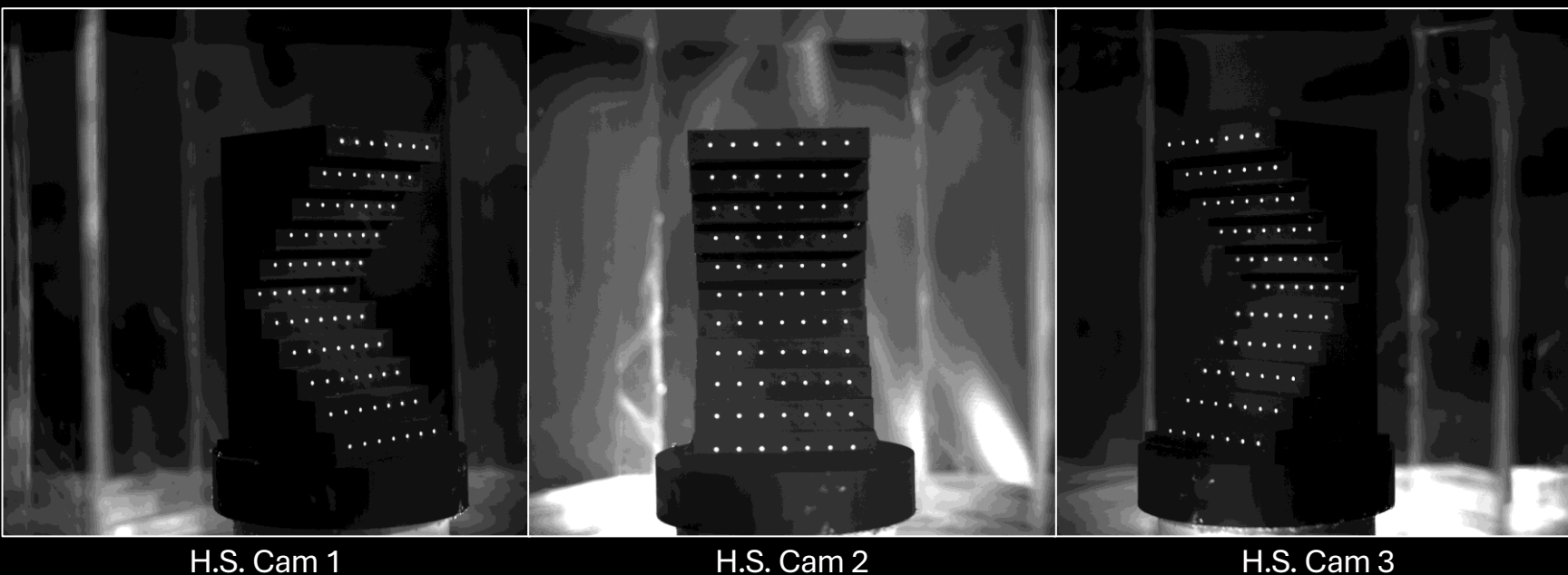
- Without the filter, good enough contrast is not possible due to much higher intensity of the green light compared to the red fluorescent light in the monochrome camera.
- A color high speed camera might allow us to selectively filter out different wavelengths

- Using green filter and High Speed camera removes most of the noise/reflections from printing defects and bubbles.

# Calibration Target



3D printed  
Calibration target

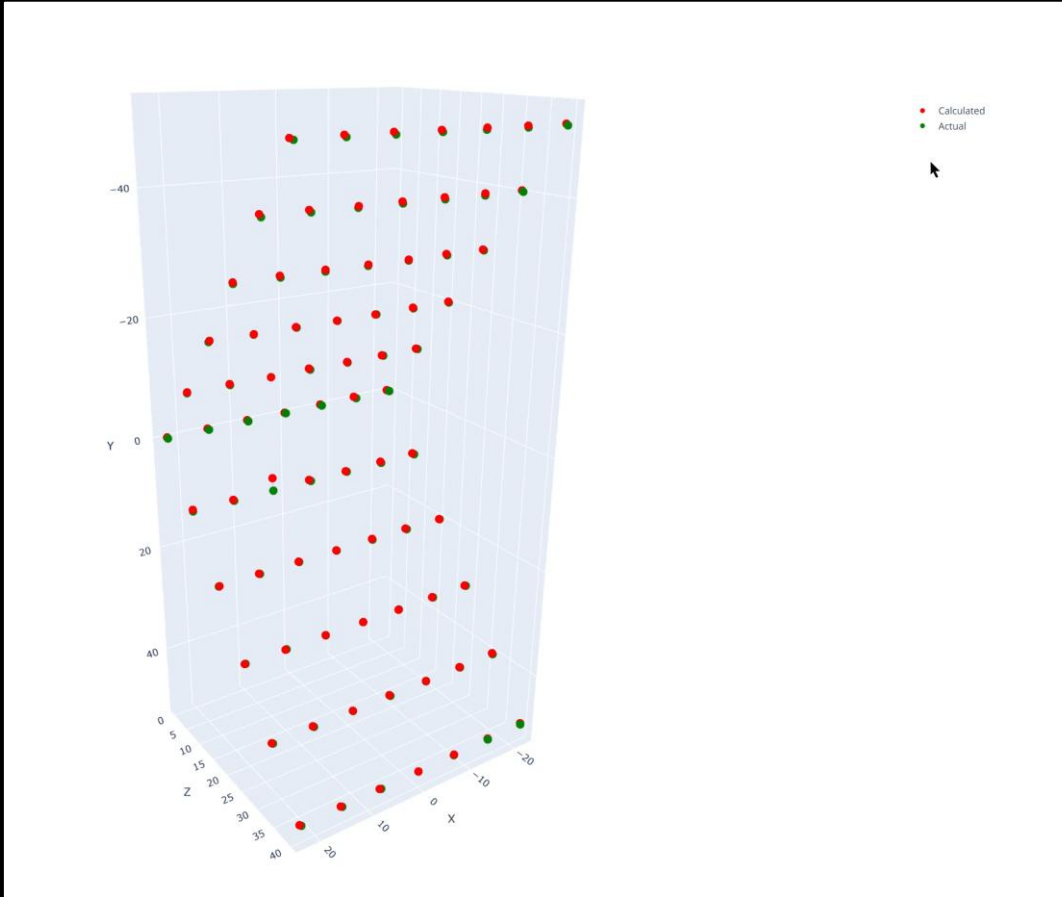
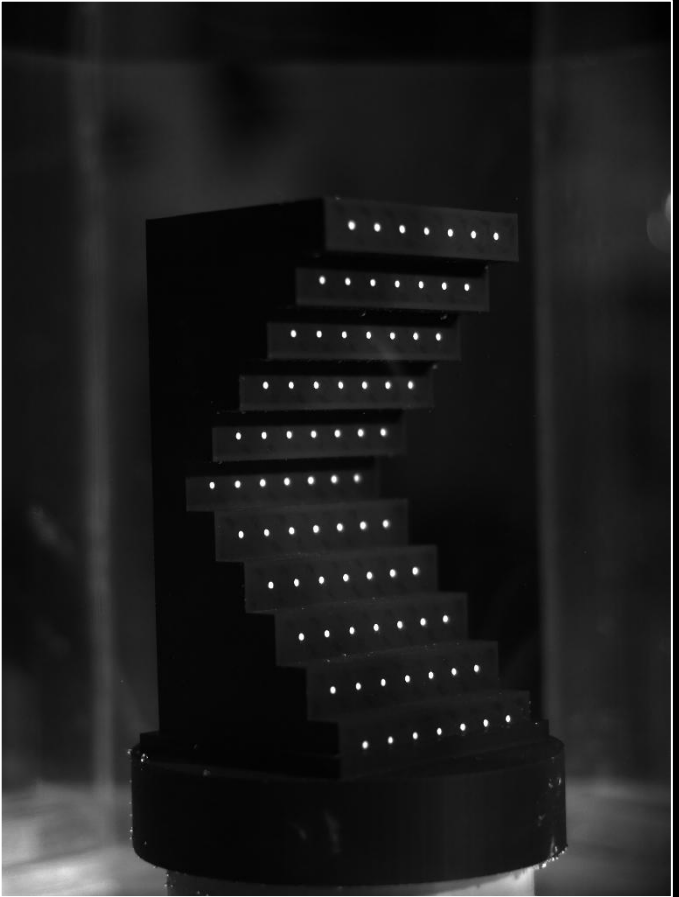


H.S. Cam 1

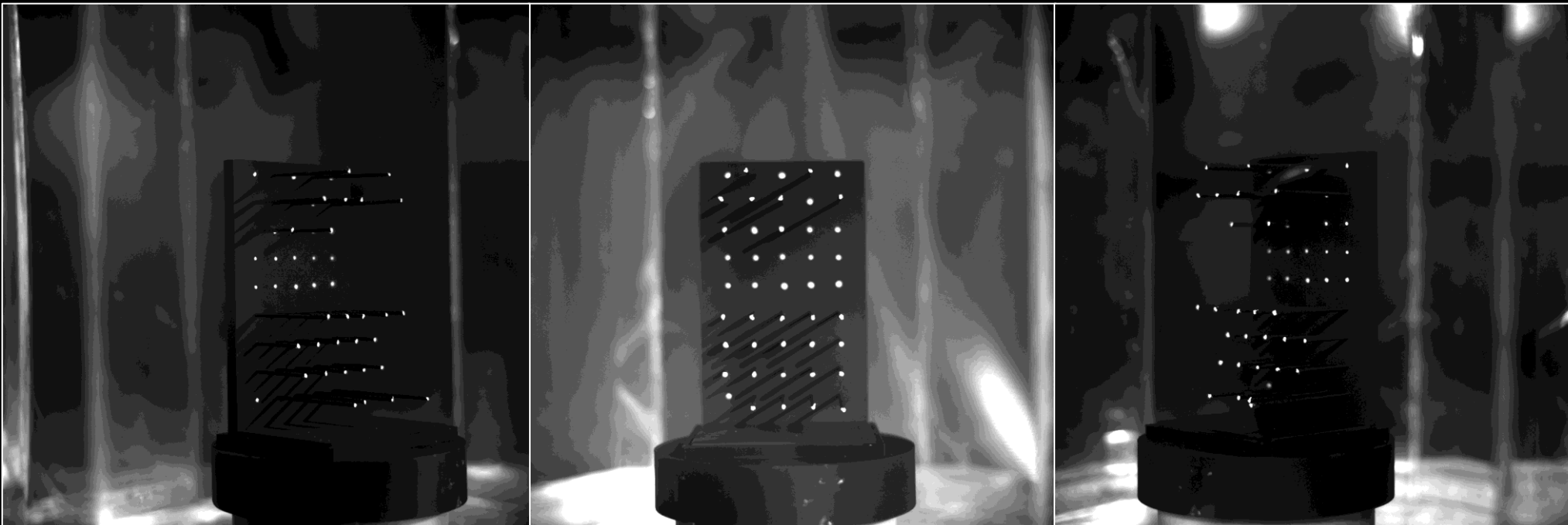
H.S. Cam 2

H.S. Cam 3

# Calibration Target reconstruction



# Test Target for calibration validation



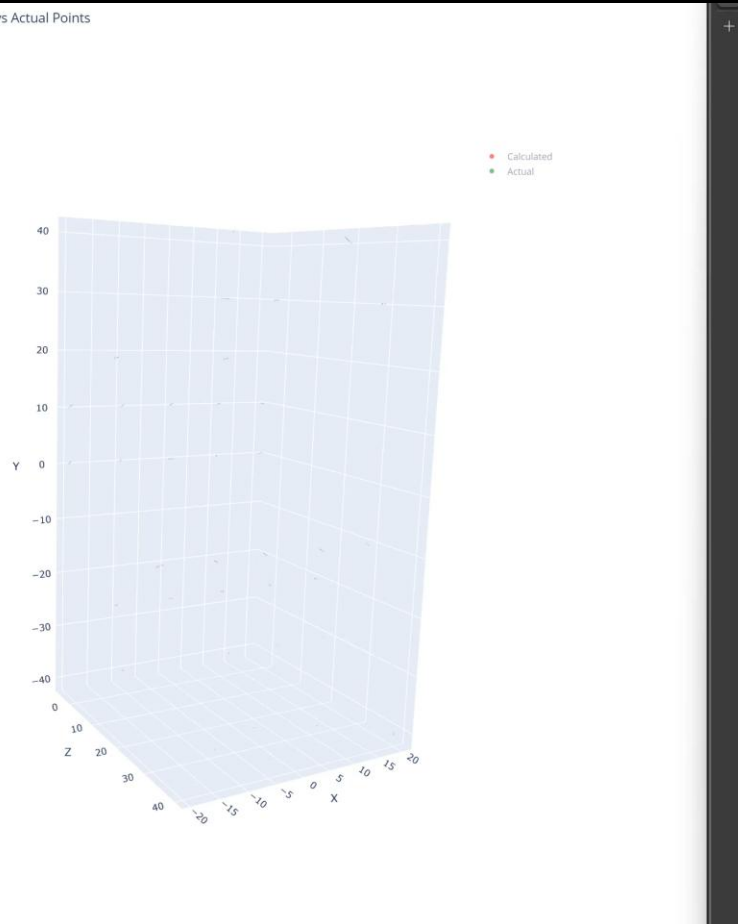
H.S. Cam 1

H.S. Cam 2

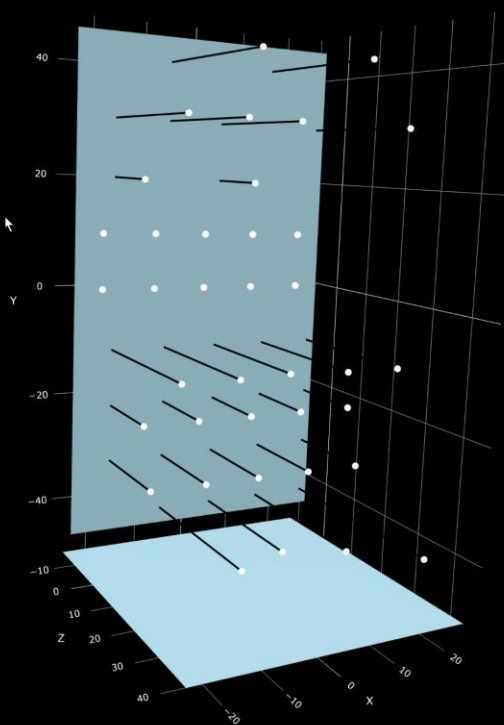
H.S. Cam 3

# Test target reconstruction

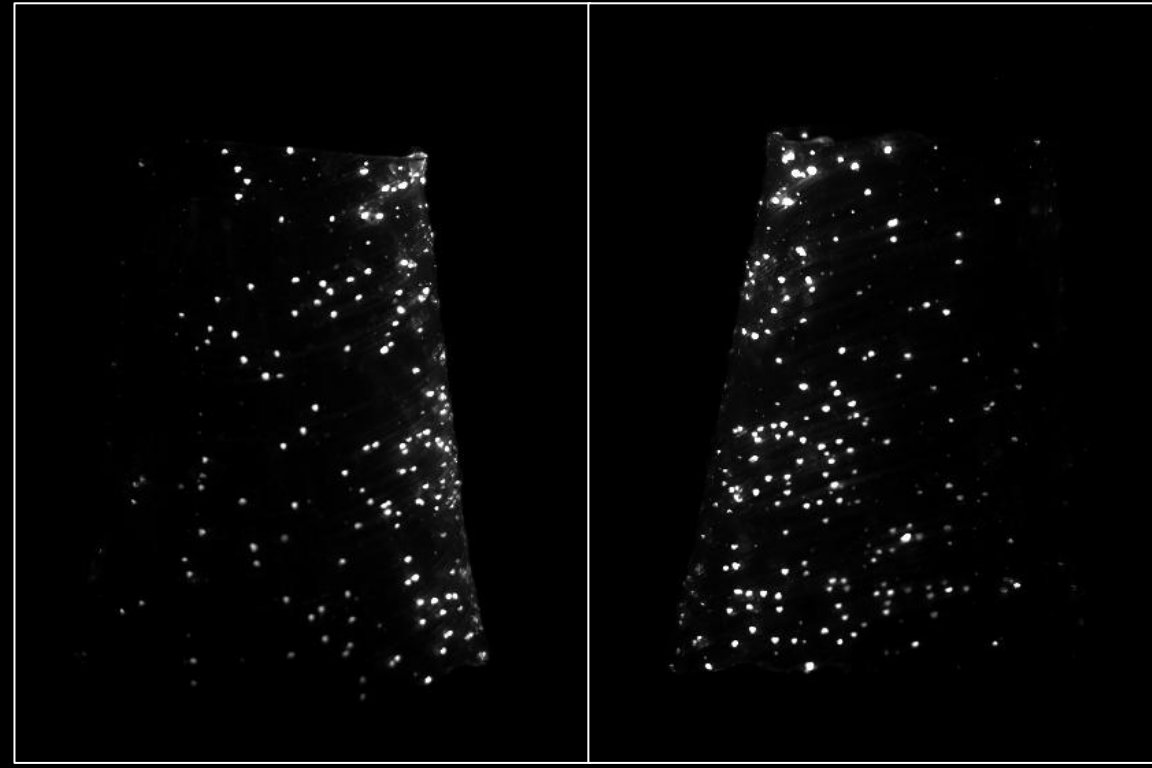
3D Comparison of Calculated vs Actual Points



3D Rod Target with Z=5 Plane (Black Background)



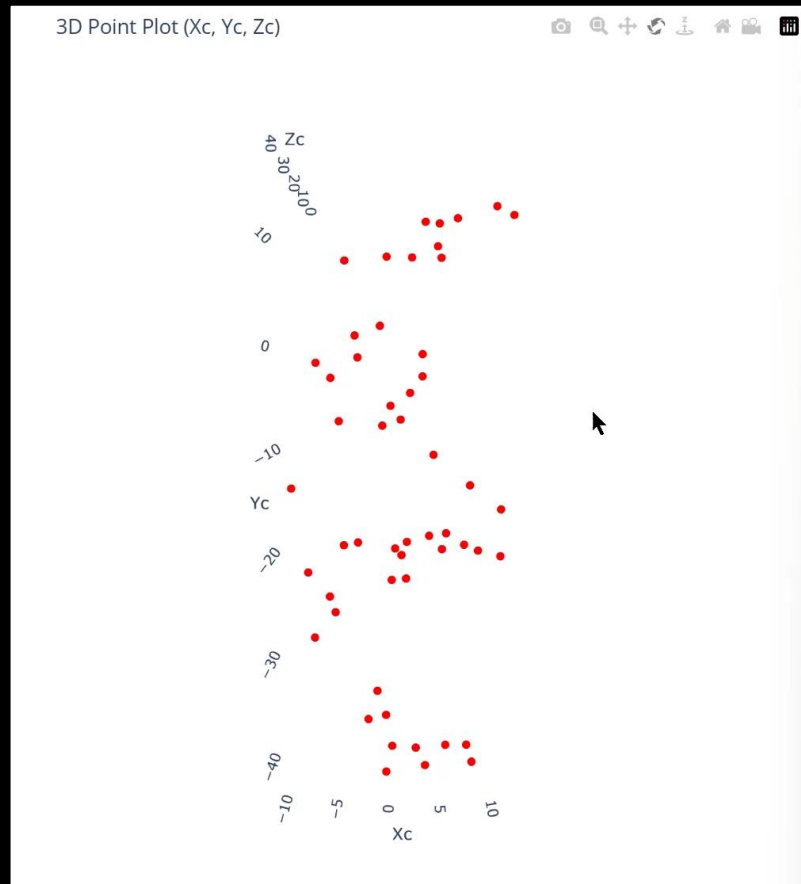
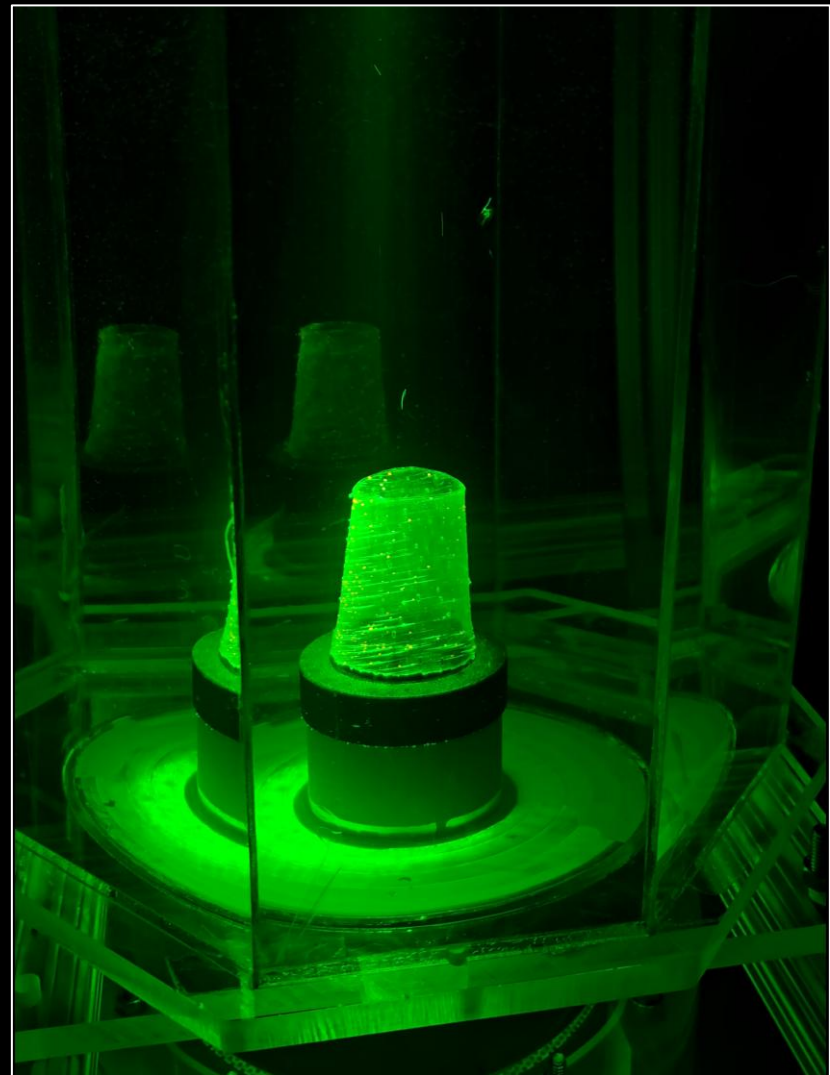
# Conical nozzle reconstruction



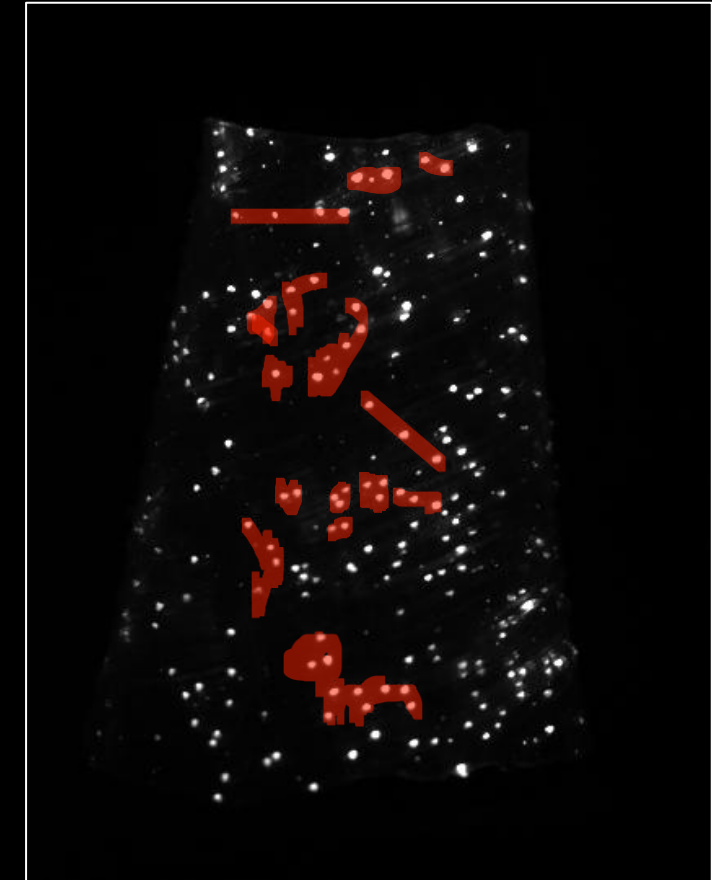
H.S. Cam 1  
(Left)

H.S. Cam 3  
(Right)

# Conical nozzle reconstruction

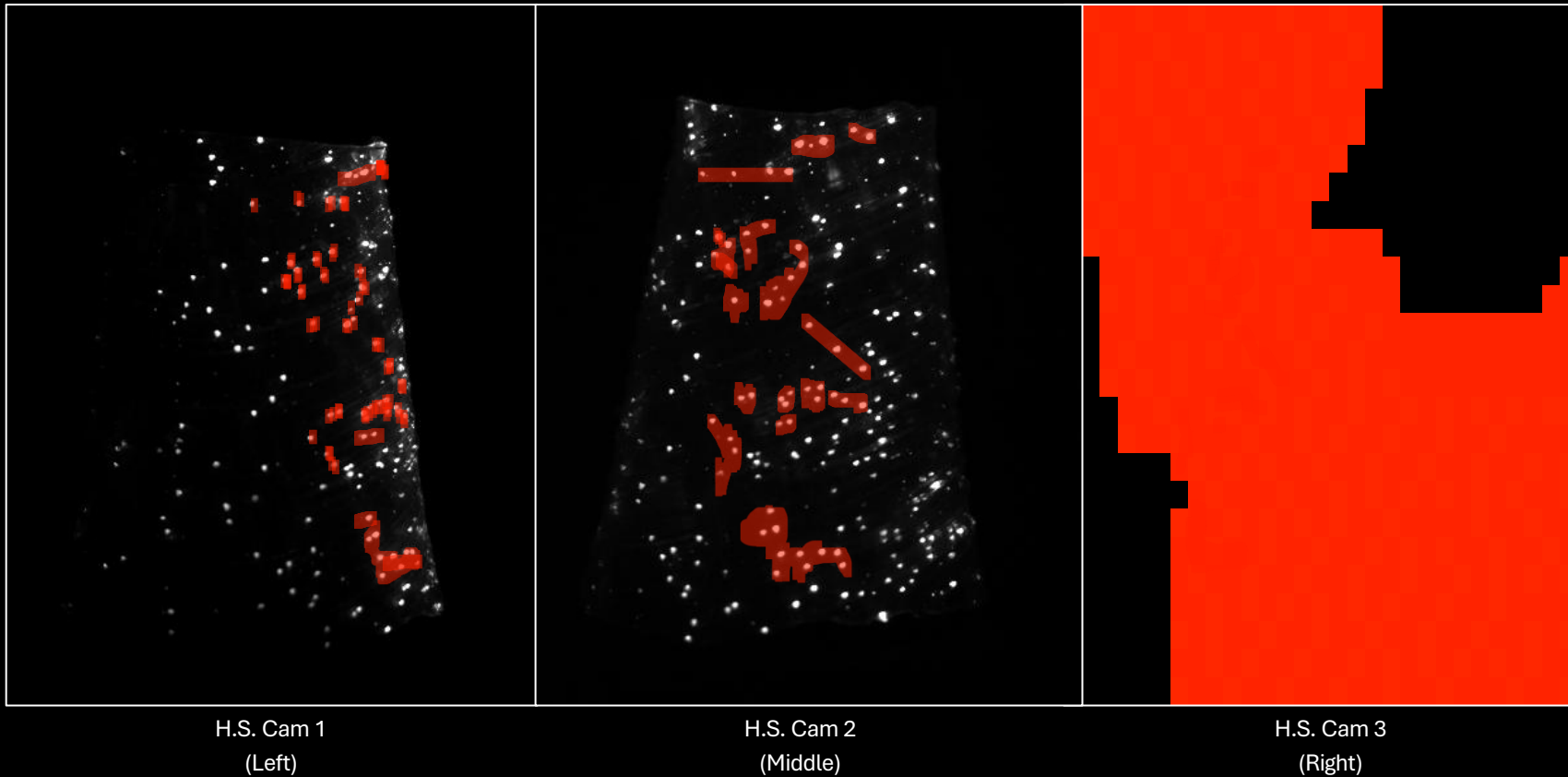


3D reconstruction using  
Extended Zolof Method

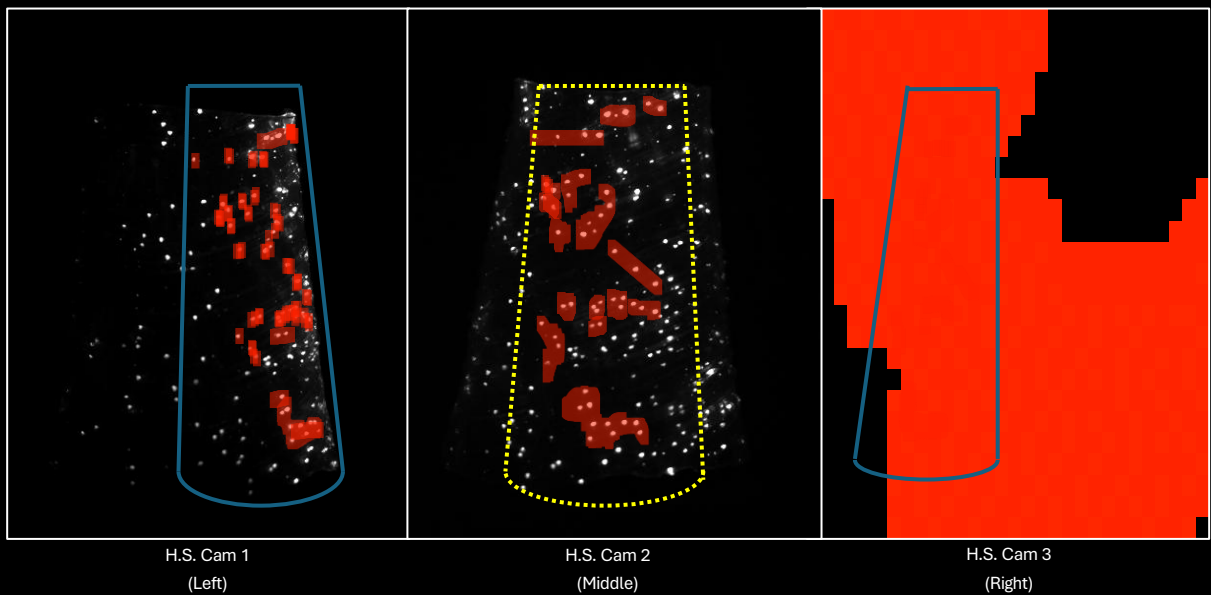
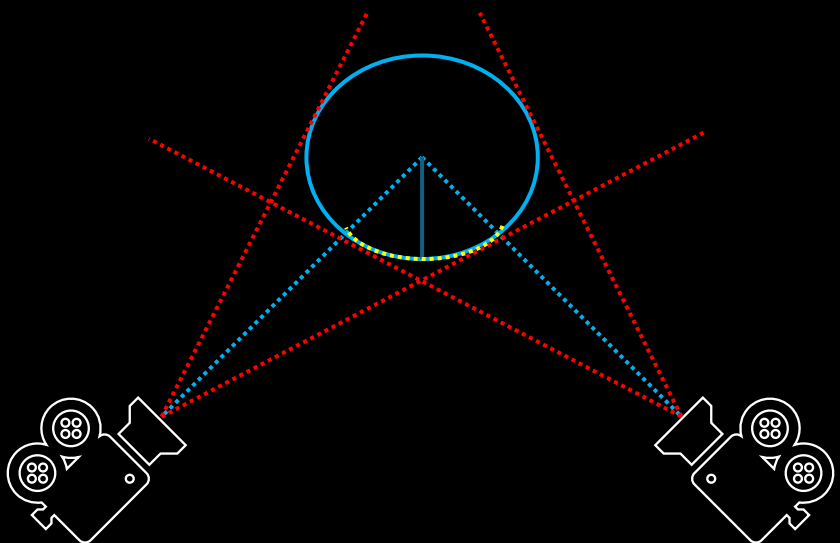


H.S. Cam 2

# Conical nozzle reconstruction

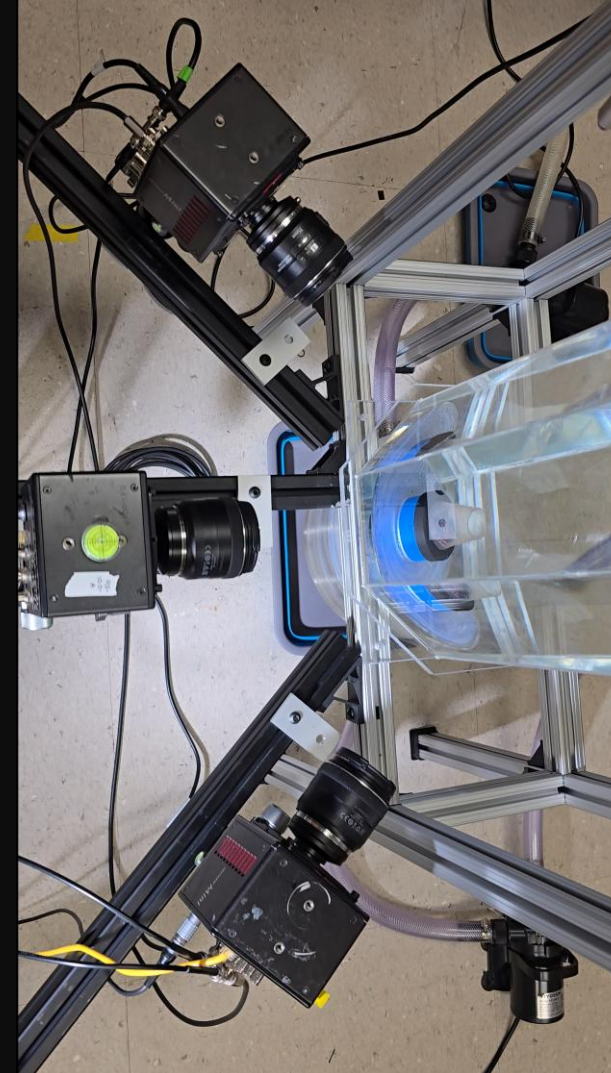


# Conical nozzle reconstruction

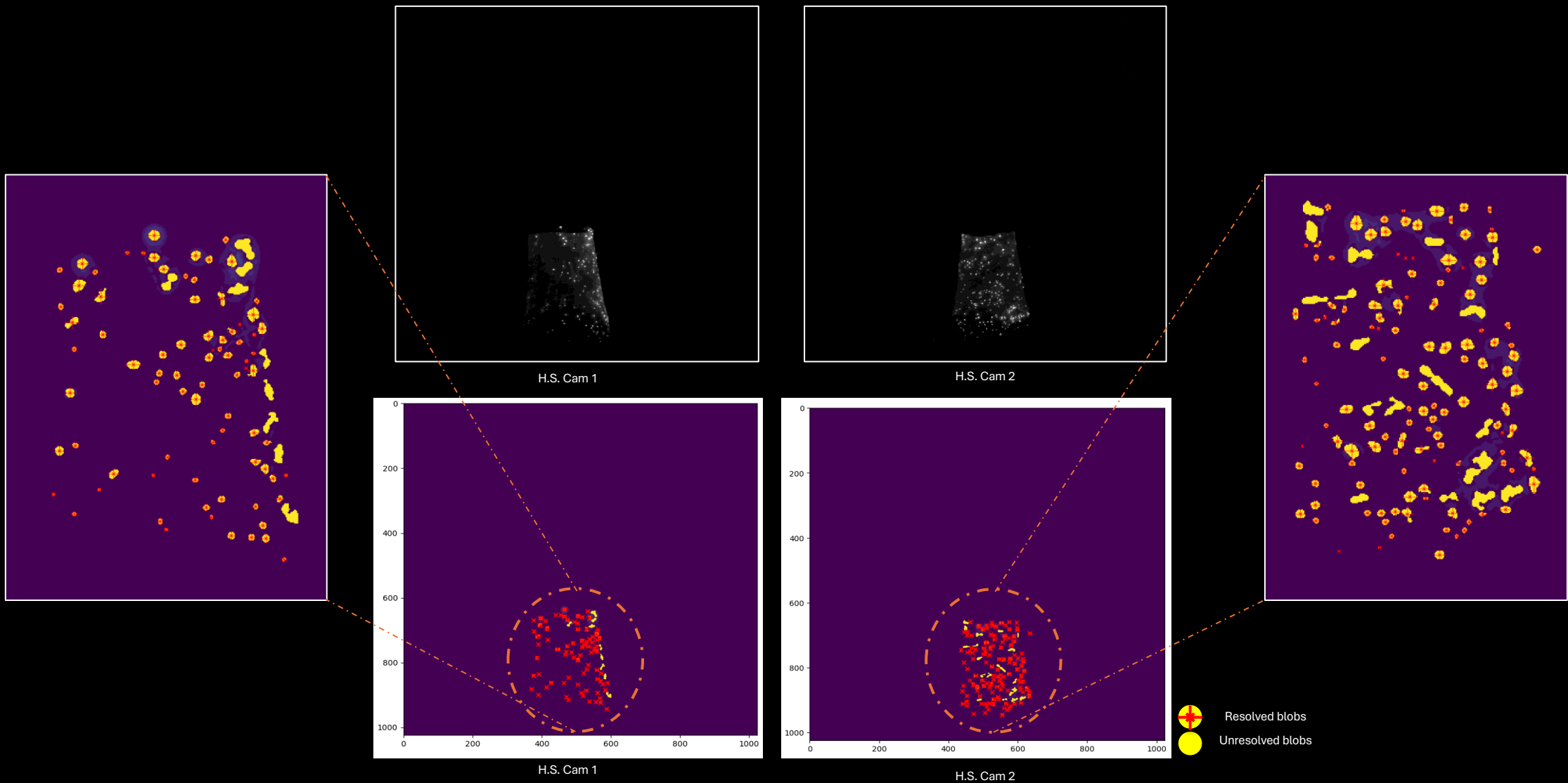


- Limited common field of view leads to partial nozzle mapping
- More cameras required for full nozzle mapping

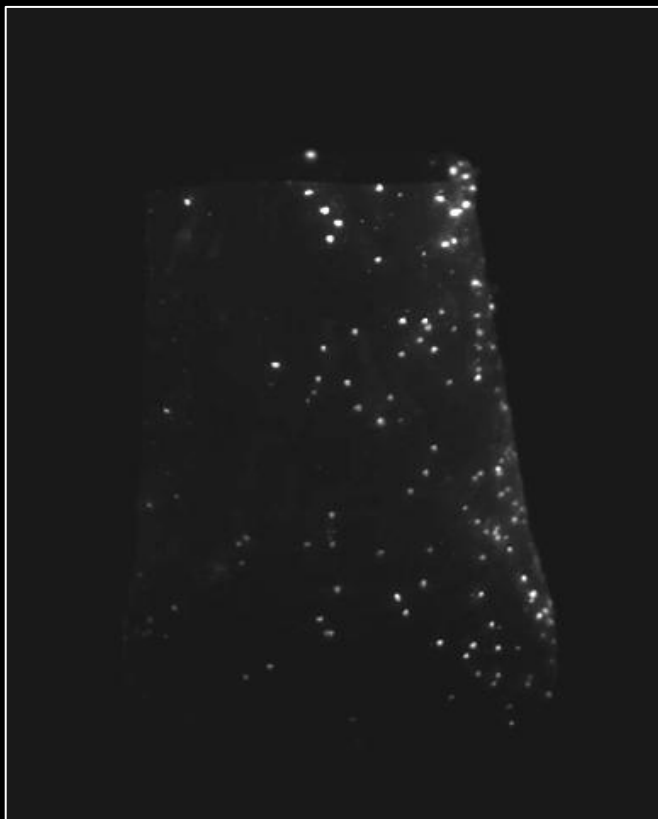
# Current PTV Setup



# Embedded particles segmentation and Matching



# High speed nozzle deformation footage



H.S. Cam 1



H.S. Cam 1

# Next Steps: Deformation mapping and particle tracking

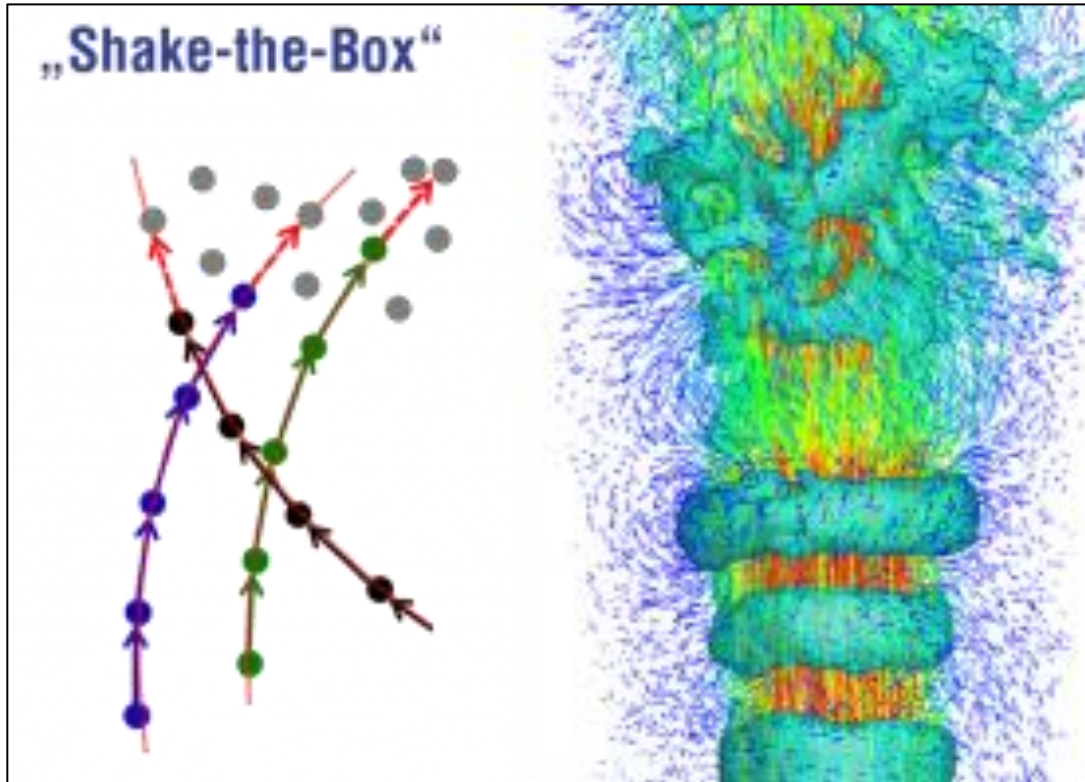
## Key accomplishments

- ✓ Camera calibration with Extended Zolof method
- ✓ Fabricated the flexible nozzle with embedded orange fluorescent beads
- ✓ Automated the particle segmentation and matching pipeline
- ✓ Nozzle reconstruction in 3D

## Immediate goals

- ❑ full nozzle reconstruction with 1000 fps capture with error of +/- 1% (0.5mm) for simple conical shape
- ❑ reproducible manufacturing setup with particles embedded in the nozzle
- ❑ Pulsed illumination setup to interleave deformation and flow capture
- ❑ Finalizing the MLOS based flow field reconstruction
- ❑ Tracking nozzle deformation using fluorescent markers
- ❑ Tracking flow field using polyamide tracer particles

# Next Steps: Deformation mapping and particle tracking



- Shake-The-Box (STB) is a novel time-resolved 3D Lagrangian particle tracking method for measuring densely seeded flows.
- STB overcomes the ill-posed reconstruction problem for 3D particle distributions at high seeding densities present for each single time-step (as known for tomo-PIV and classical PTV) by pre-solving the problem for each predicted time-step using an extrapolation strategy.
- Temporal filtering is applied to already known trajectories from previous time-steps and extrapolated to the current time-step.
- This central step is followed by a ‘shake’-process, which corrects the involved prediction error by an accurate image-matching scheme (a method that is also applied within the Iterative Particle Reconstruction technique).



# Squid-Inspired Nozzle for Underwater Propulsion

**Daehyun Choi<sup>1</sup>, Halley J. Wallace<sup>1</sup>, Paras Singh<sup>1</sup>, Gourav Samal<sup>1</sup>, William F. Gilly<sup>2</sup>, Chandan Bose<sup>3</sup>, and Saad M. Bhamla<sup>1</sup>**

<sup>1</sup>School of Chemical and Biomolecular Engineering, Georgia Institute of Technology

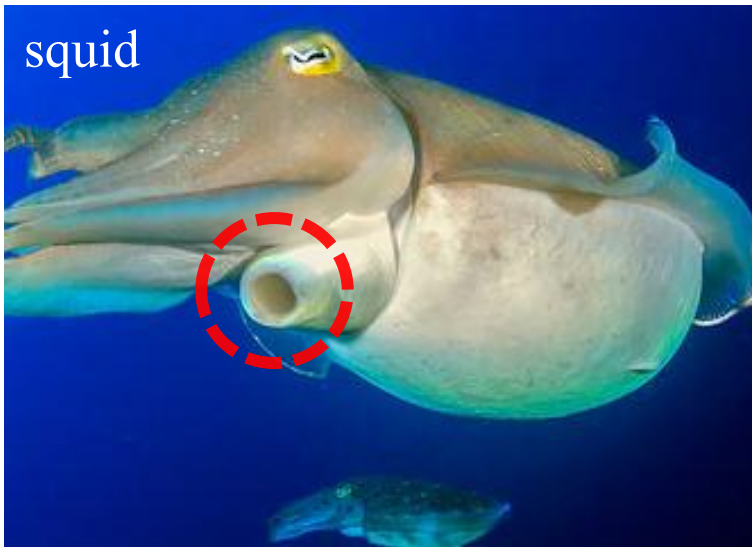
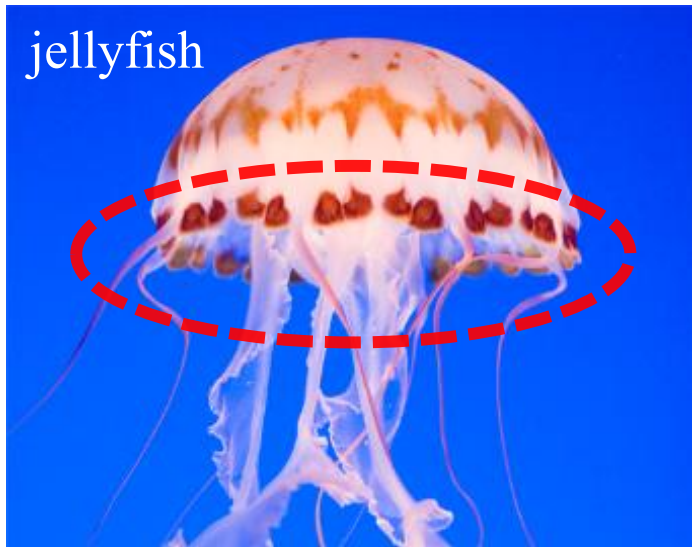
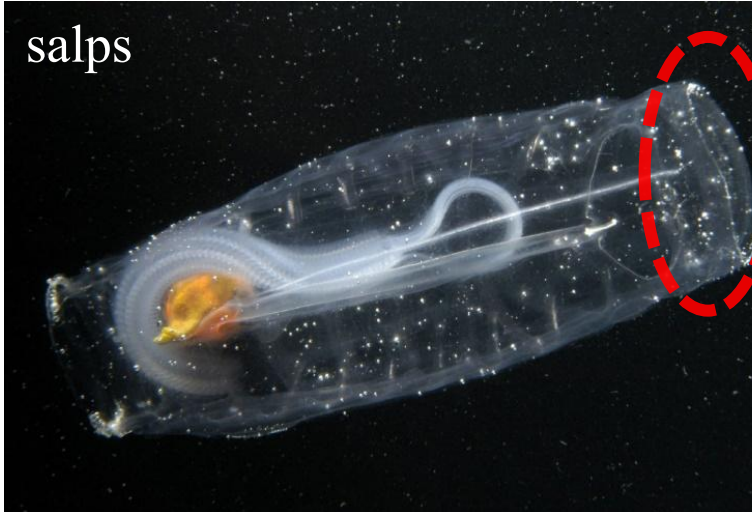
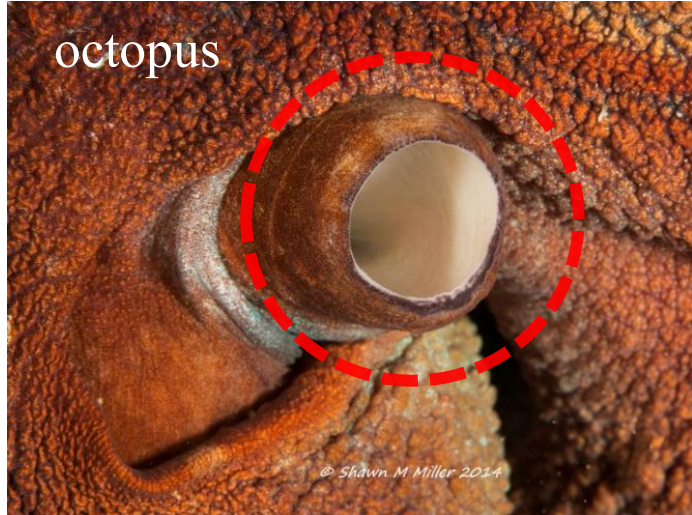
<sup>2</sup>Hopkins Marine Station, Stanford University

<sup>3</sup>Aerospace Engineering, University of Birmingham

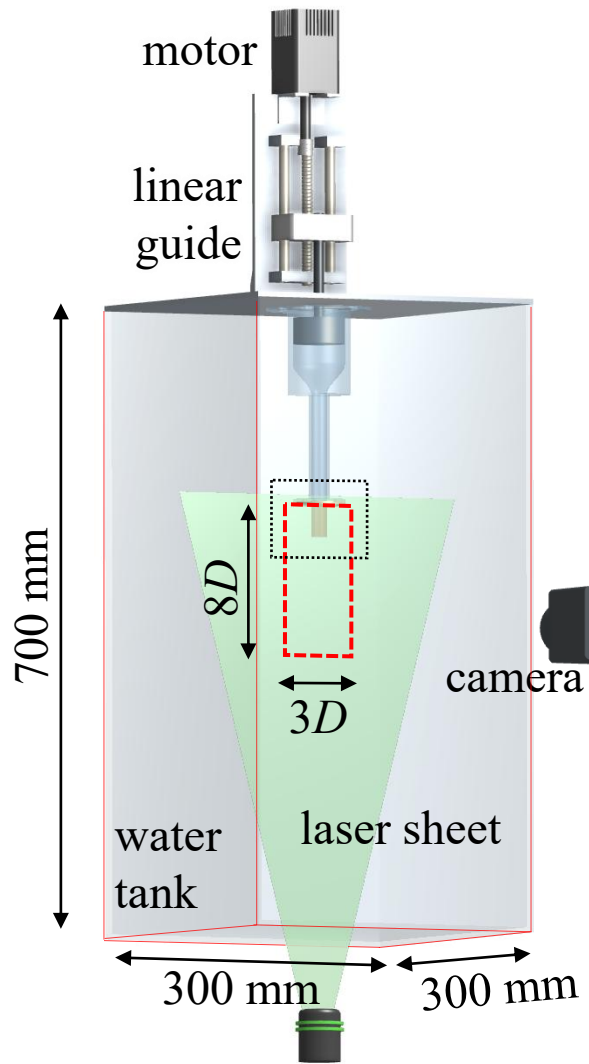
14<sup>th</sup> July 2025, Fluid and Biodynamics Seminar,  
Max-Planck-Institut für Dynamik und Selbstorganisation (MPIDS)



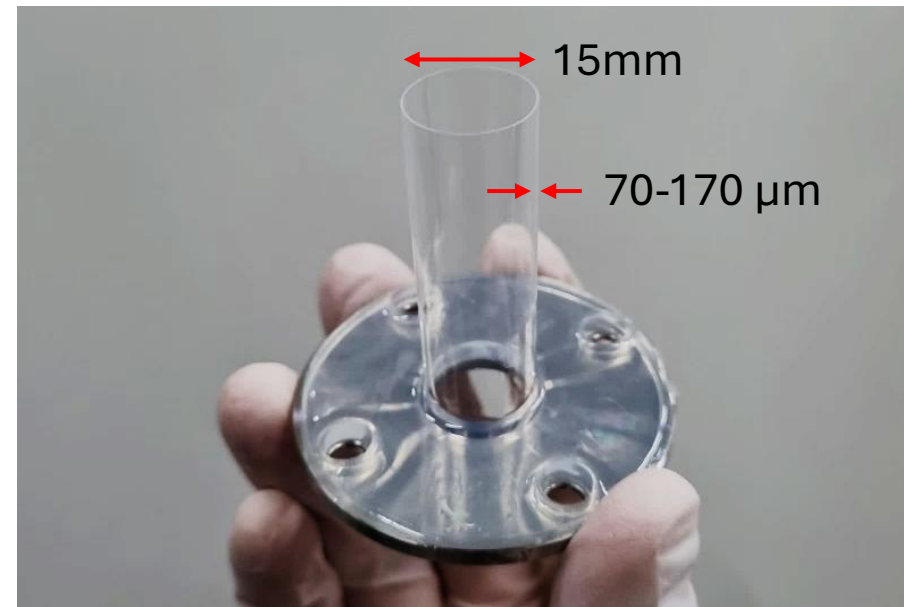
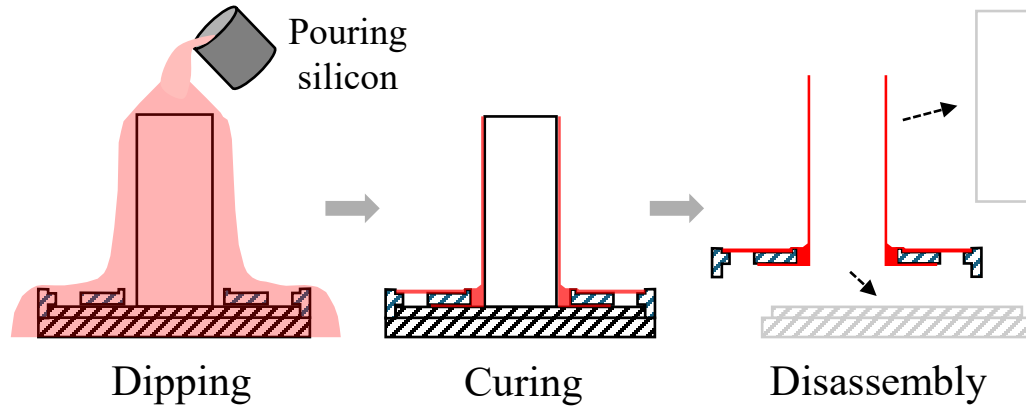
# Flexible nozzle in nature



# Flexible cylindrical nozzle

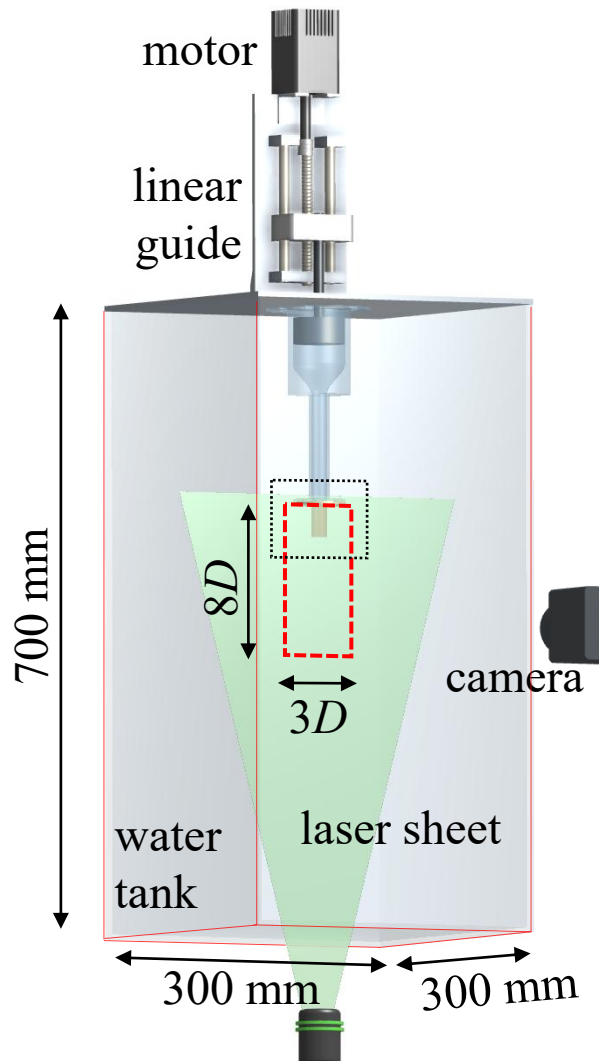


Jet generator

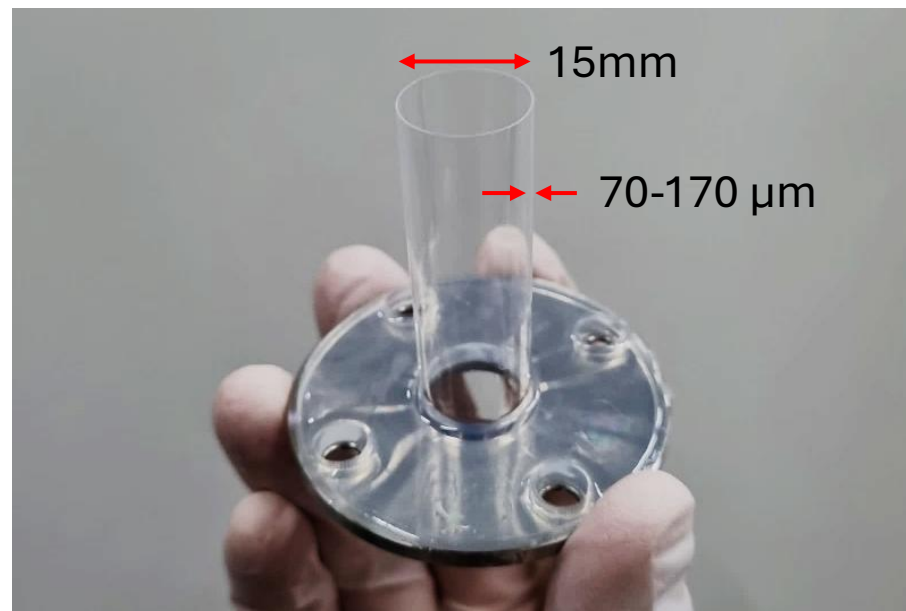
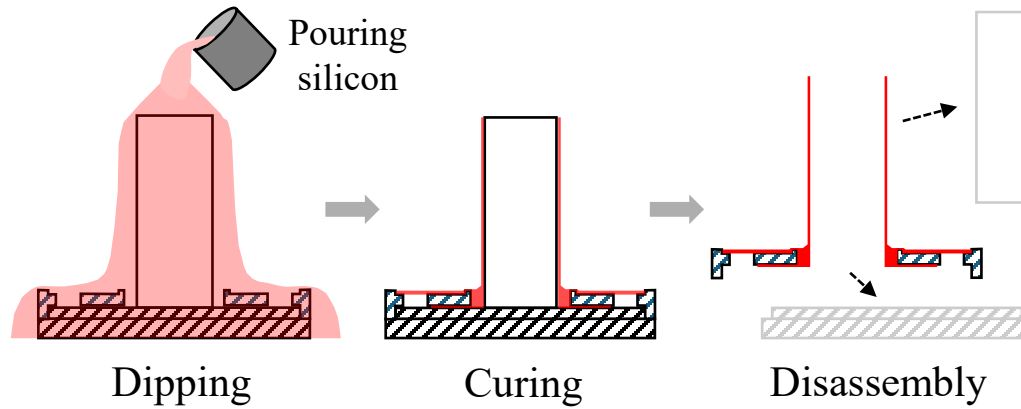


Nozzle fabrication

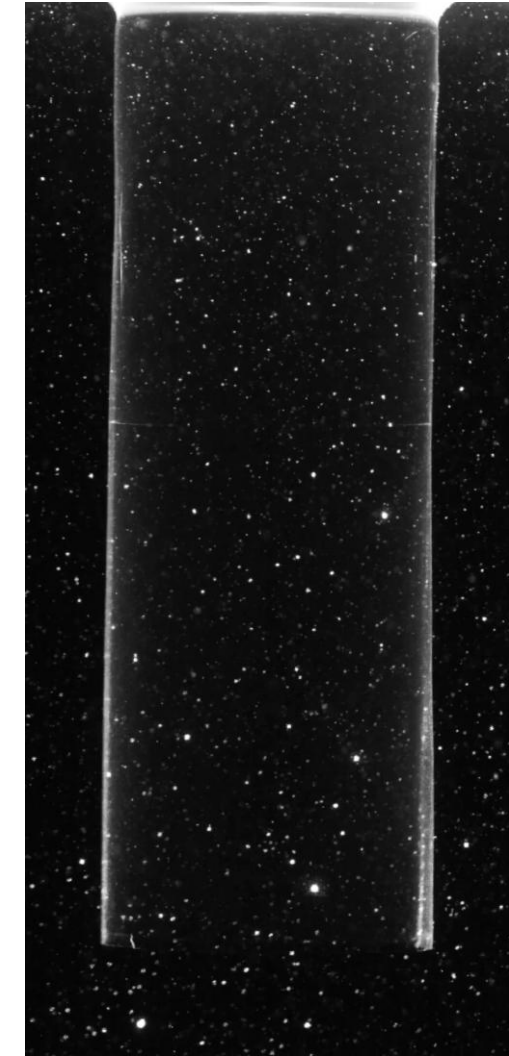
# Flexible cylindrical nozzle



Jet generator



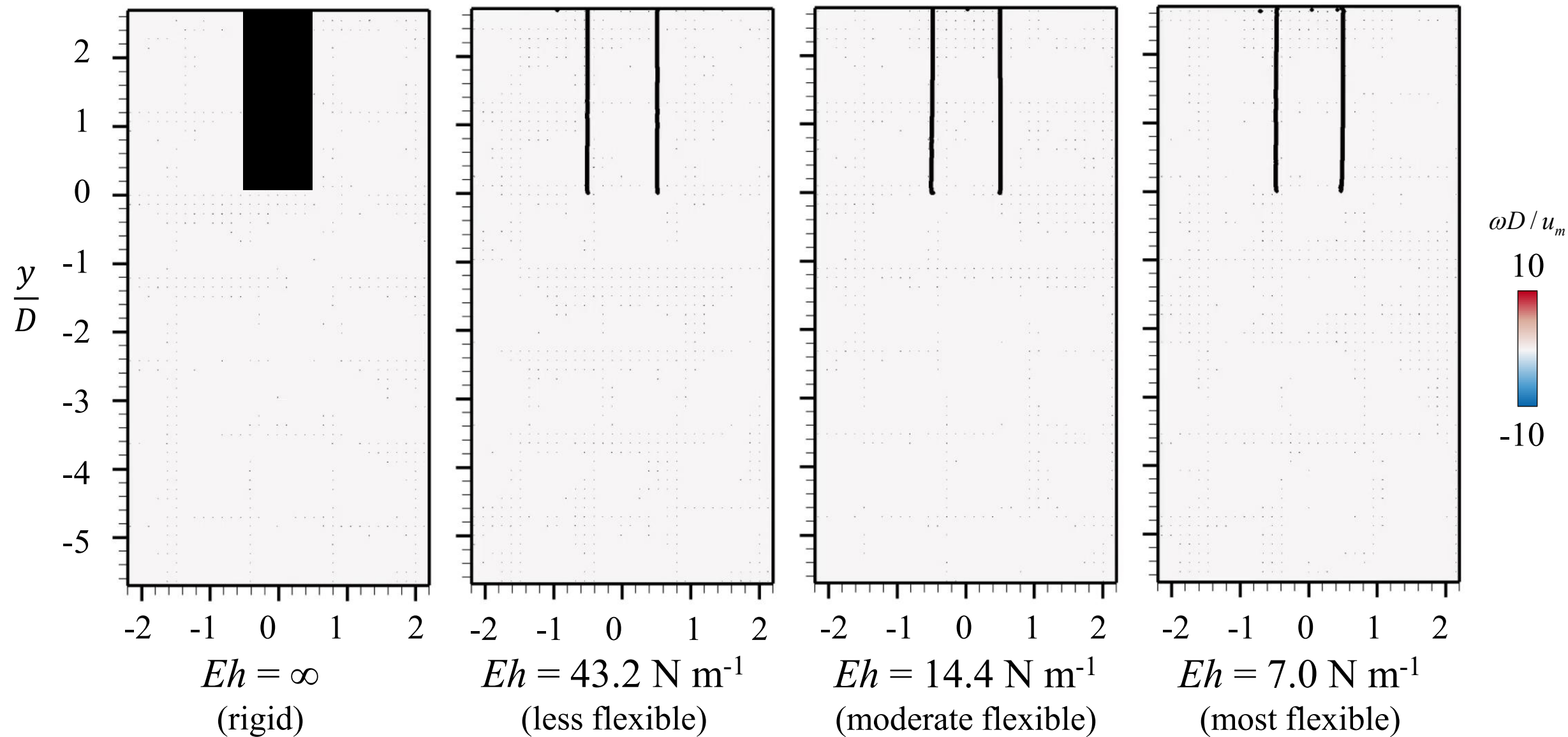
Nozzle fabrication



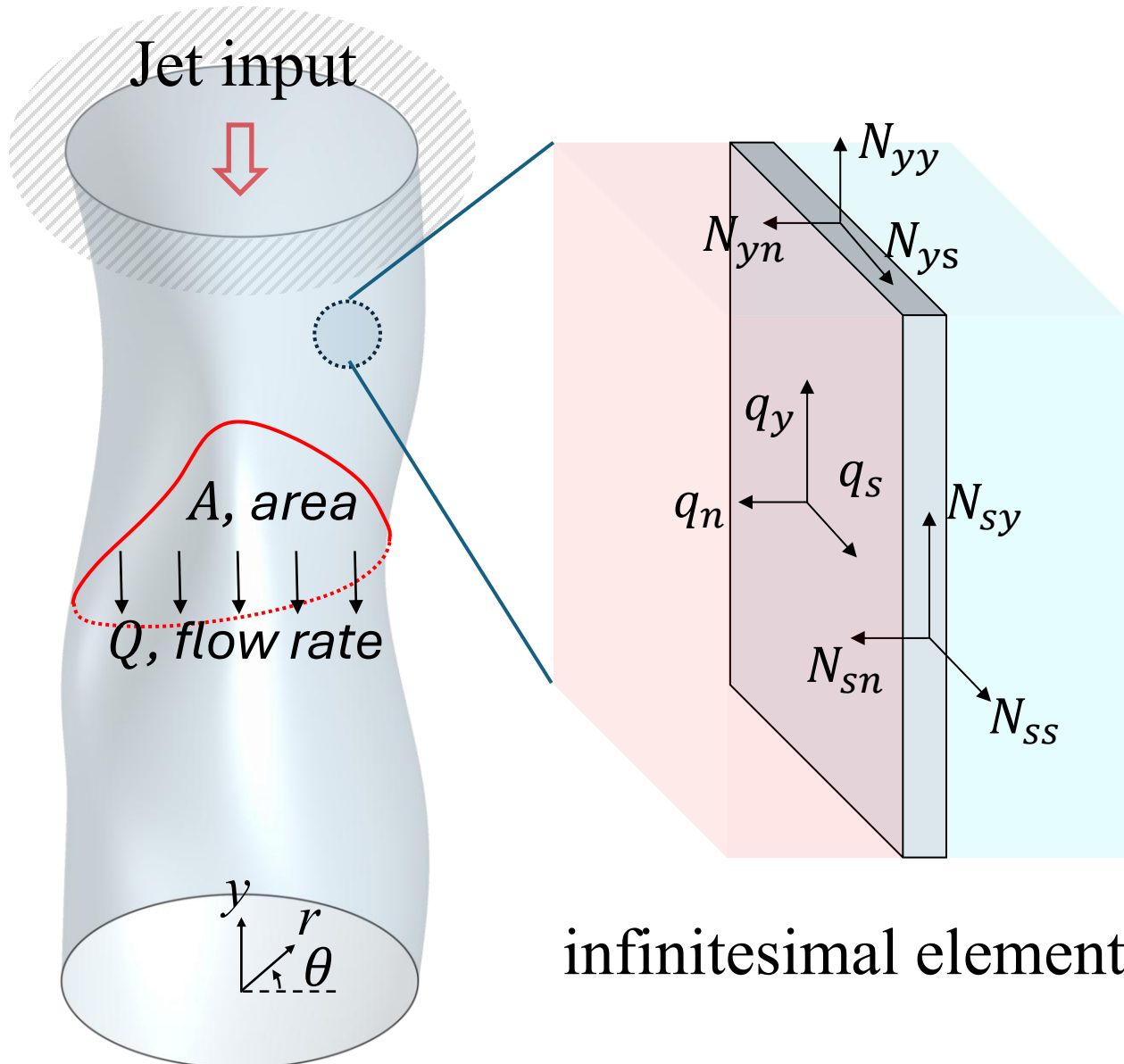
Flow measurement

Choi & Park 2022 *J. Fluid Mech.*

# Flexible nozzle amplifies starting jet ( $Re = 3,000$ )



# FSI Governing equation



Flow-rate equation (Shapiro 1977)

$$\frac{\partial A}{\partial t} + \frac{\partial Q}{\partial y} = 0$$

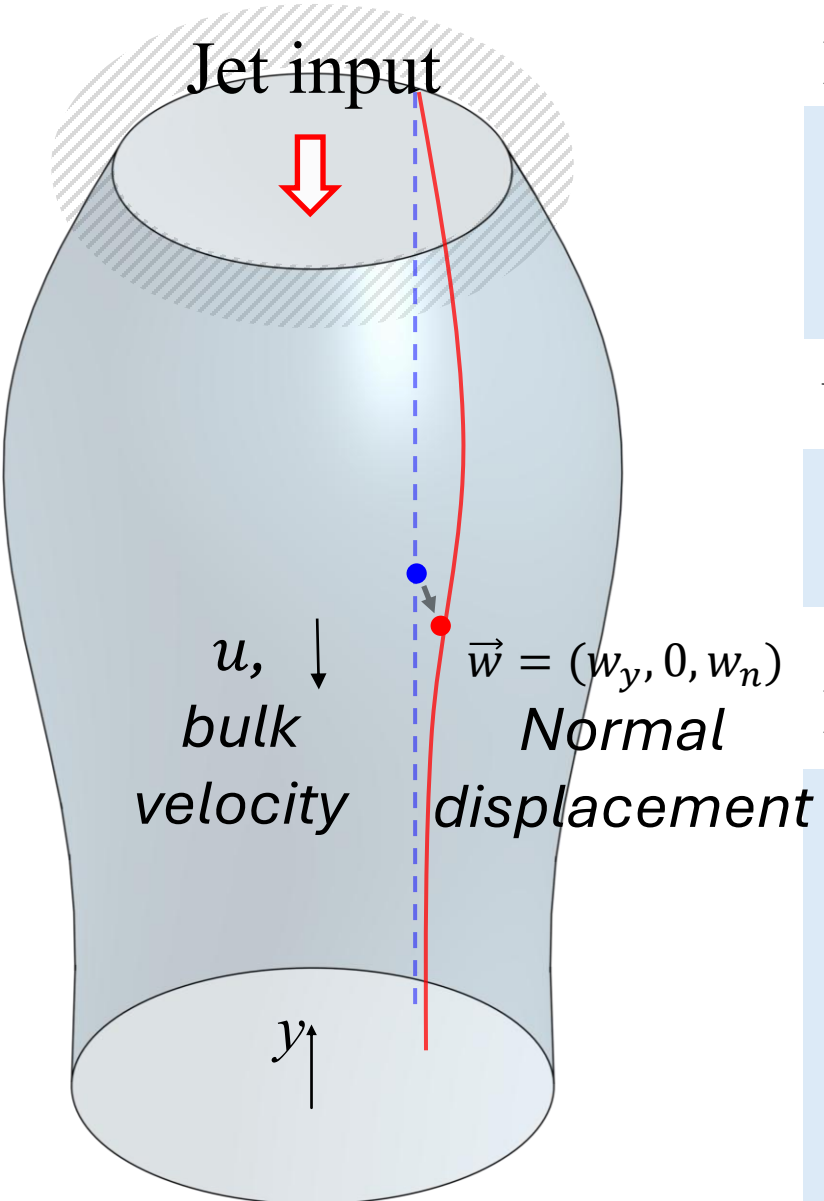
$$\frac{\partial Q}{\partial t} + \frac{\partial(uQ)}{\partial y} + \frac{A}{\rho_f} \frac{\partial \mathbf{q}_n}{\partial y} = -C_R u$$

Force balance of nozzle wall (Flügge 1968)

$$\frac{\partial N_{yy}}{\partial y} + \frac{\partial N_{ys}}{\partial s} + q_y = \rho_n h \frac{\partial^2 w_y}{\partial t^2}$$

$$\frac{\partial N_{yn}}{\partial y} + \frac{\partial N_{sn}}{\partial s} - \frac{N_{ss}}{R} - \mathbf{q}_n = \rho_n h \frac{\partial^2 w_n}{\partial t^2}$$

# Dimensionless equation



Displacement-velocity relations

$$u \cdot w' + (1 + w)u'/2 = -\Pi_0^{-1}\dot{w}$$

$$u \cdot u' + \Pi_1 w_n = -\Pi_0^{-1}\dot{u}$$

Nozzle wave equation

$$\ddot{w}_n - \hat{c}^2 w_n'' = 0$$

Dimensionless parameters

$$\Pi_0 = \frac{u T_{acc}}{L}$$

Effective jet duration

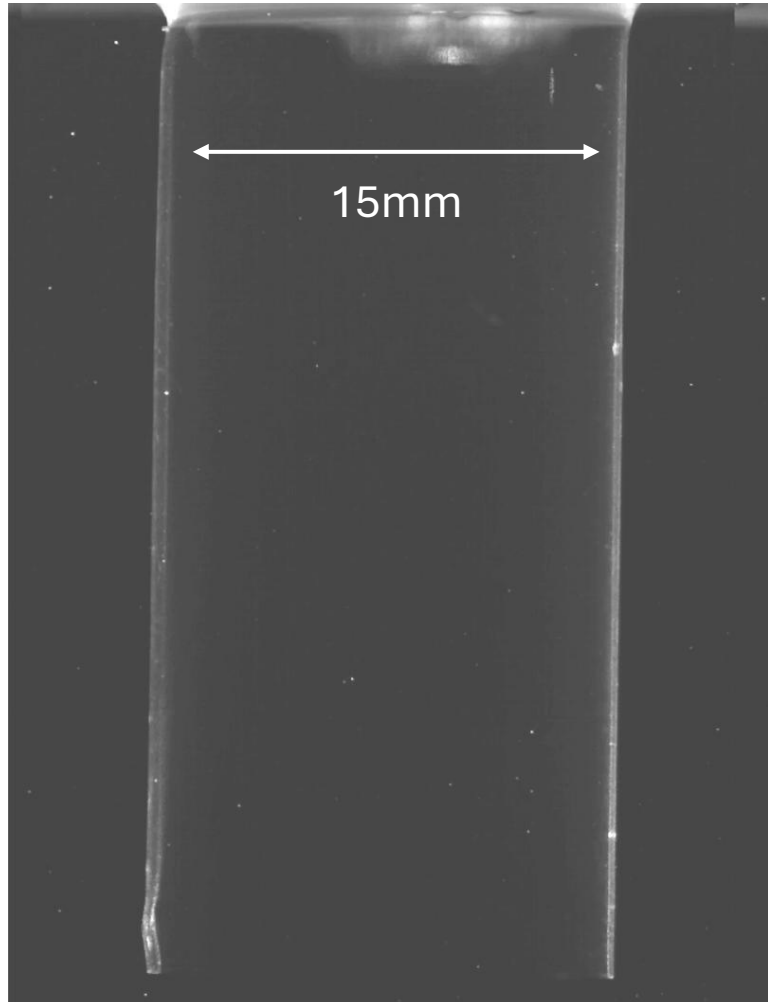
$$\Pi_1 = \frac{Eh}{\rho_f u D}$$

Effective nozzle stiffness

$$\hat{c} = \sqrt{\frac{Eh T_{acc}^2}{\rho_f D L}}$$

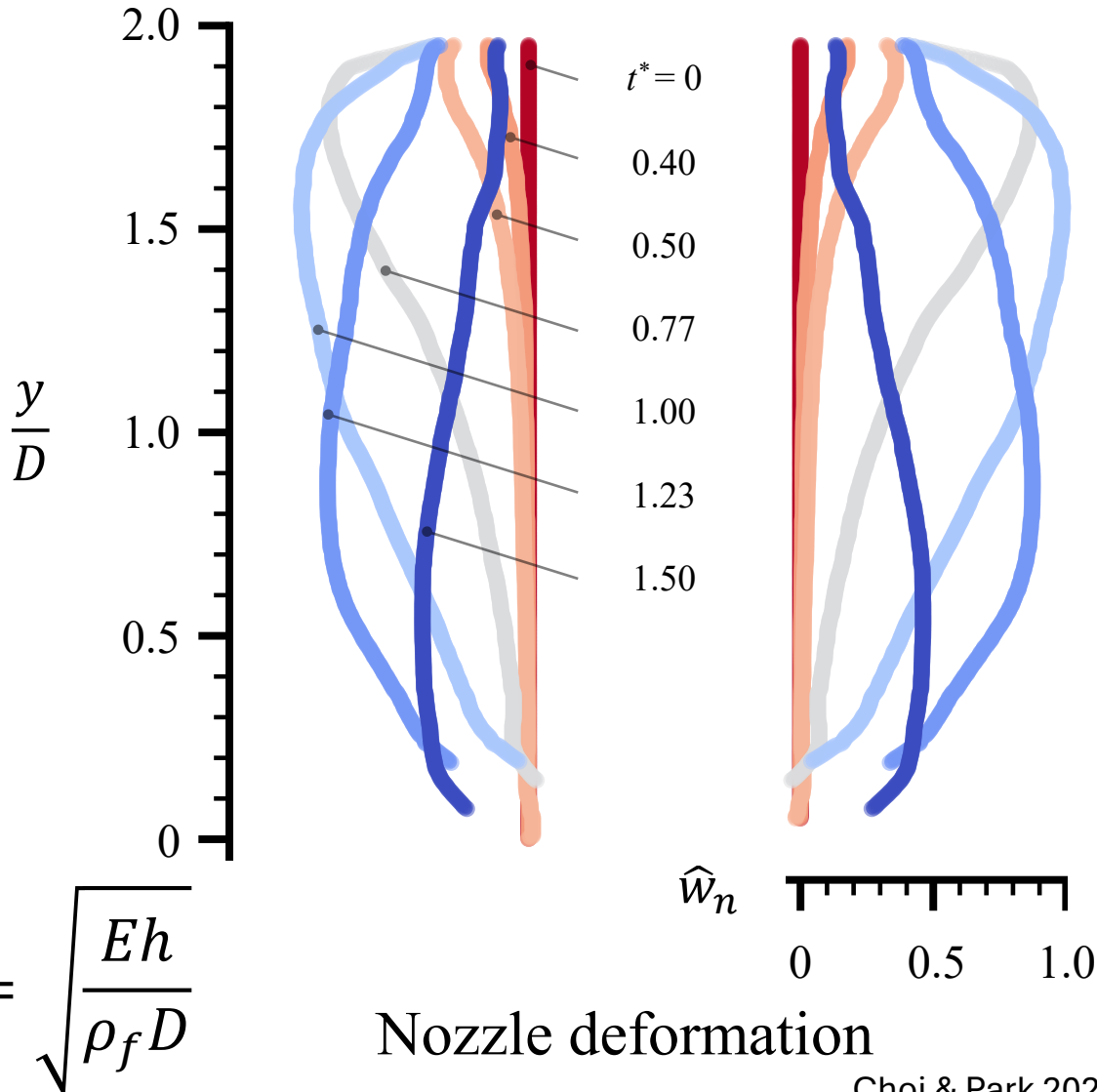
dimensionless wave speed

# Nozzle deformation is governed by the wave propagation

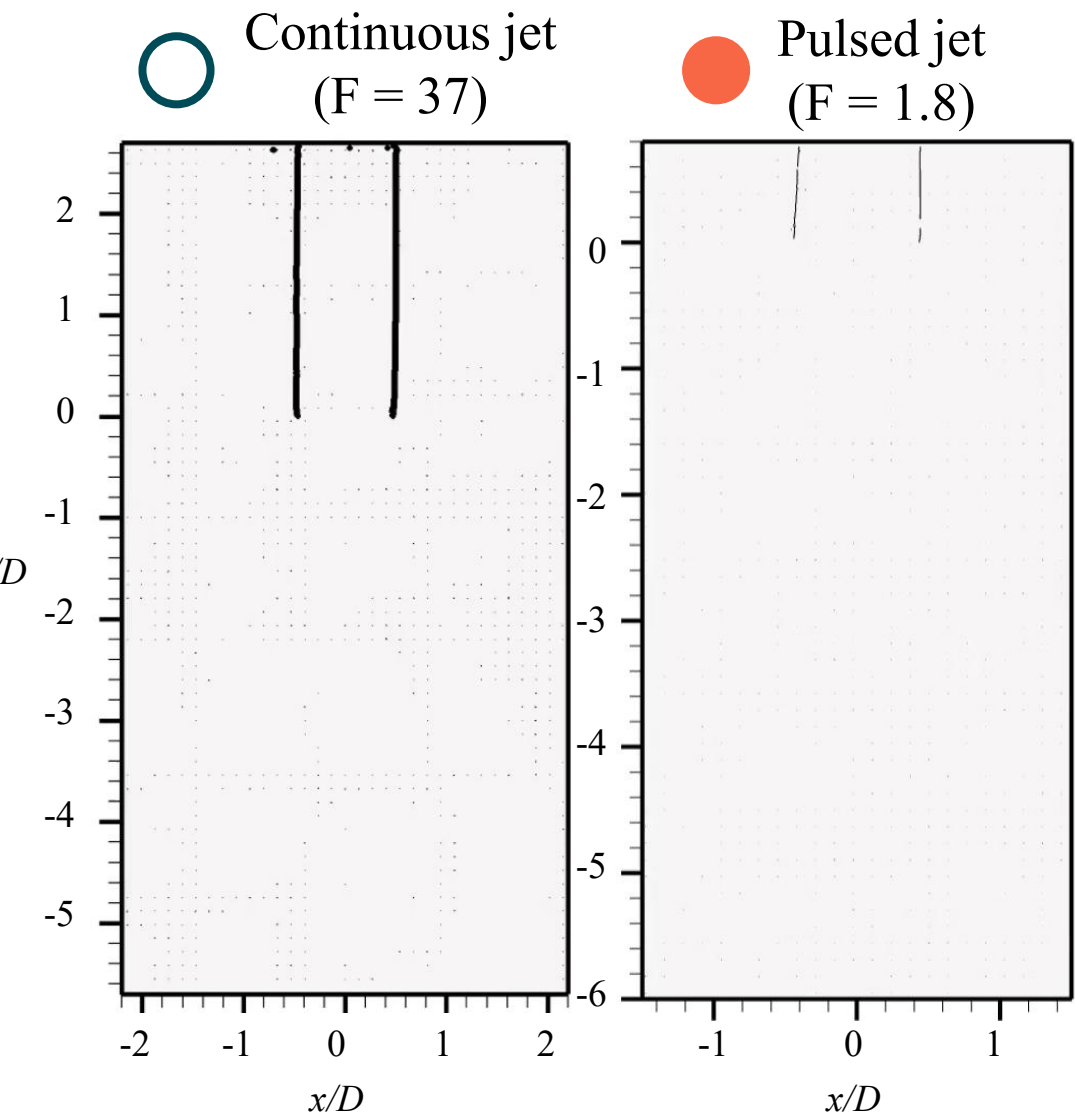
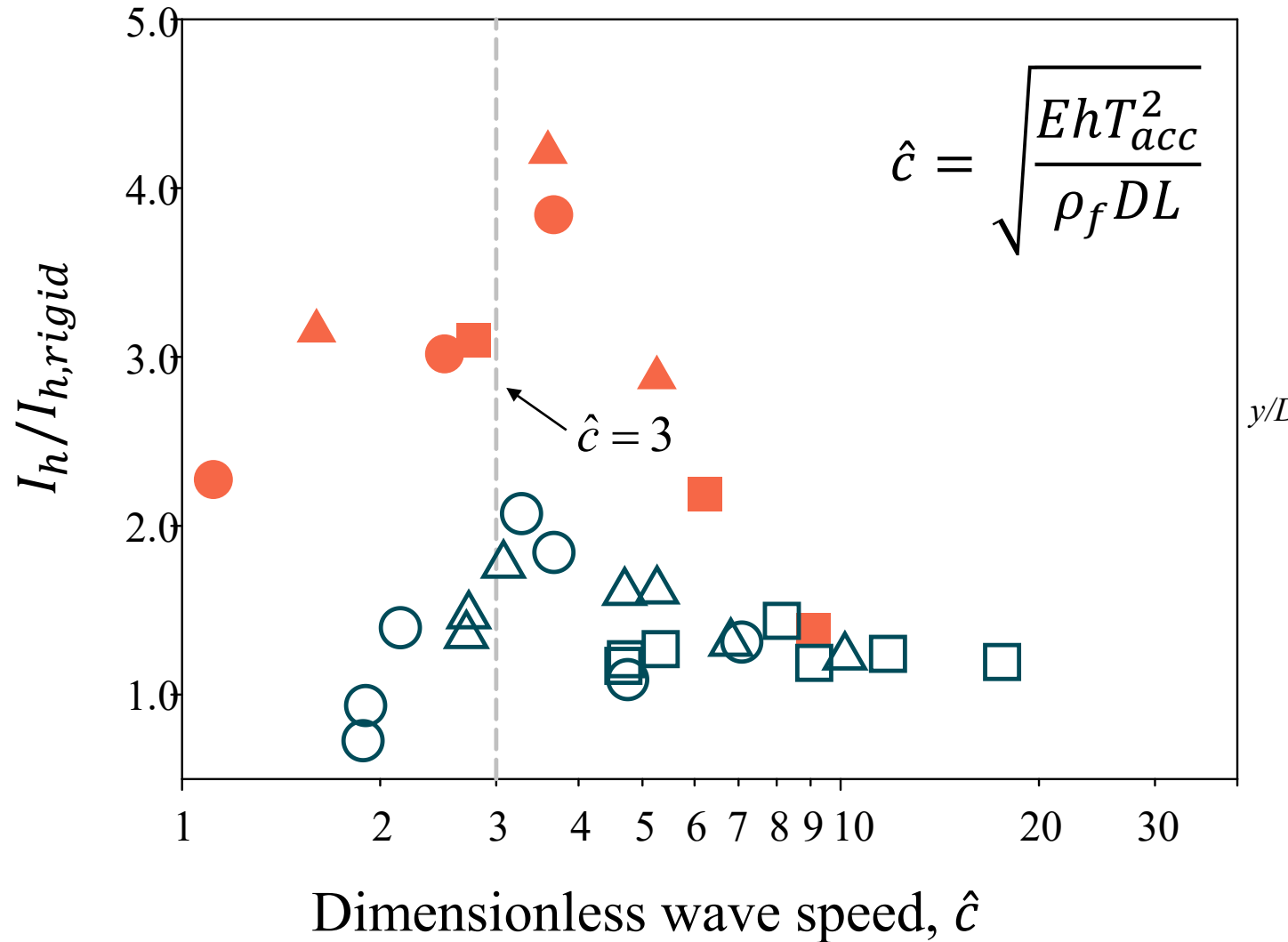


Raw video

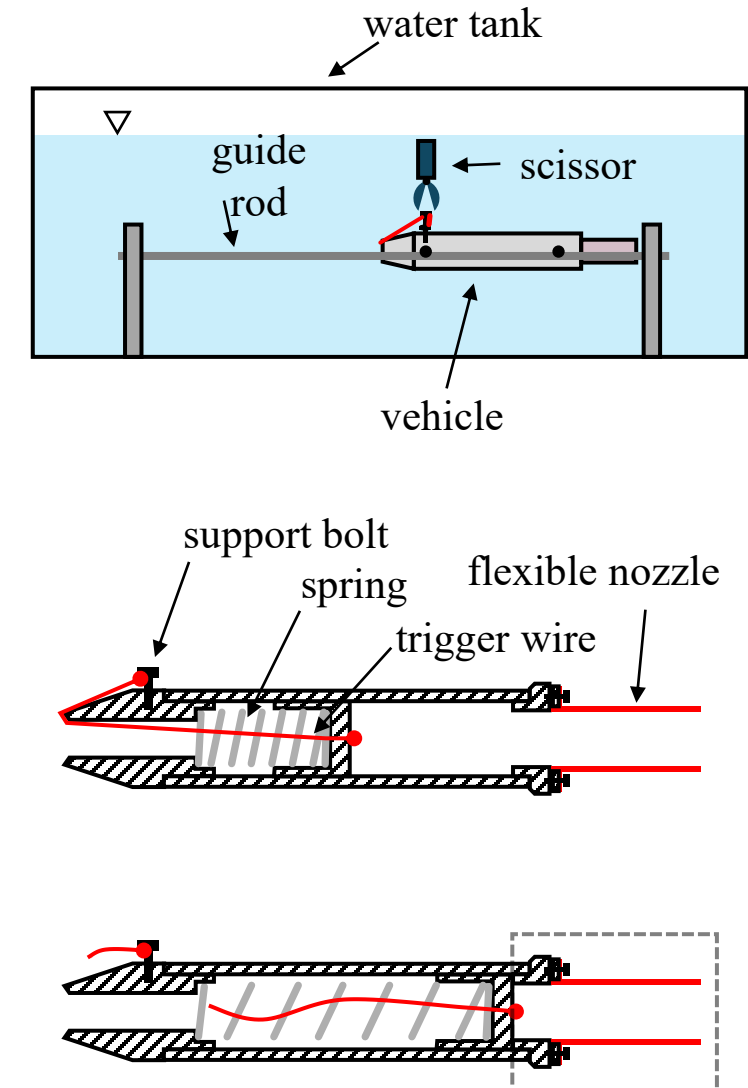
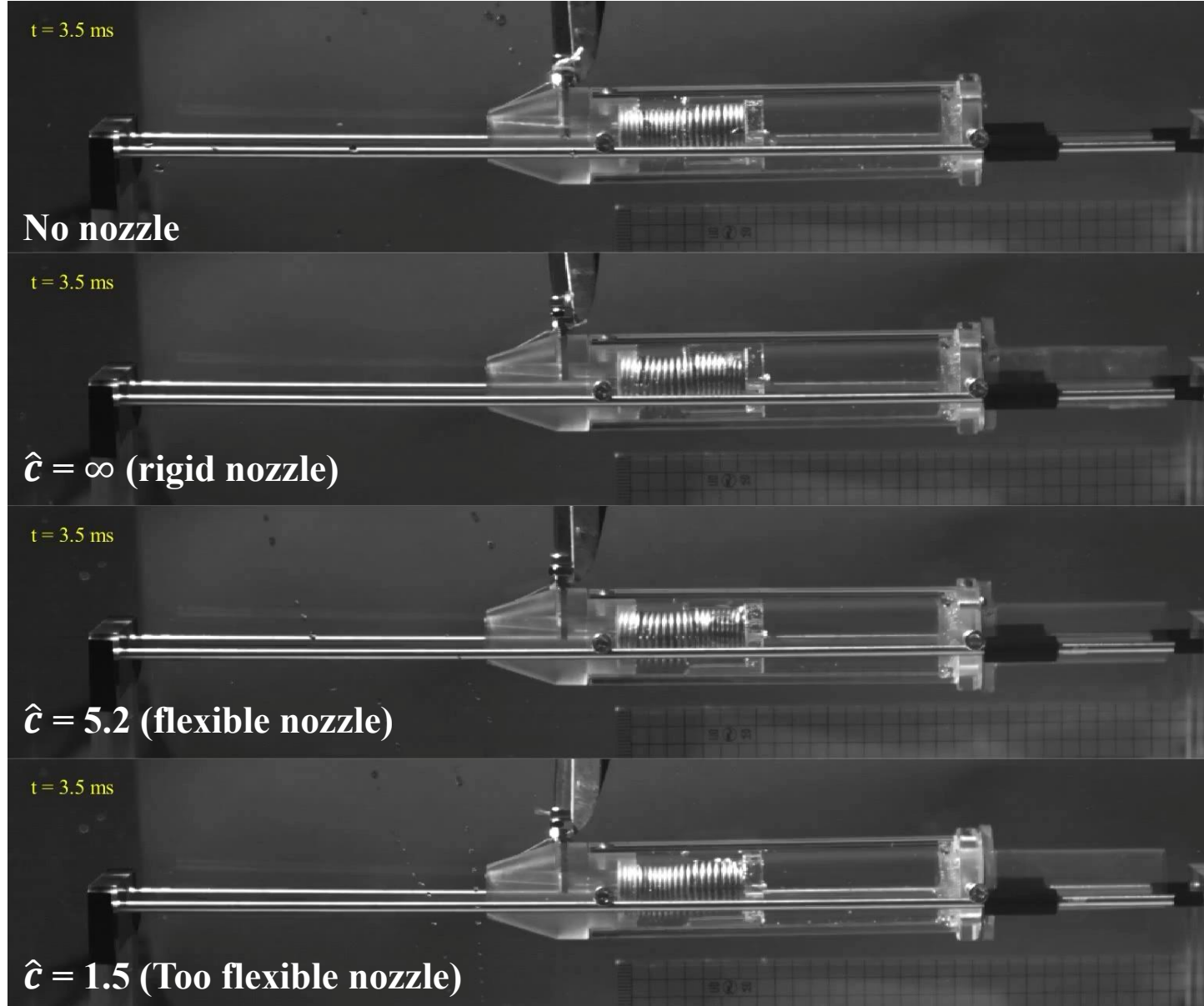
$$c_{wave} = \sqrt{\frac{Eh}{\rho_f D}}$$



# Jet impulse maximizes at $\hat{c} = 3$

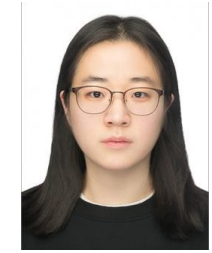


# Flexible nozzle accelerates underwater vehicle

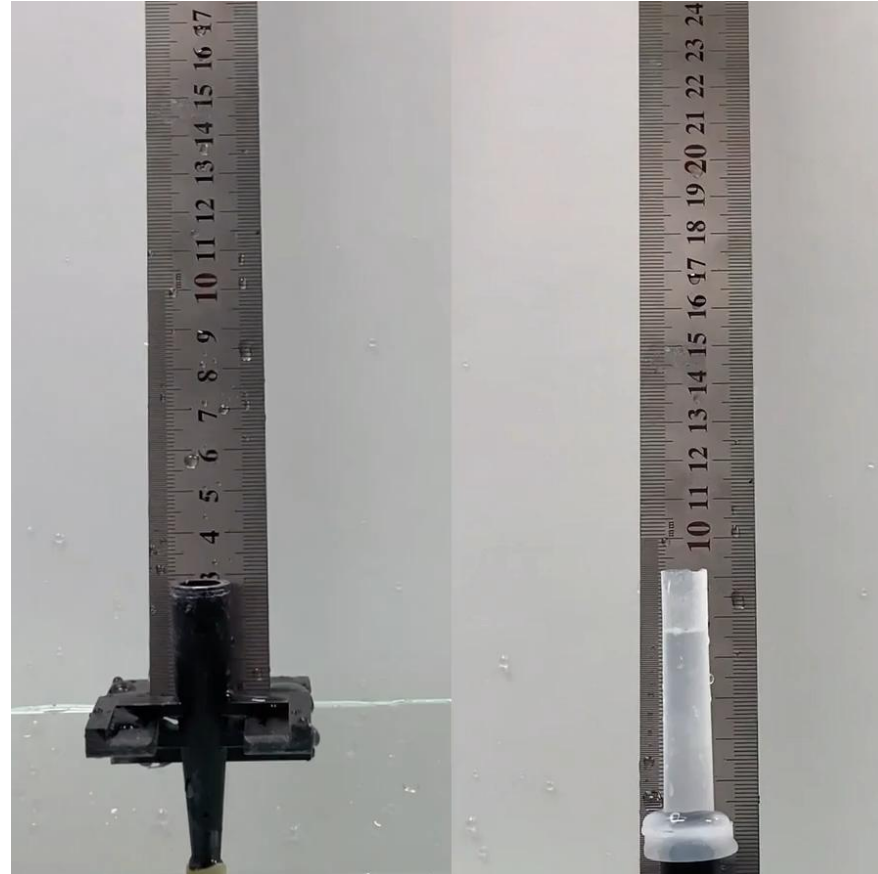


# Aerial jet reaches greater height

$$\hat{c} = \sqrt{\frac{EhT_{acc}^2}{2\rho_f DL^2}}$$



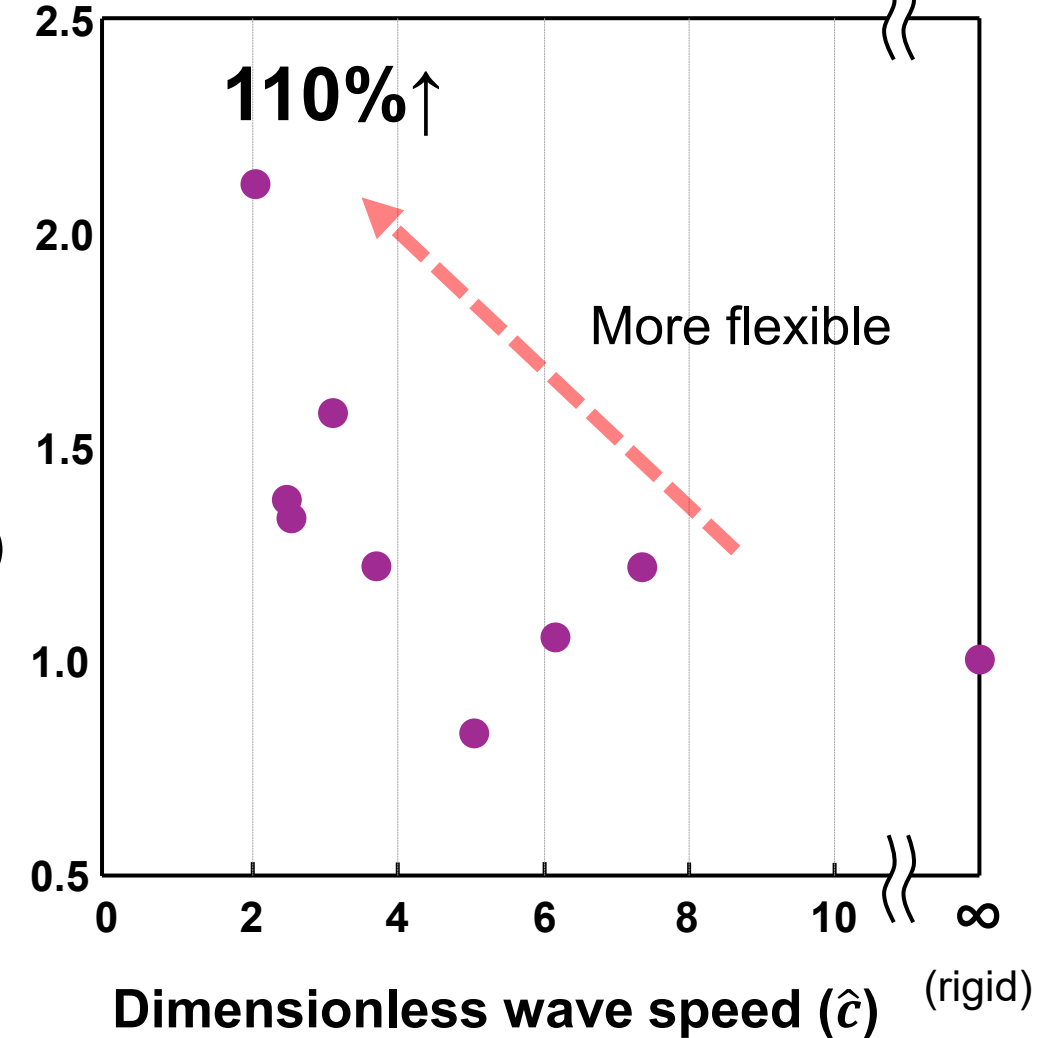
Minho Kim Jieun Park



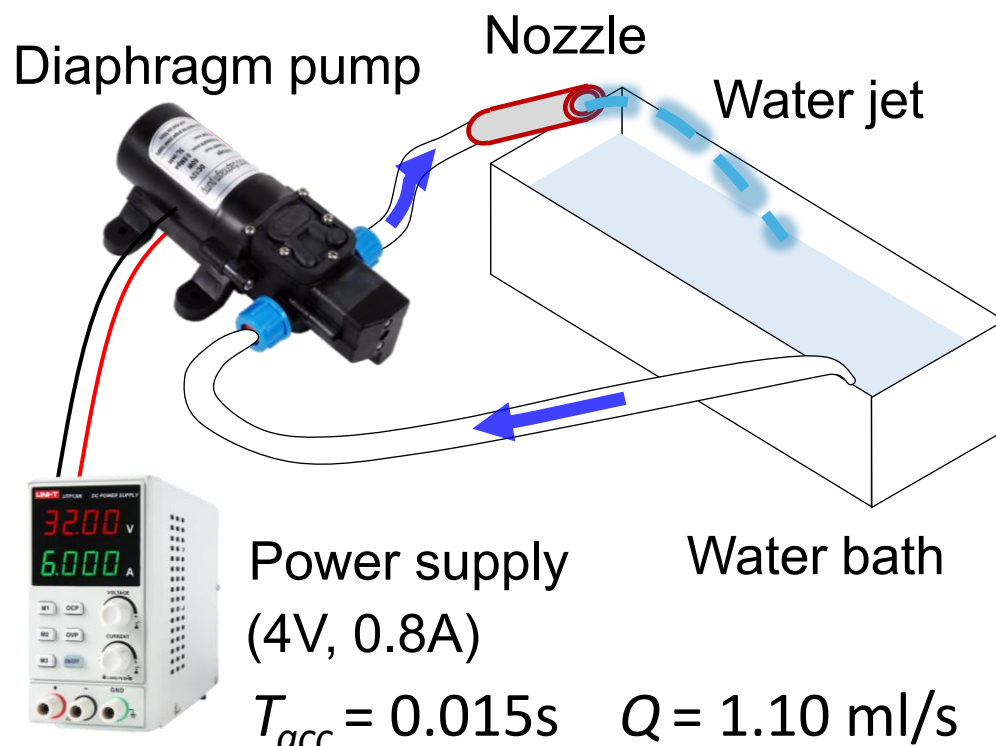
Rigid nozzle  
 $\hat{c} = \infty$

Flexible nozzle  
 $\hat{c} = 2.0$

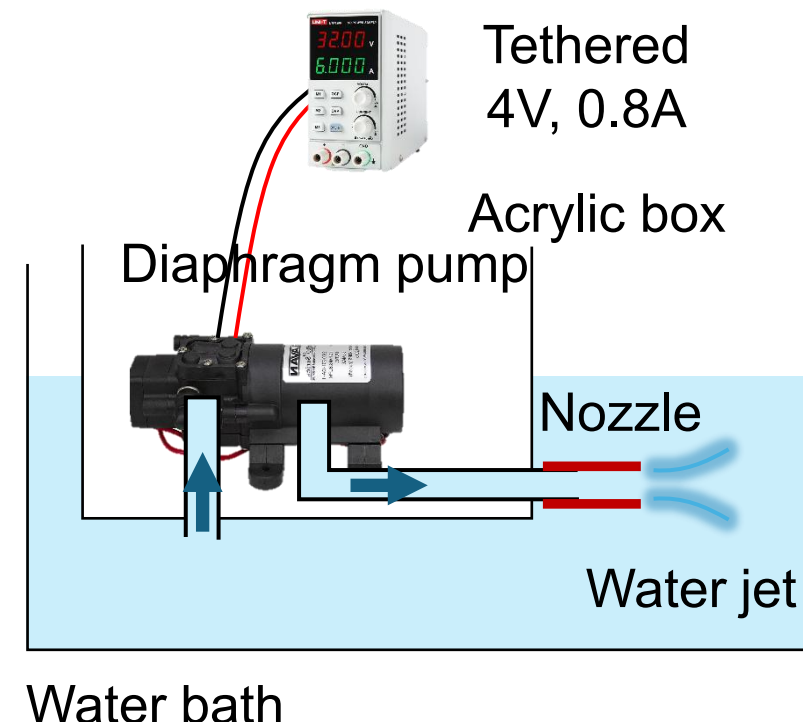
Relative maximum height  
( $h_{flexible}/h_{rigid}$ )



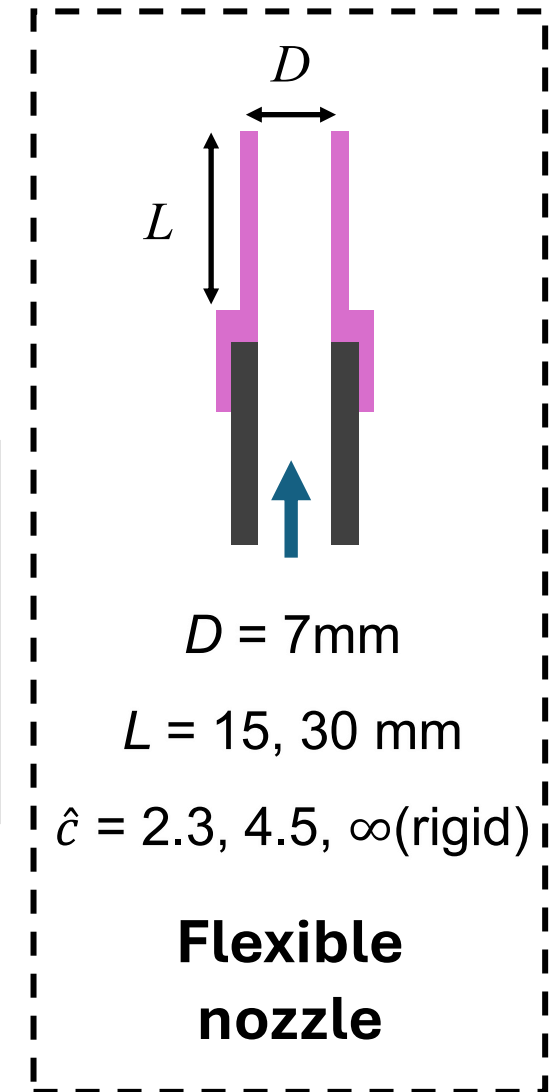
# Demonstration



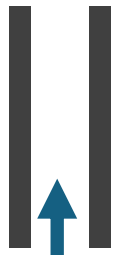
Aerial ejection



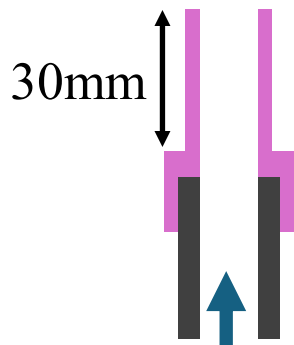
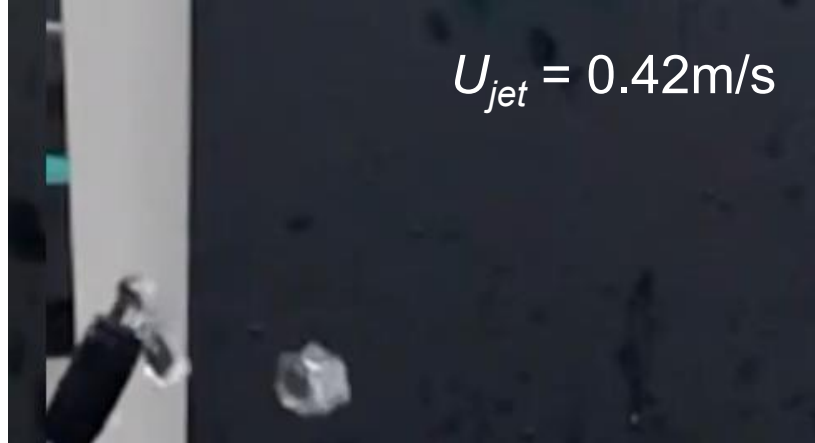
Pulsed-jet boat



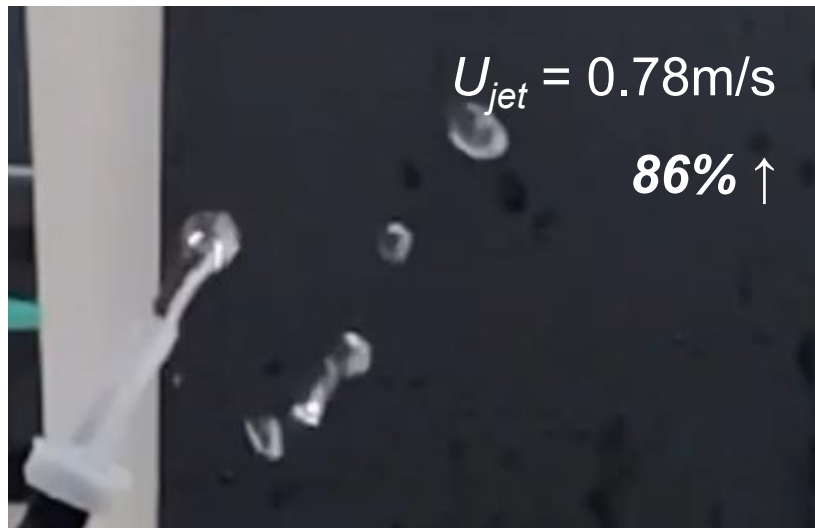
# Aerial jet



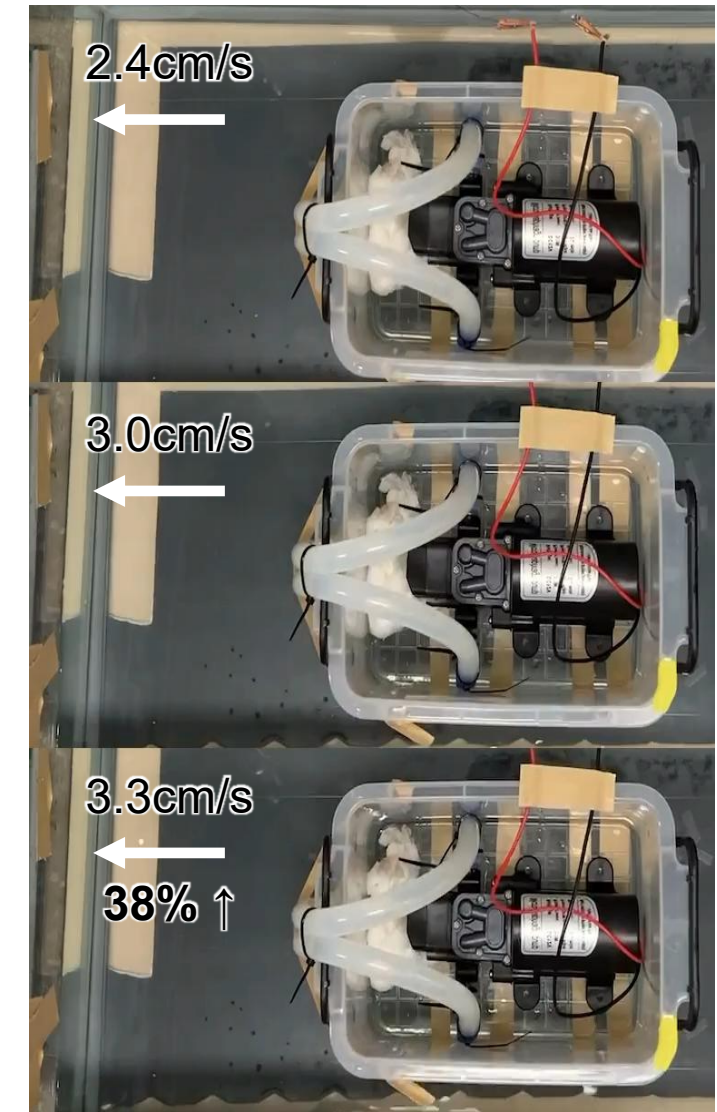
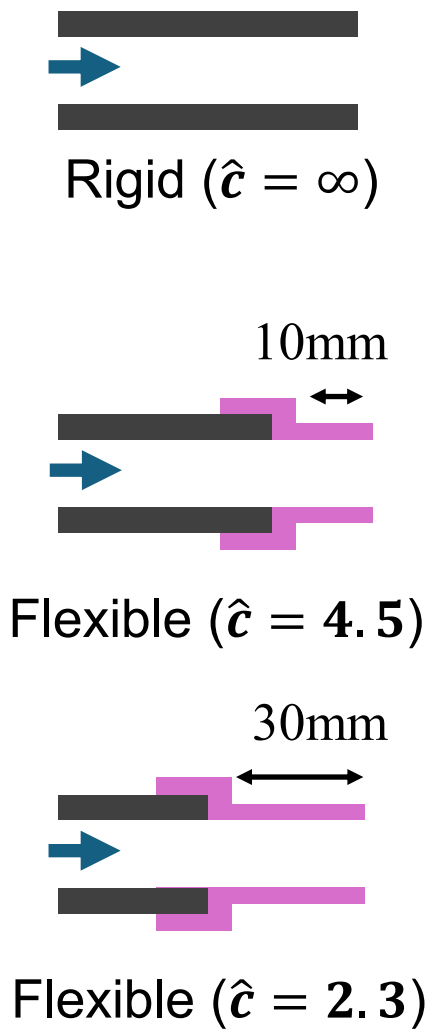
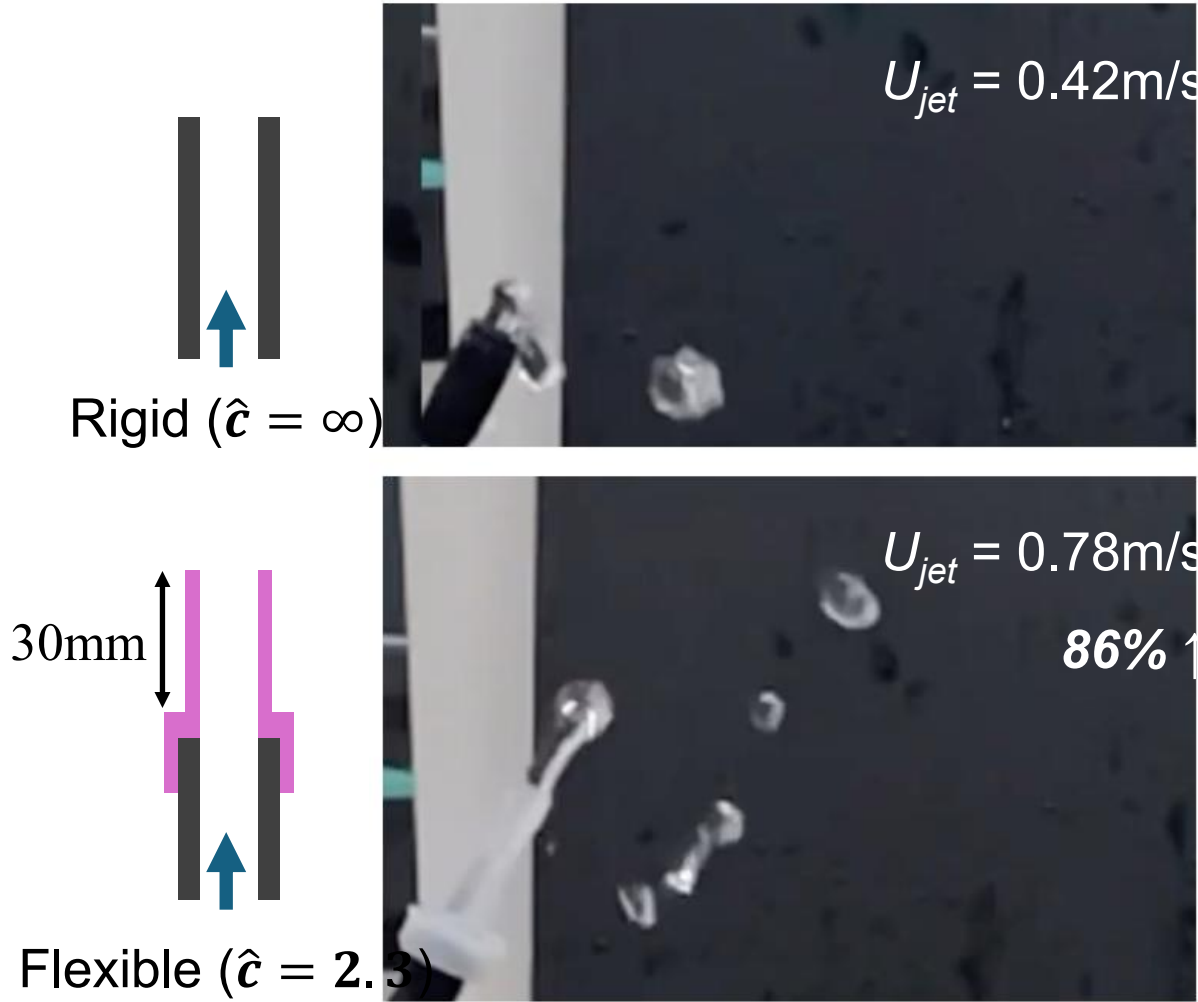
Rigid ( $\hat{c} = \infty$ )



Flexible ( $\hat{c} = 2.3$ )



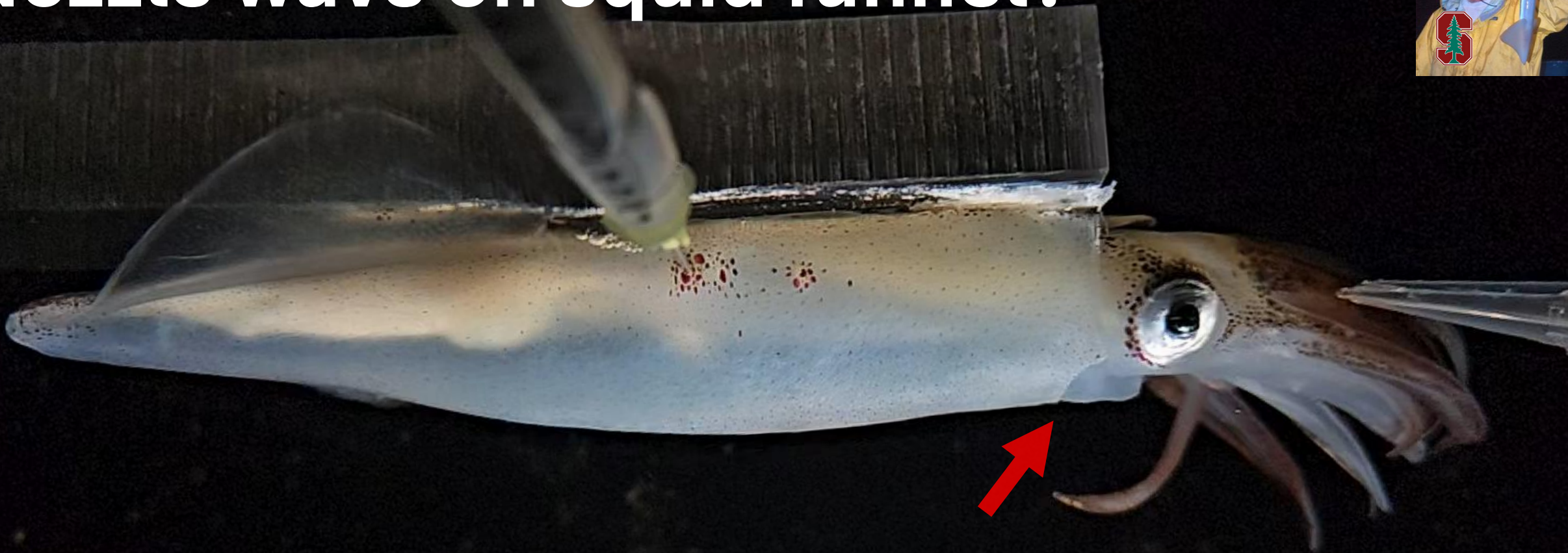
# Propulsion



Dr. William Gilly  
at Stanford Univ.



# Nozzle wave on squid funnel?



*Doryteuthis opalescens*  
(California market squid)

—  
10 mm

# Funnel actively moves during jetting

Mantle

Funnel

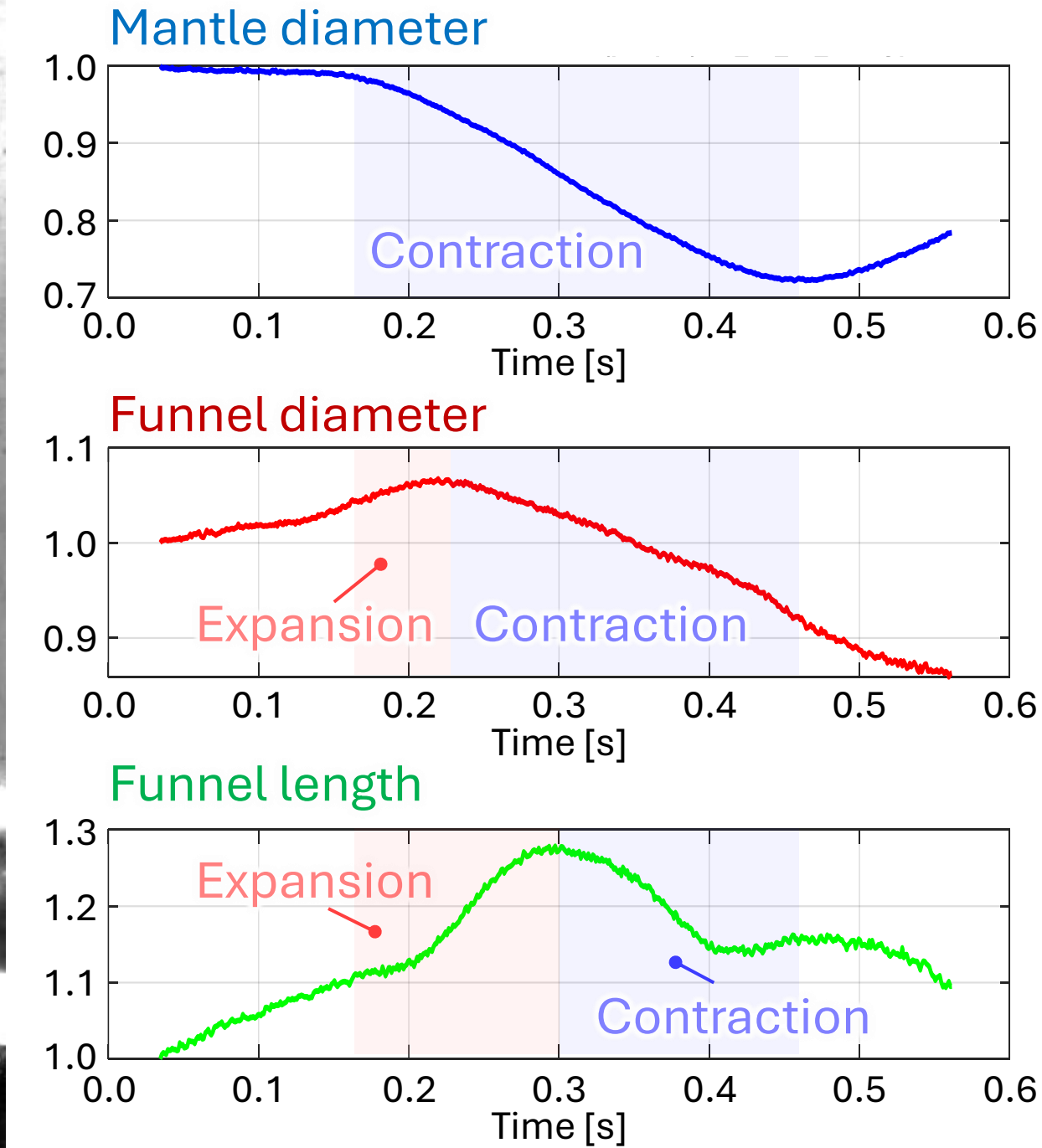
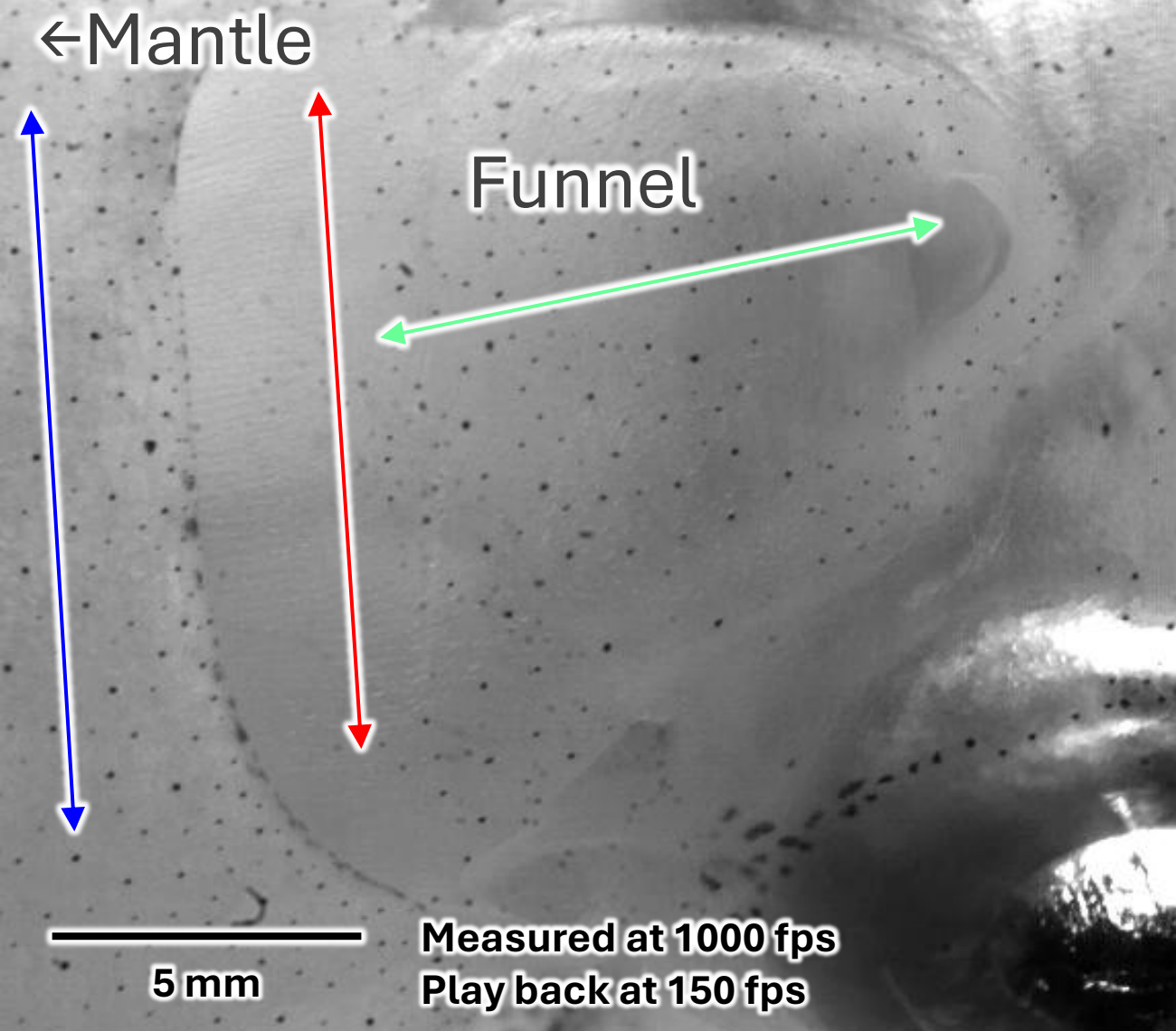
Arm →

Eye

5 mm

Measured at 1000 fps  
Playback at 150 fps

# Funnel deforms late



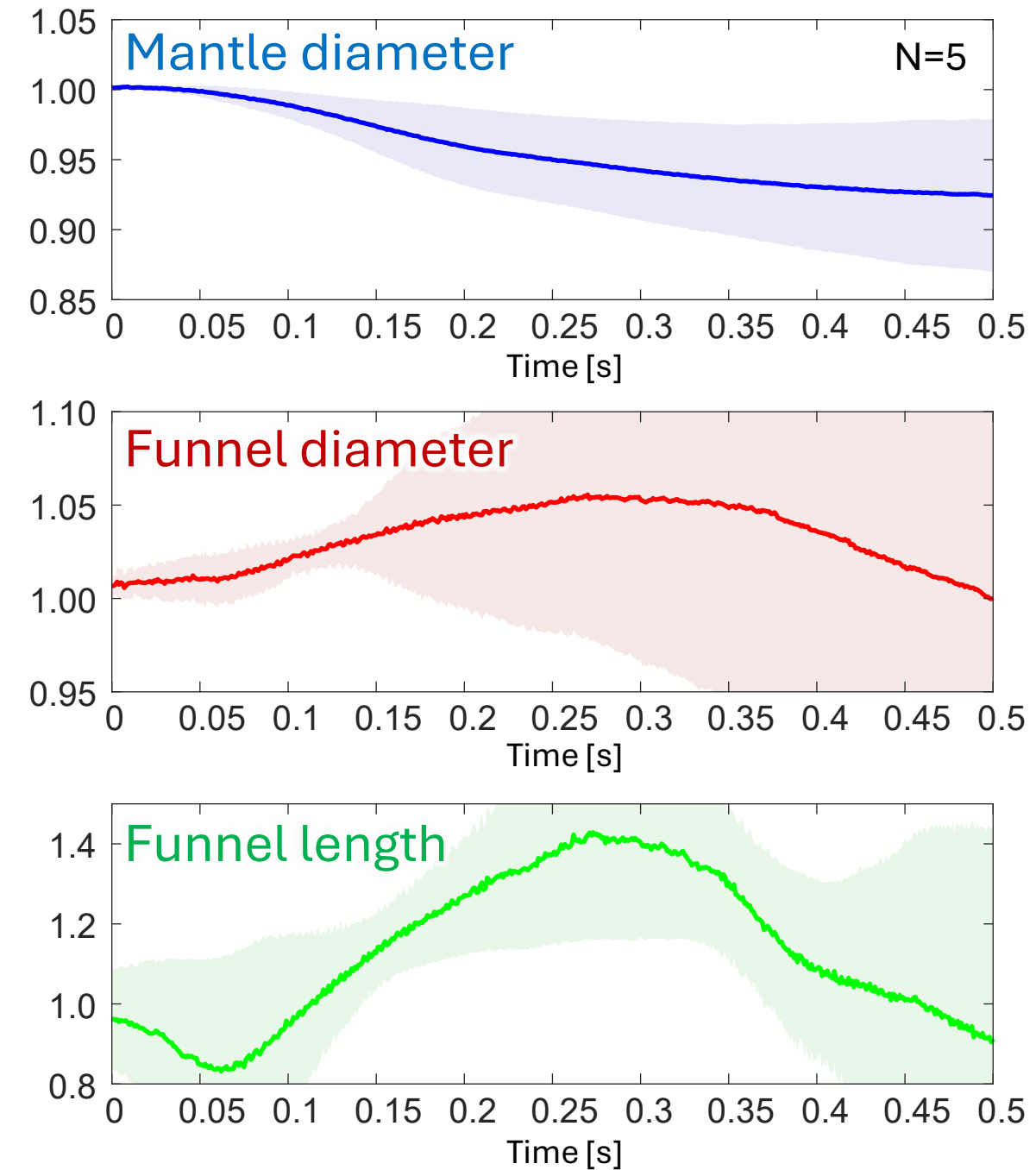
# Funnel deforms late

←Mantle

Funnel

5 mm

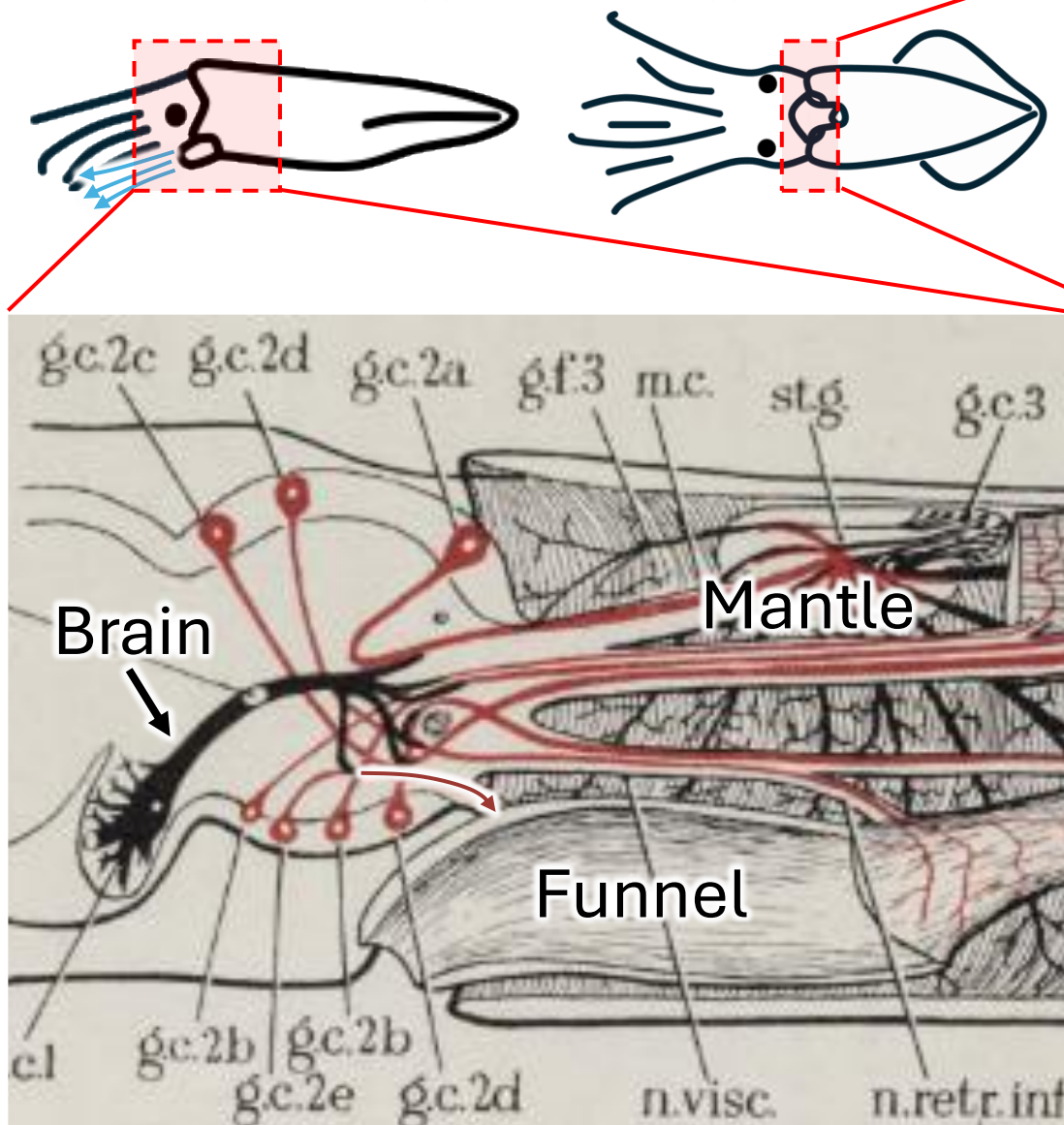
Measured at 1000 fps  
Playback at 150 fps



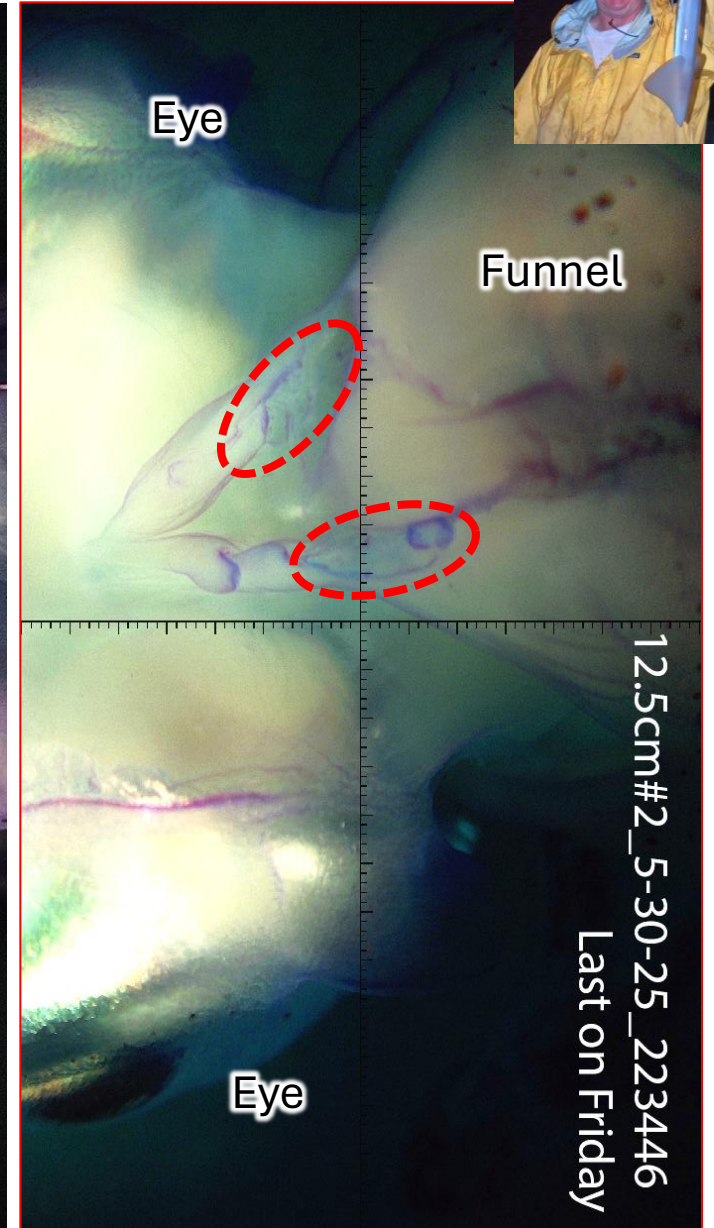
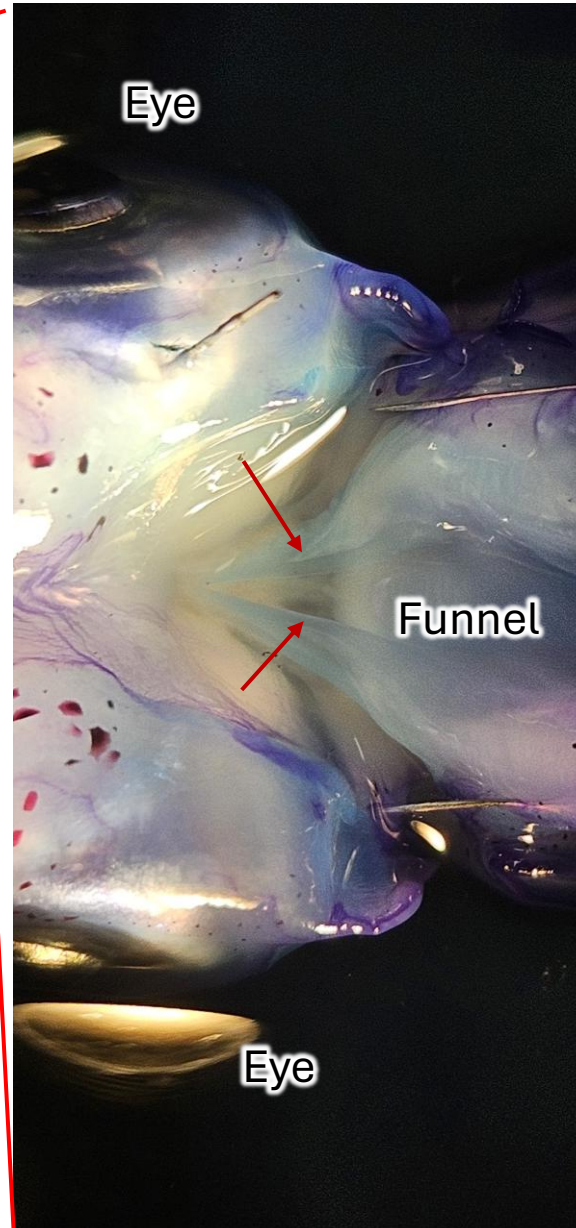
Dr. William Gilly  
at Stanford Univ.



# Funnel paralysis

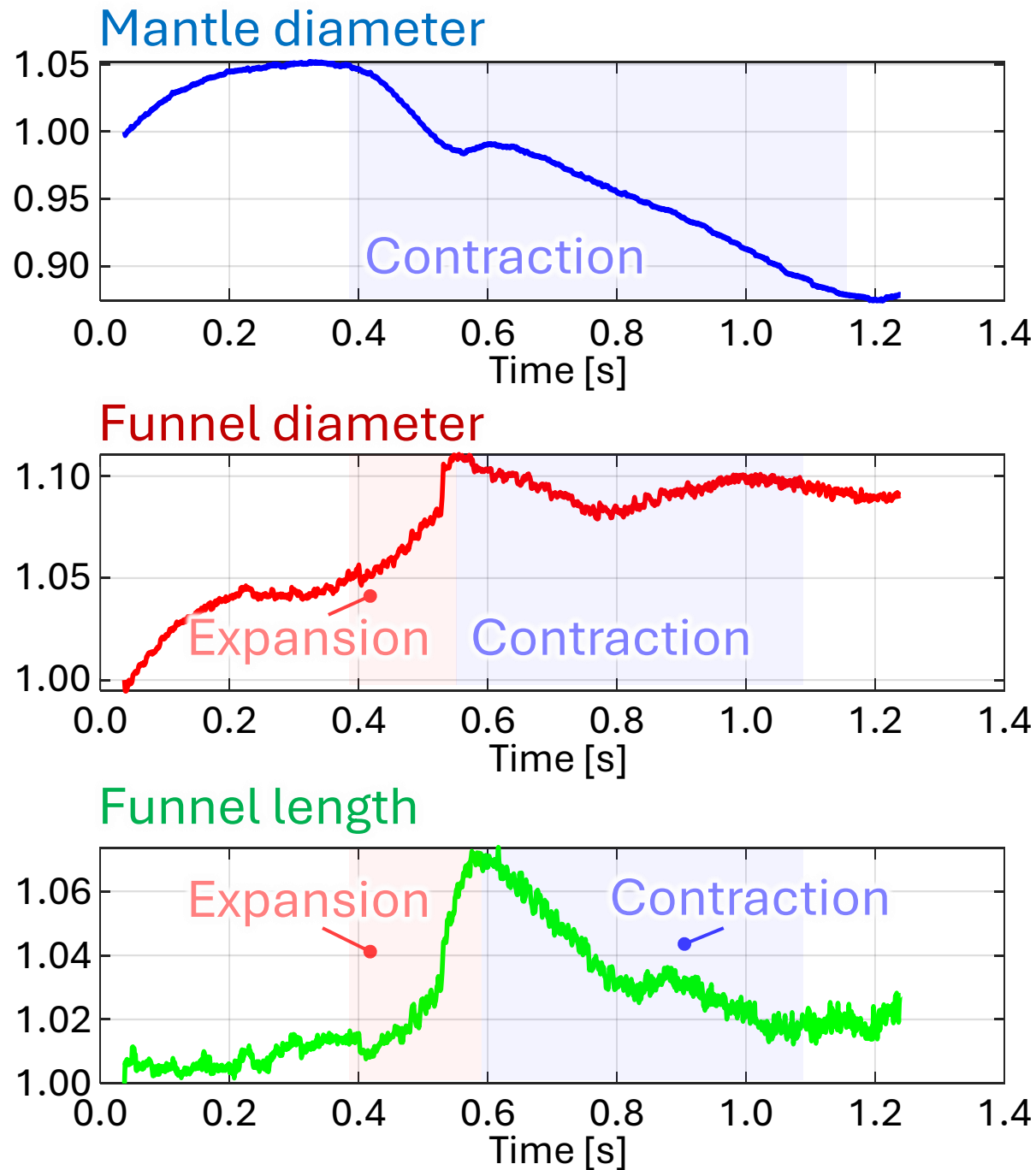
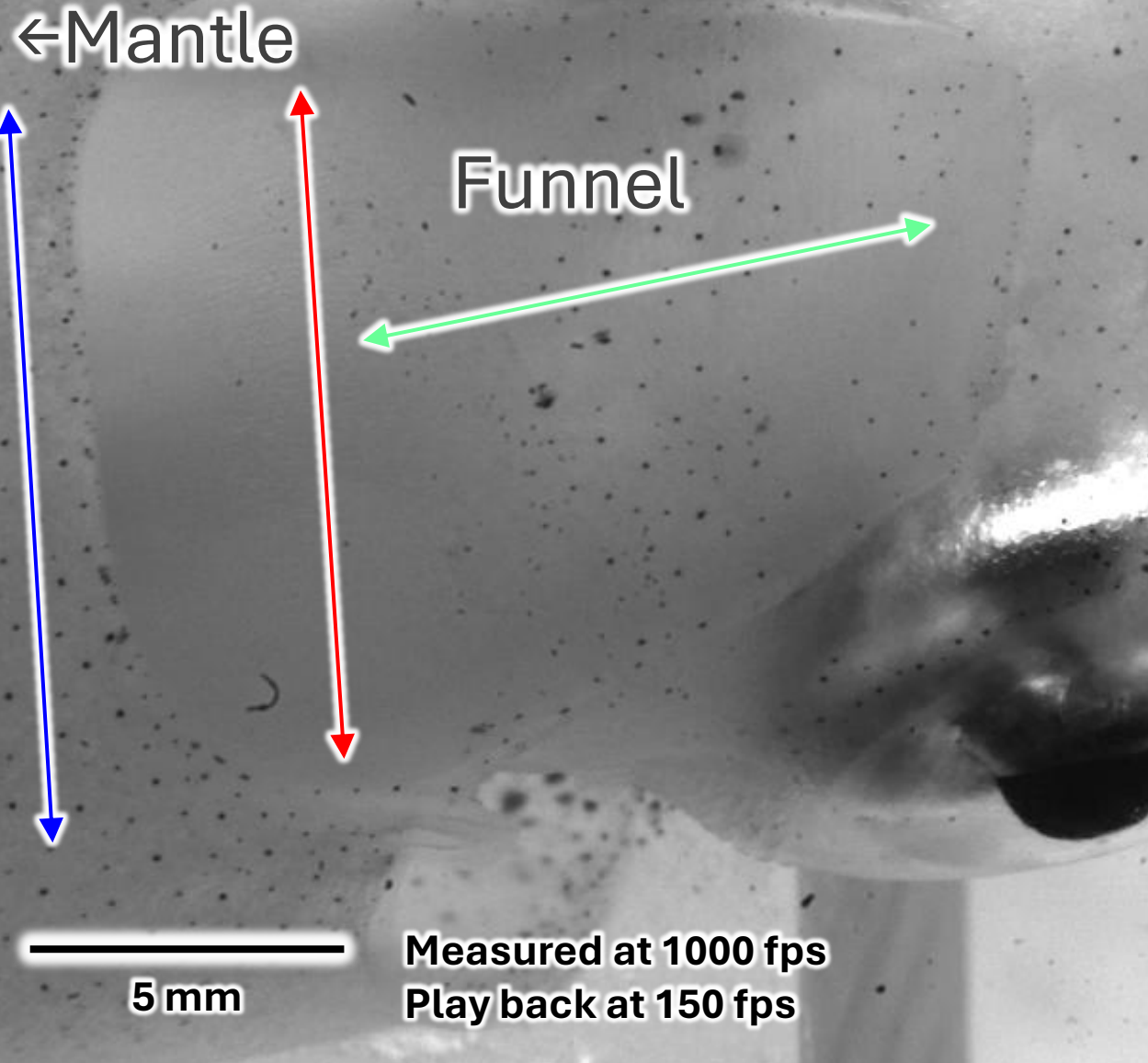


Young (1978)

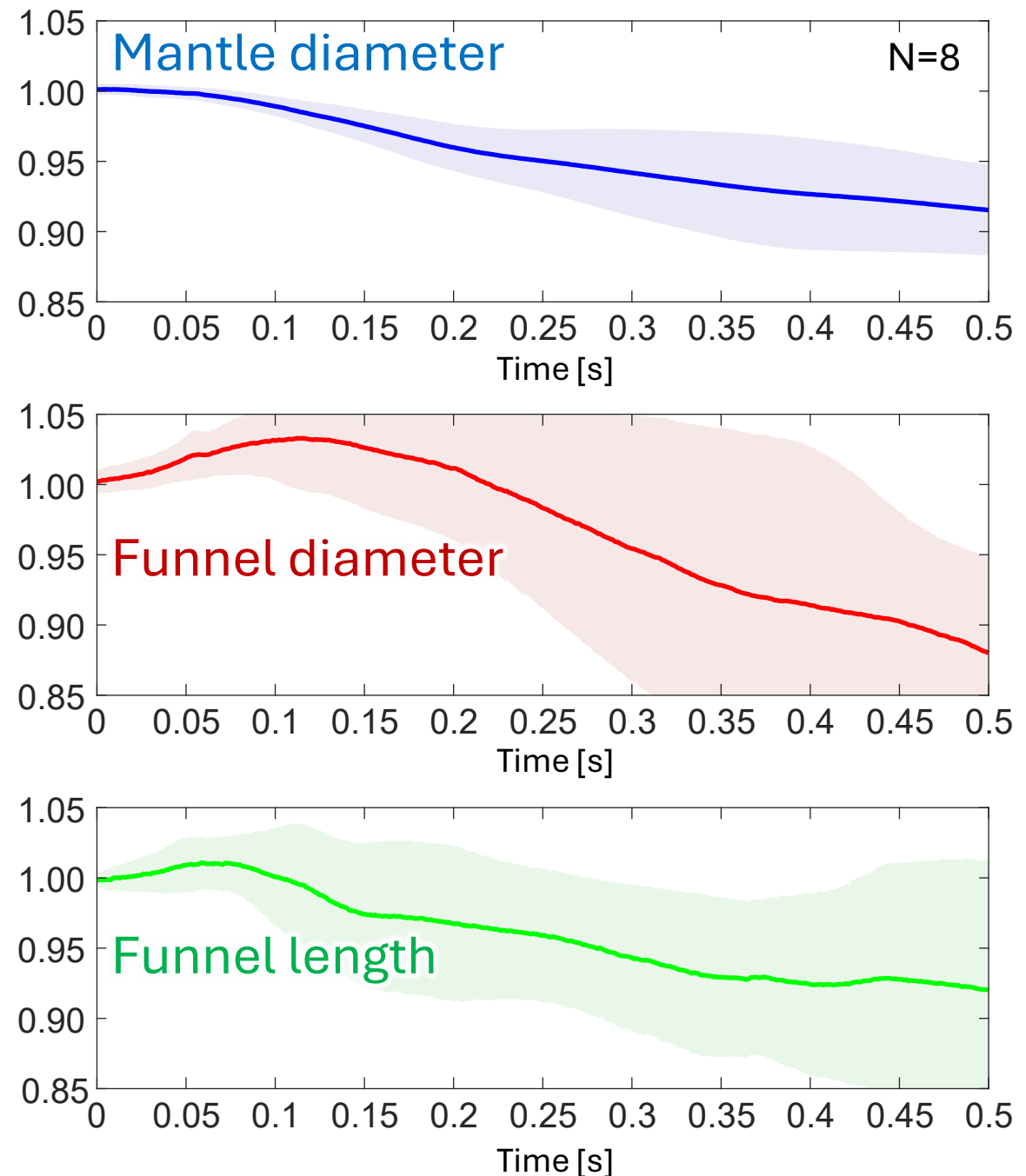
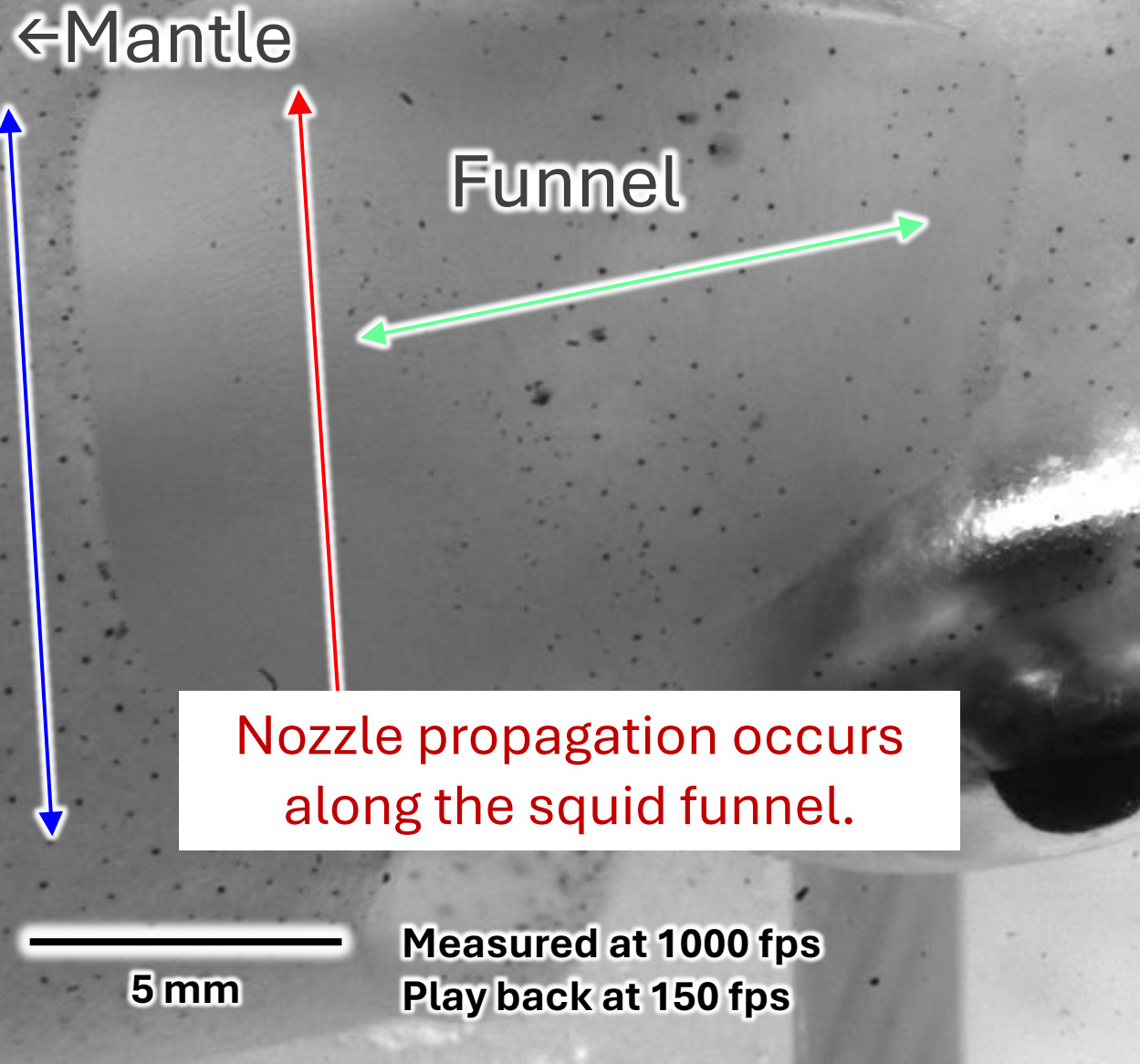


12.5cm#2\_5-30-25\_223446  
Last on Friday

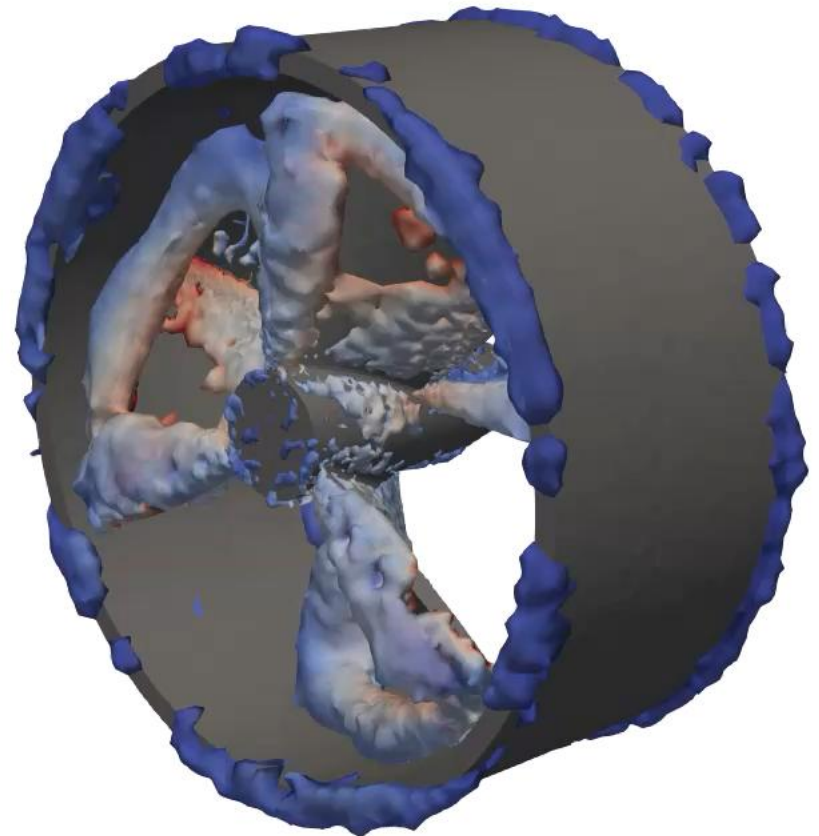
# Paralyzed funnel



# Paralyzed funnel



# Application to propeller jet



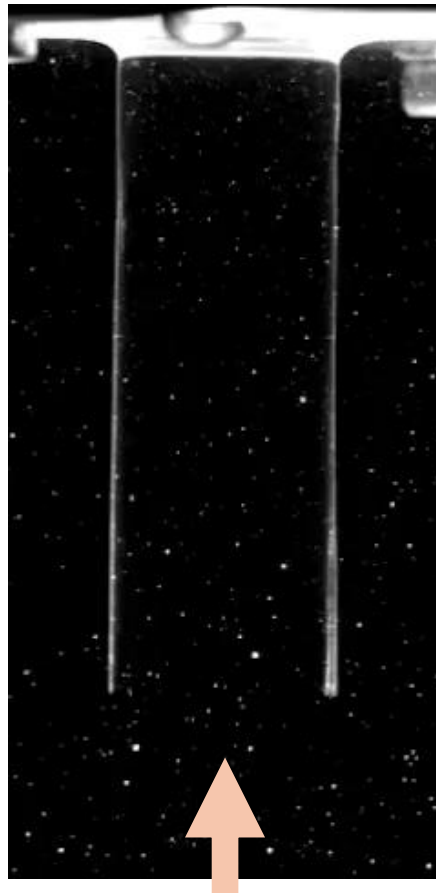
Q criterion with  
colored velocity magnitude



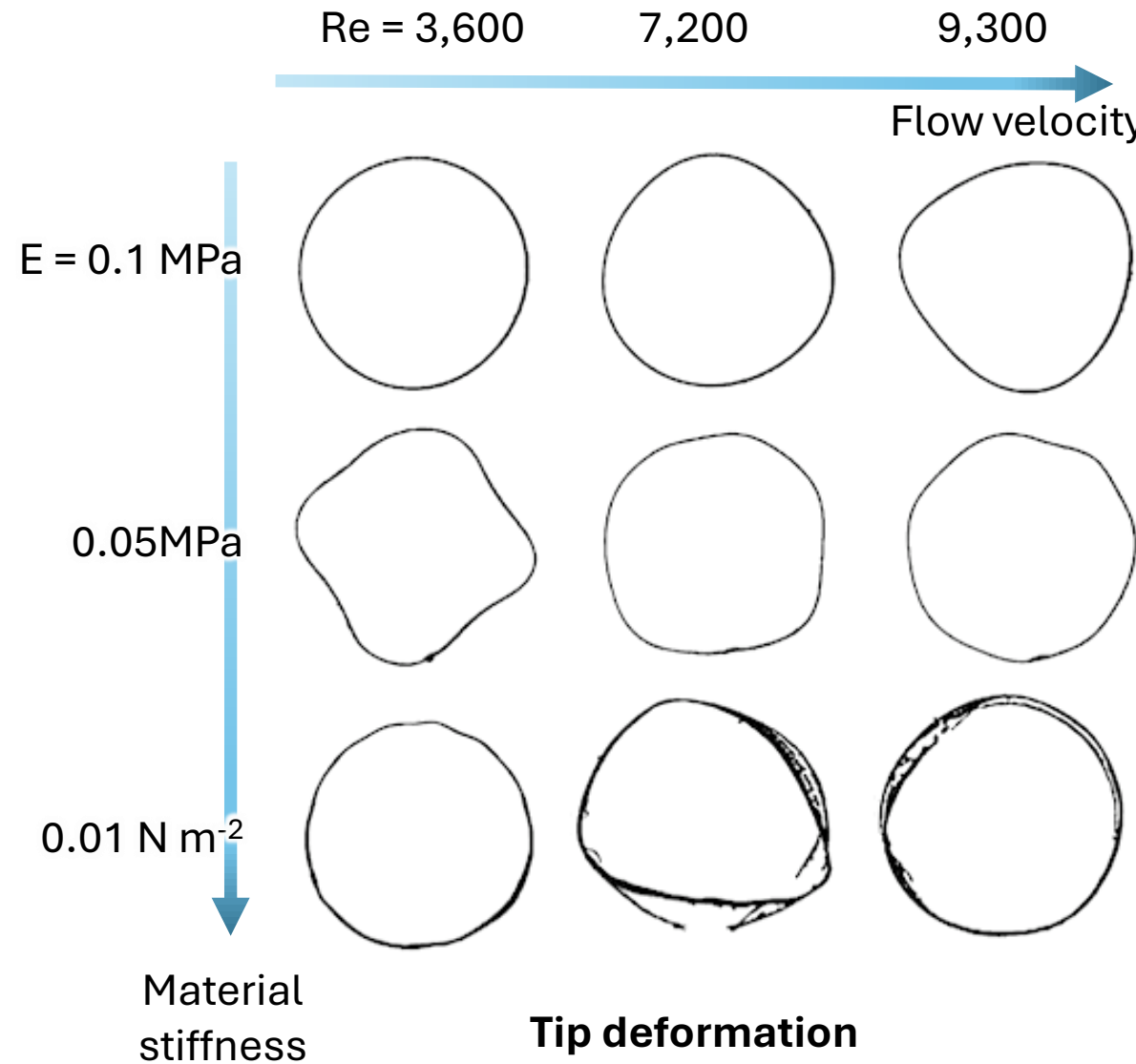
Paras Singh   Dr. Chandan  
Bose



# Non-linear response to steady jet



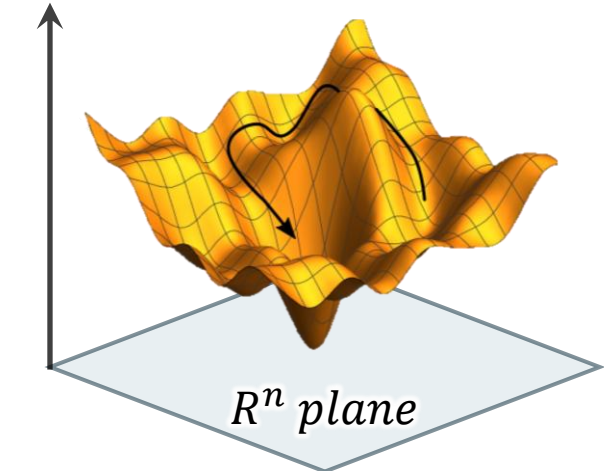
Bottom view



Choi 2022 PhD Thesis

How to find optimal design?

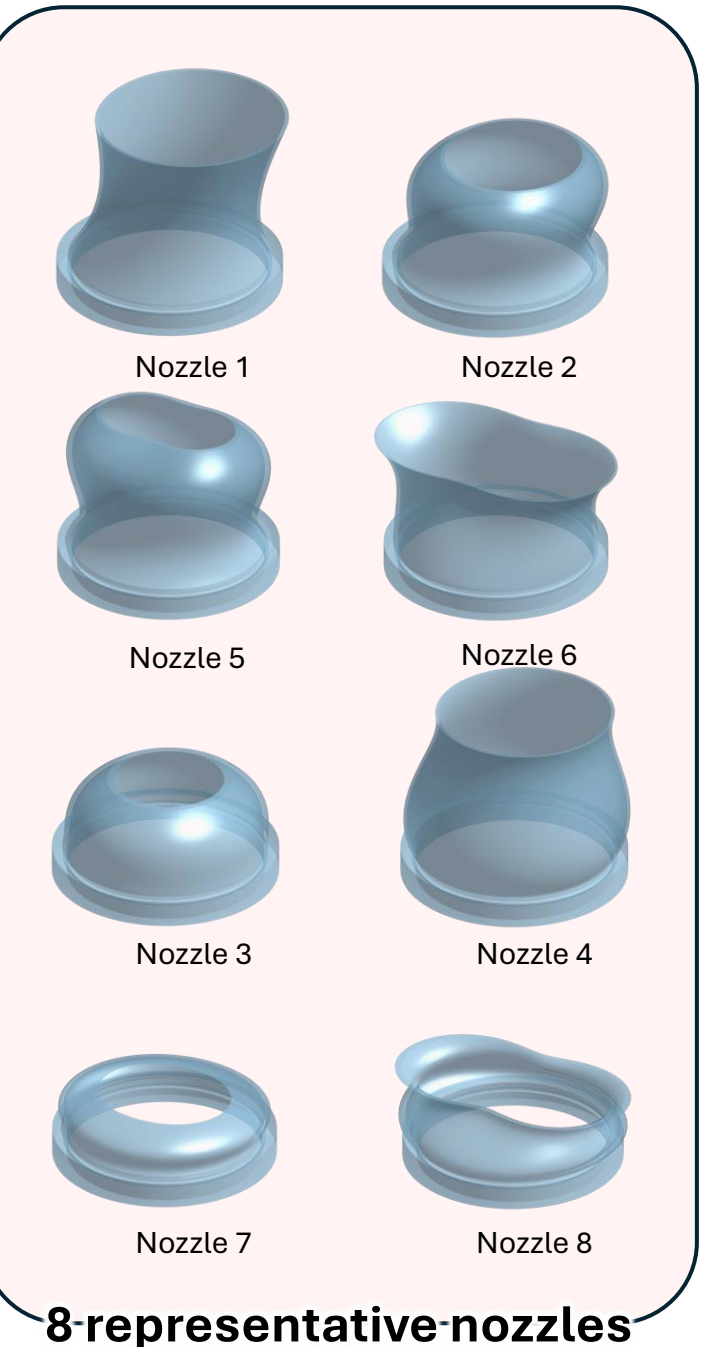
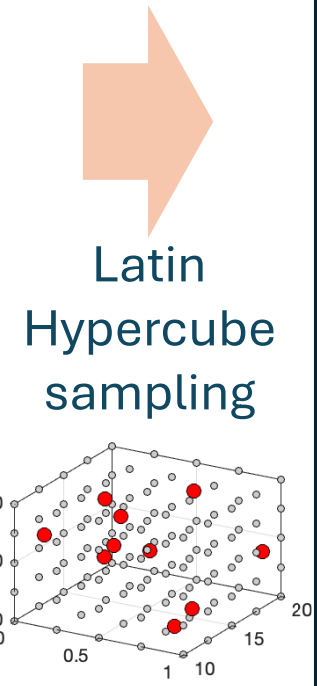
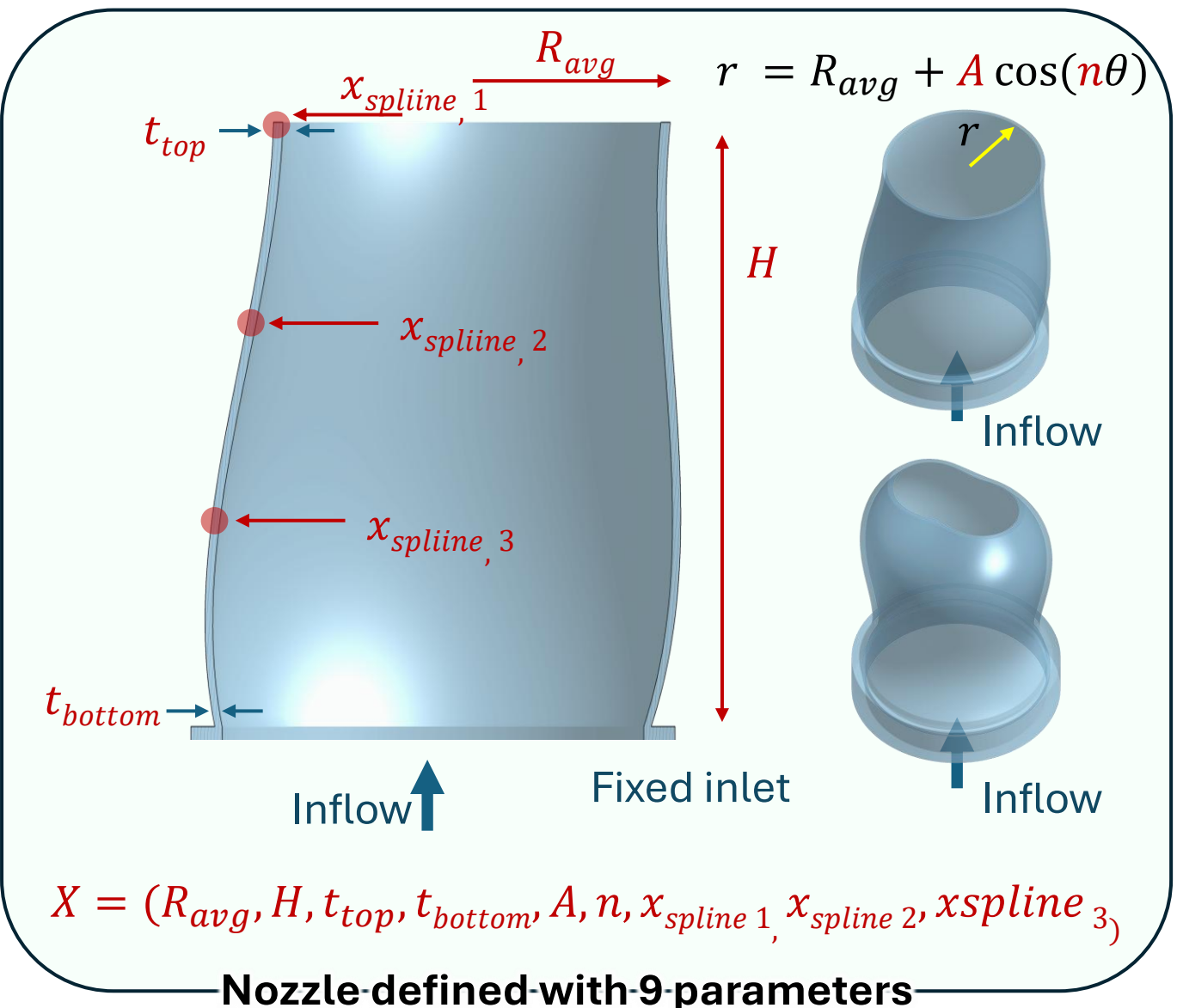
Thrust



$$\text{Thrust} = f(x_1, x_2, x_3, \dots, x_n)$$

- $x_1$ : Stiffness
- $x_2$ : Diameter
- $x_3$ : Jet velocity
- $x_4$ : Jet turbulence
- ...

# Nozzle parametrization

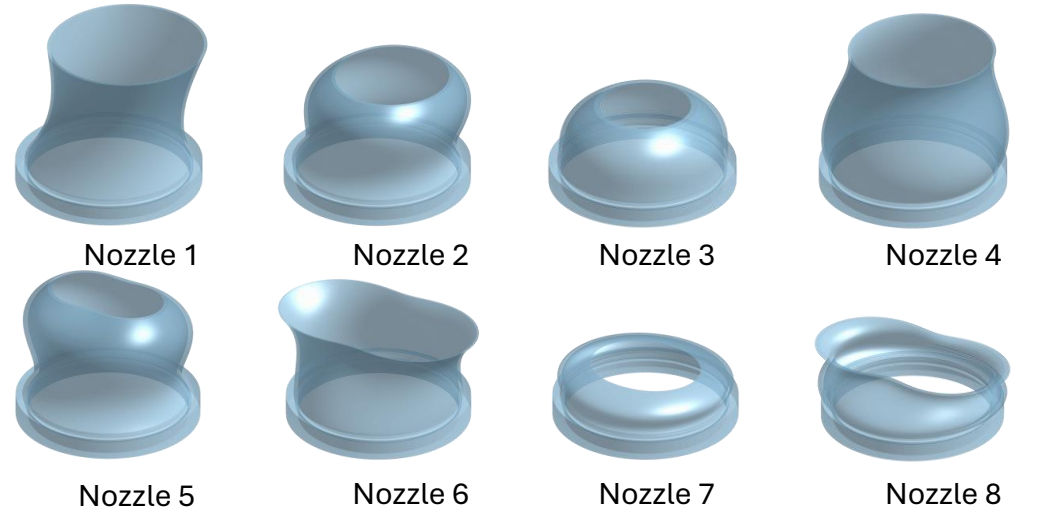


# 3D printing



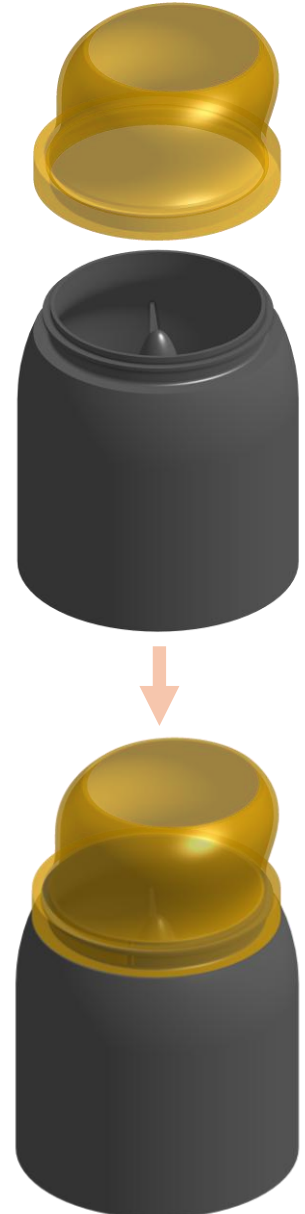
Resin printer  
(Form4)

Soft nozzle



Each takes ~3 hours (24 hours in total)

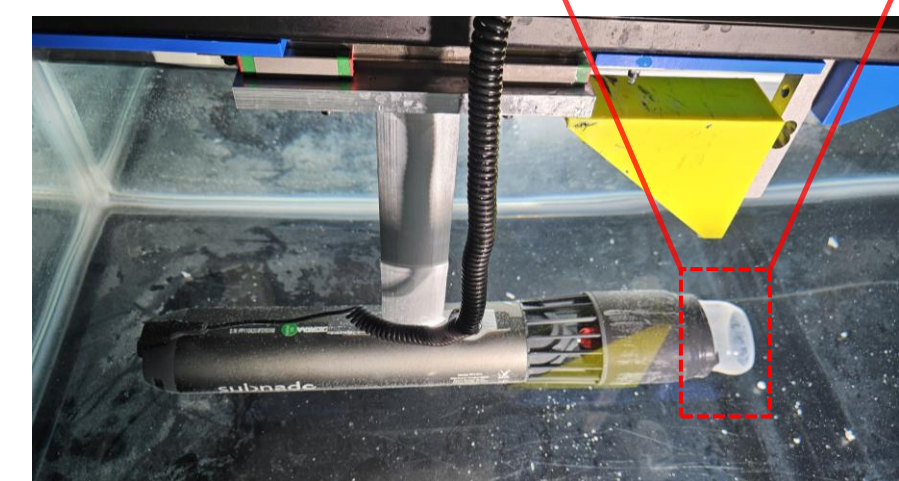
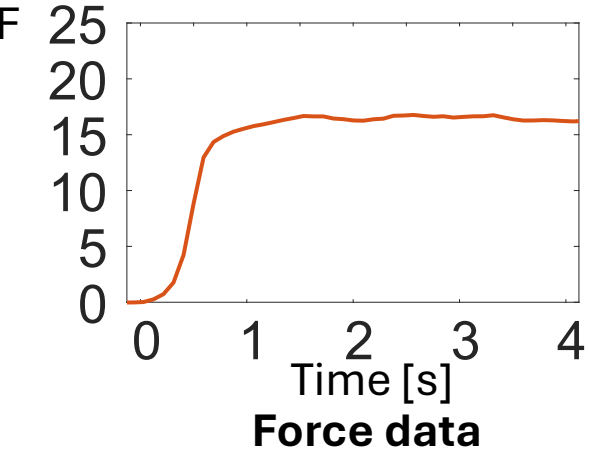
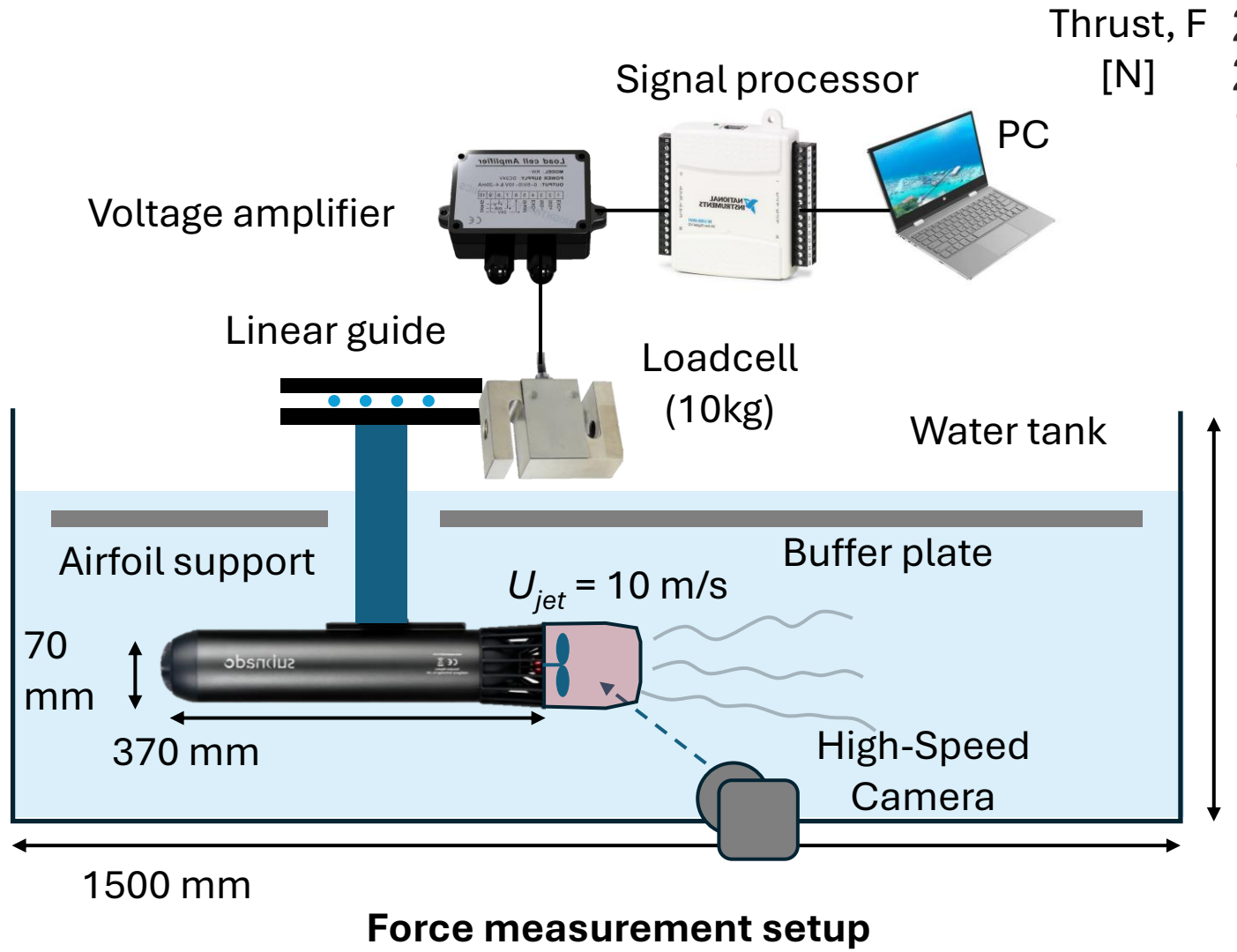
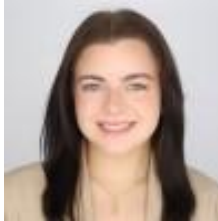
Halley  
Wallace



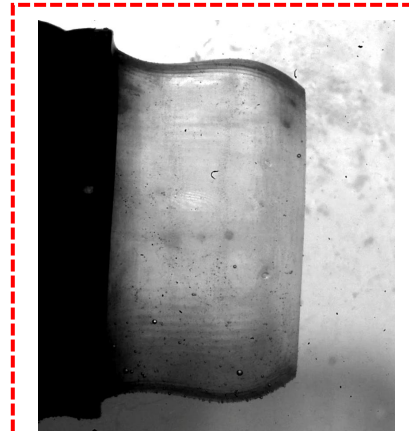
Soft nozzle  
Installation

# Thrust measurement setup

Halley  
Wallace

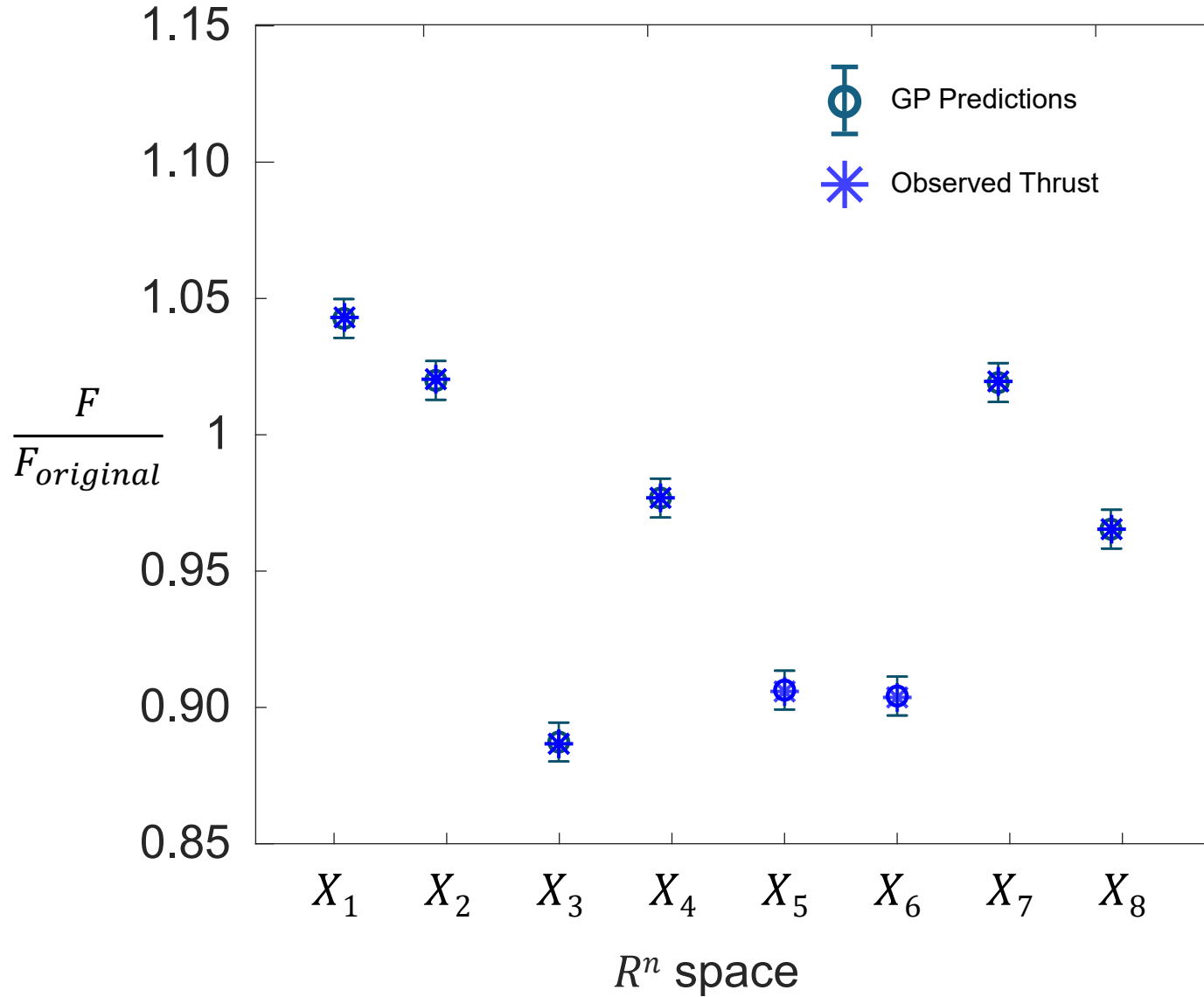


Picture

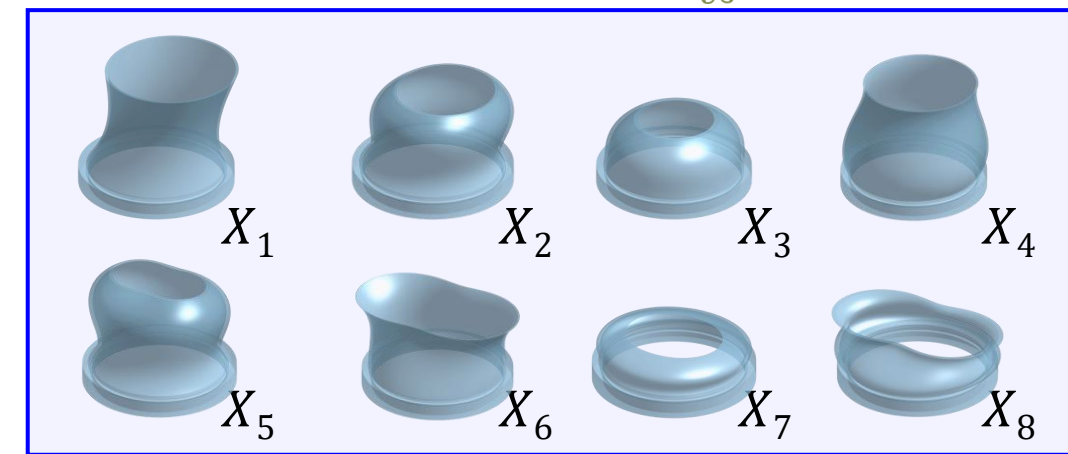


HS image

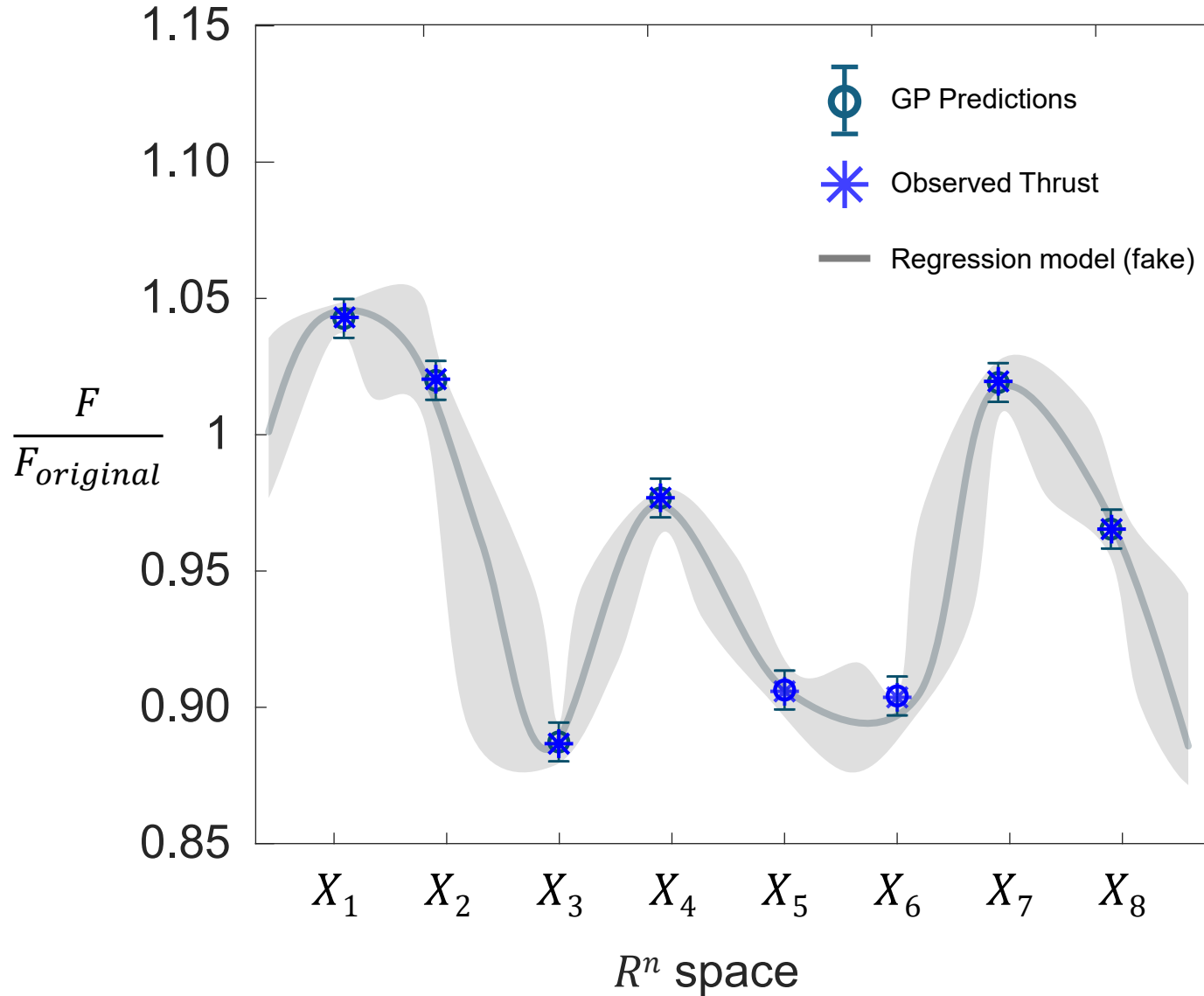
# Bayesian Optimization



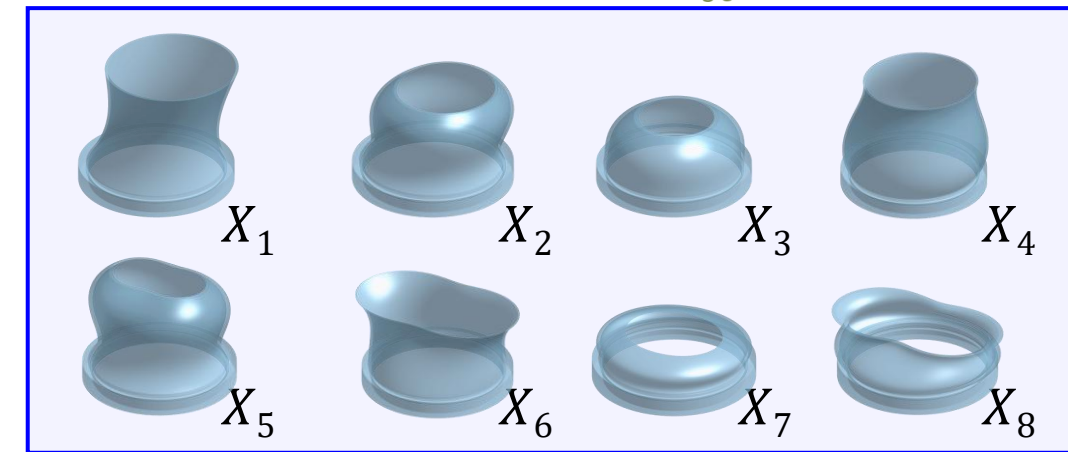
1st generation



# Bayesian Optimization



1st generation



**Gaussian process (GP) Regression model**

$$\mu_* = \beta_0 + \mathbf{k}_*^T (\mathbf{K} + \sigma_n^2 \mathbf{I}_n)^{-1} (\mathbf{y} - \beta_0 \mathbf{1})$$

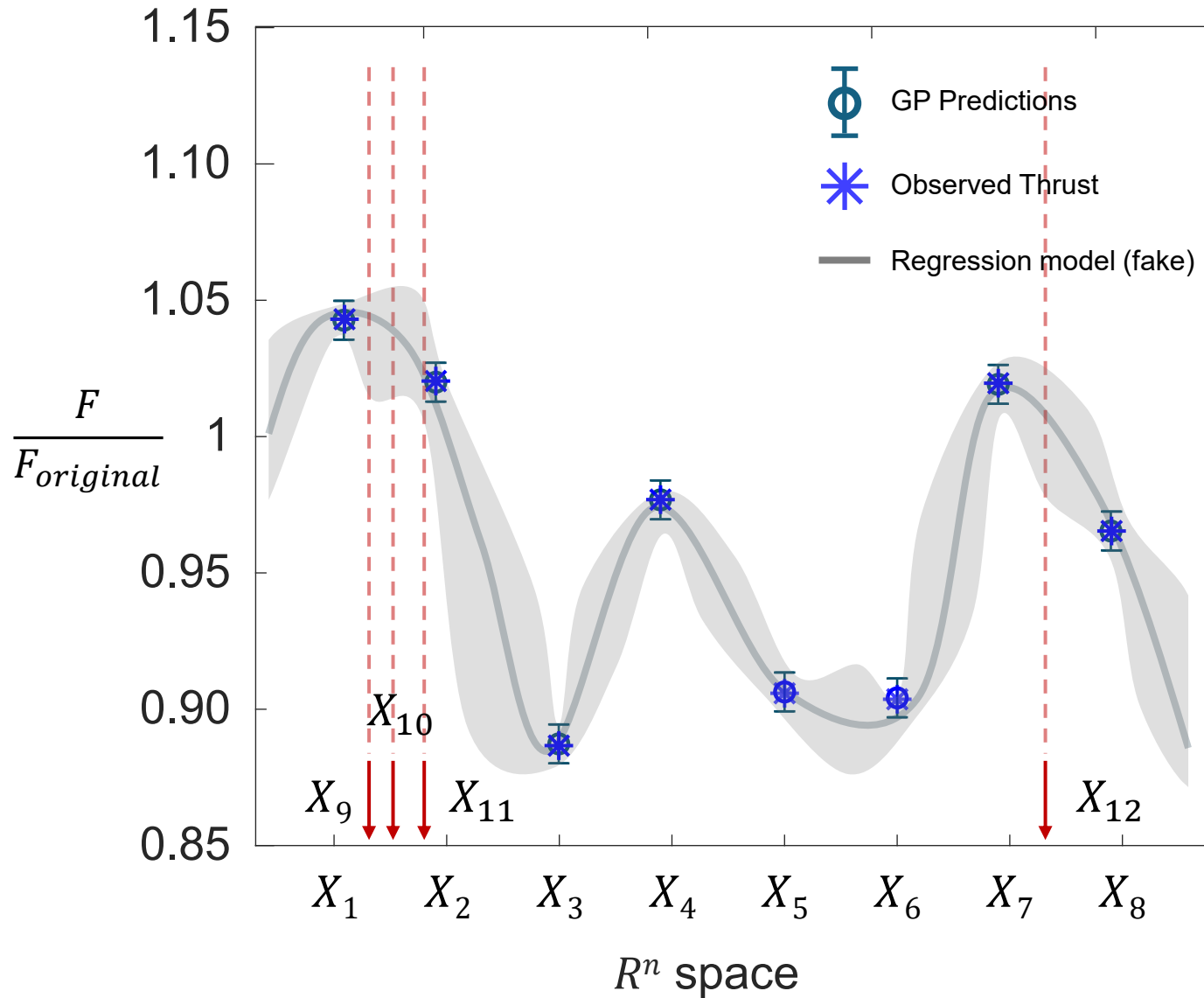
$$\sigma_*^2 = k(\mathbf{x}_*, \mathbf{x}_*) - \mathbf{k}_*^T (\mathbf{K} + \sigma_n^2 \mathbf{I}_n)^{-1} \mathbf{k}_*$$

, where  $\mathbf{k}_* = \begin{bmatrix} k(\mathbf{x}_*, \mathbf{x}_1) \\ \vdots \\ k(\mathbf{x}_*, \mathbf{x}_n) \end{bmatrix}$

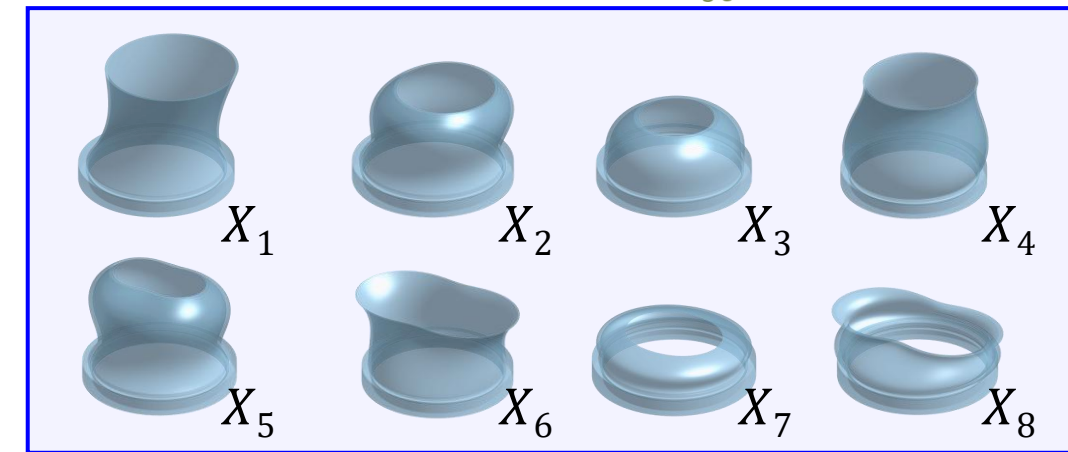
RBF kernel:  $k(\mathbf{x}_*, \mathbf{x}_i) = \sigma_f^2 \exp\left(-\frac{\|\mathbf{x}_* - \mathbf{x}_i\|^2}{2\ell^2}\right)$

Constant basis:  $\beta_0$

# Bayesian Optimization



1st generation

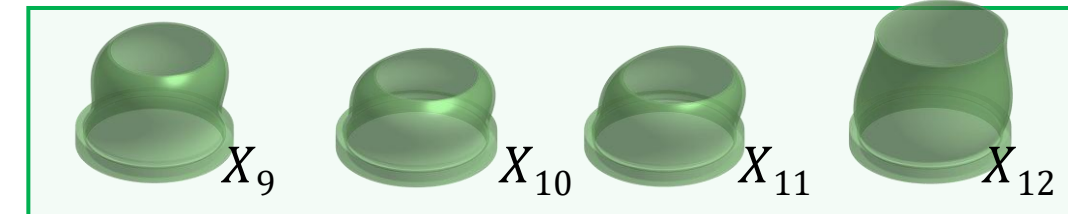


## Expected Improvement (EI)

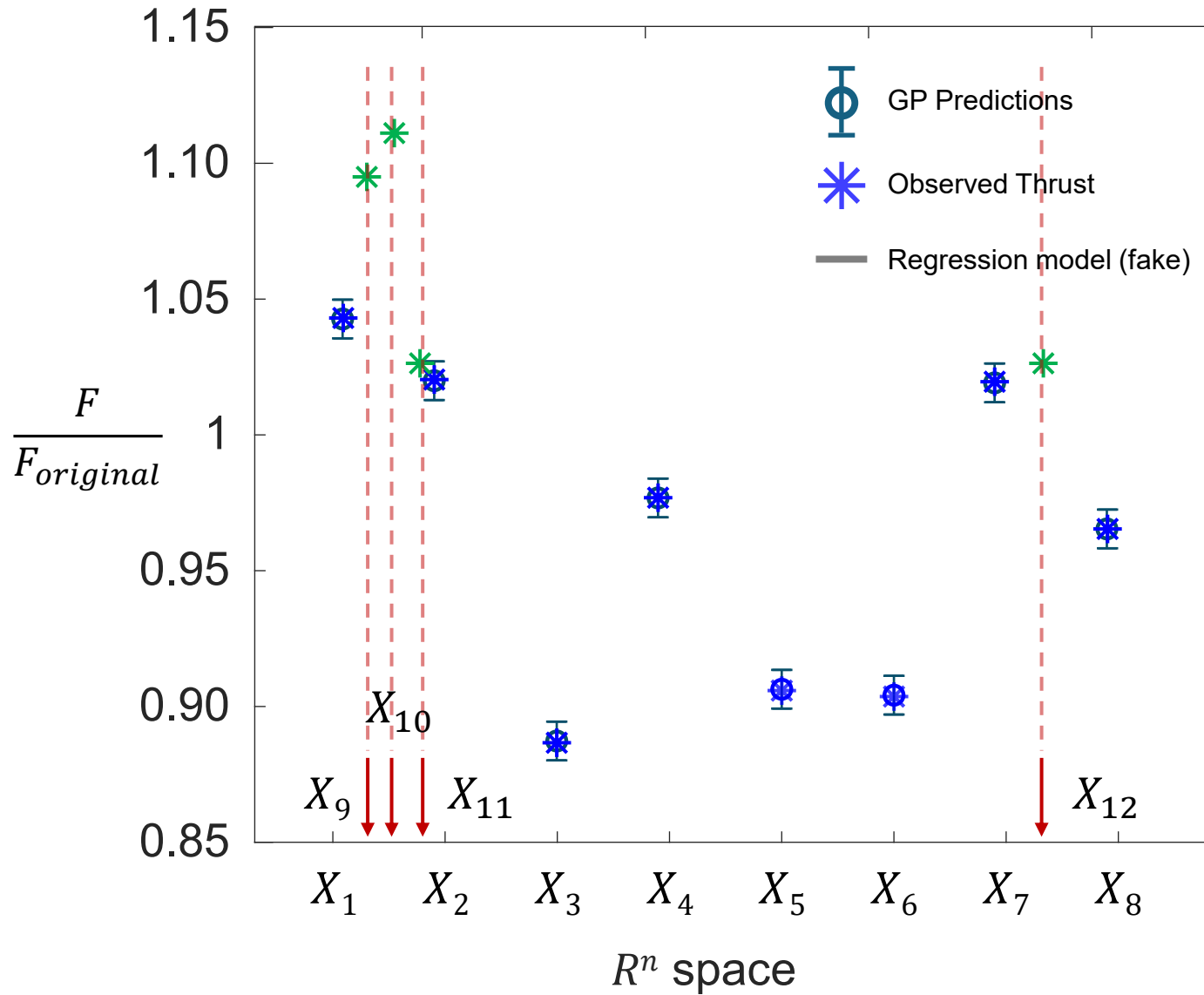
$$x^* = \arg \max \sigma(x) [Z(x)\Phi(Z(x)) + \phi(Z(x))]$$

$$\text{, where } Z(x) = \frac{\mu(x) - f^+}{\sigma(x)}$$

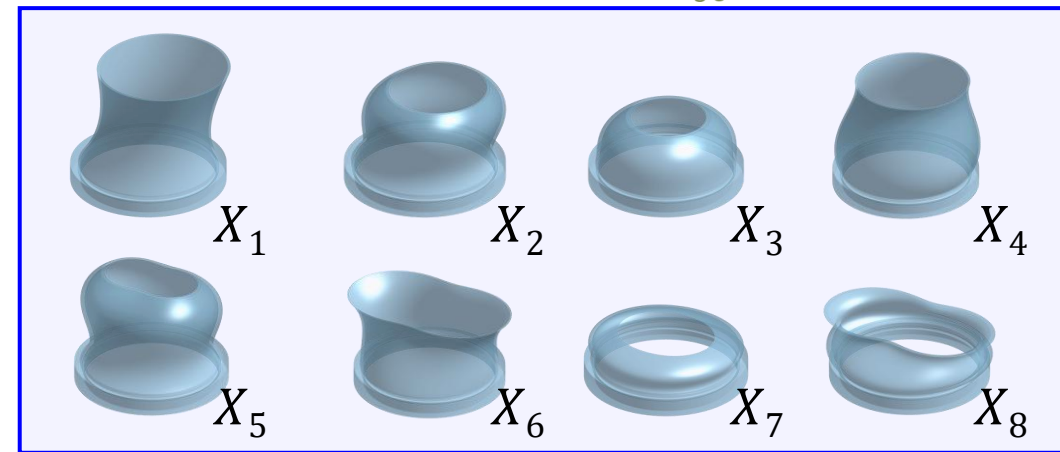
2nd generation



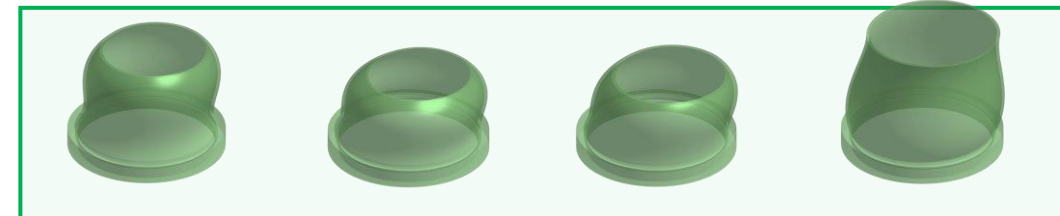
# Bayesian Optimization



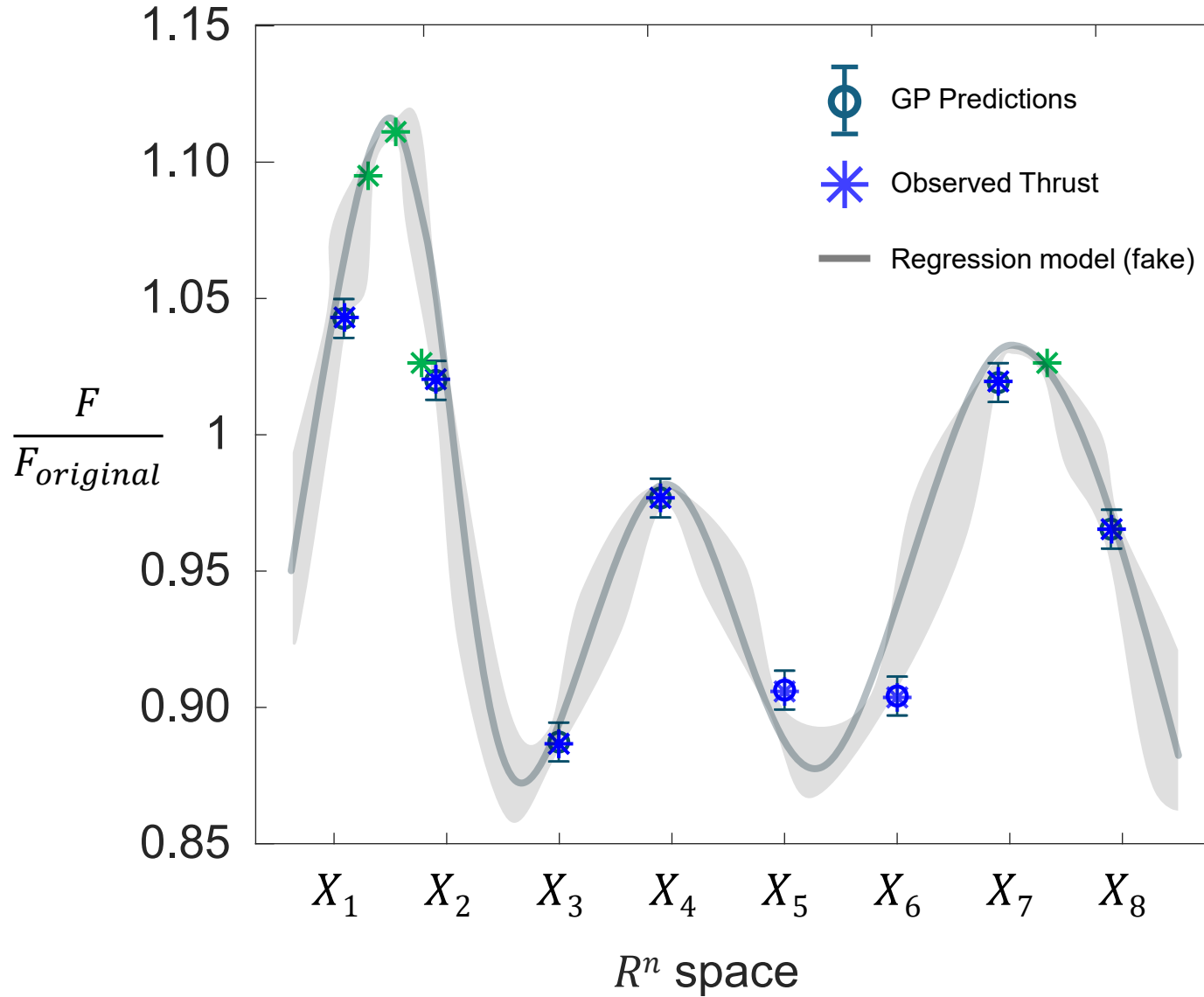
1st generation



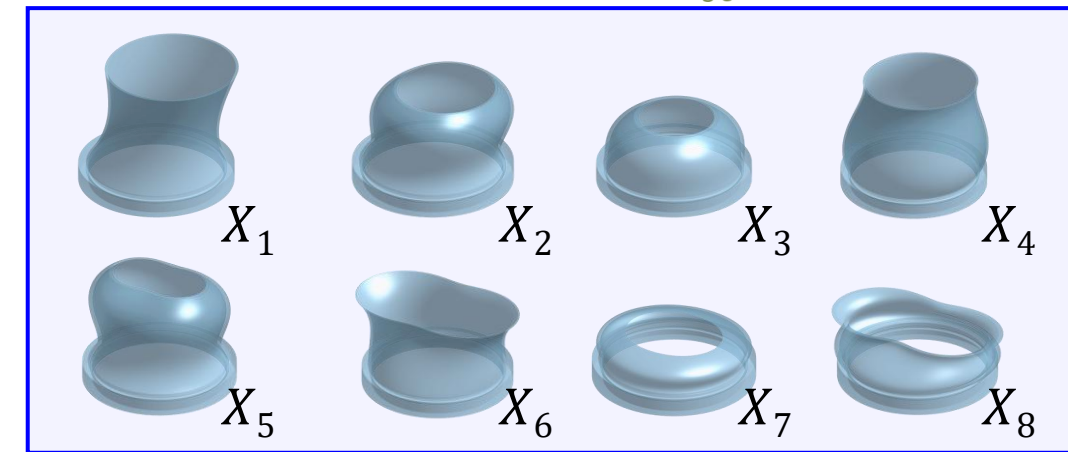
2nd generation



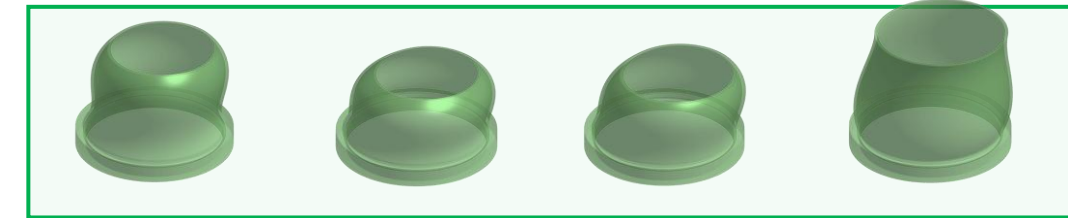
# Bayesian Optimization



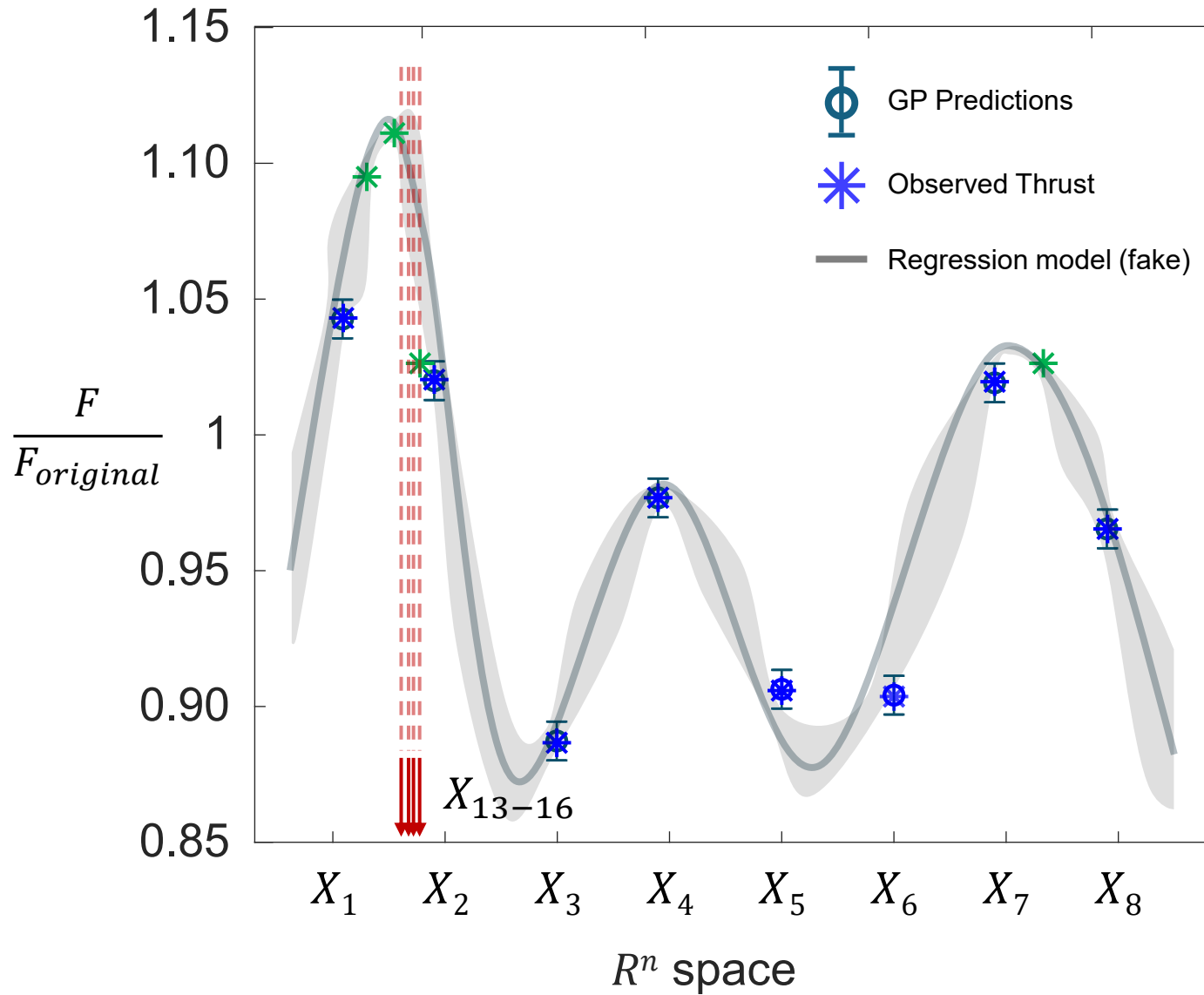
1st generation



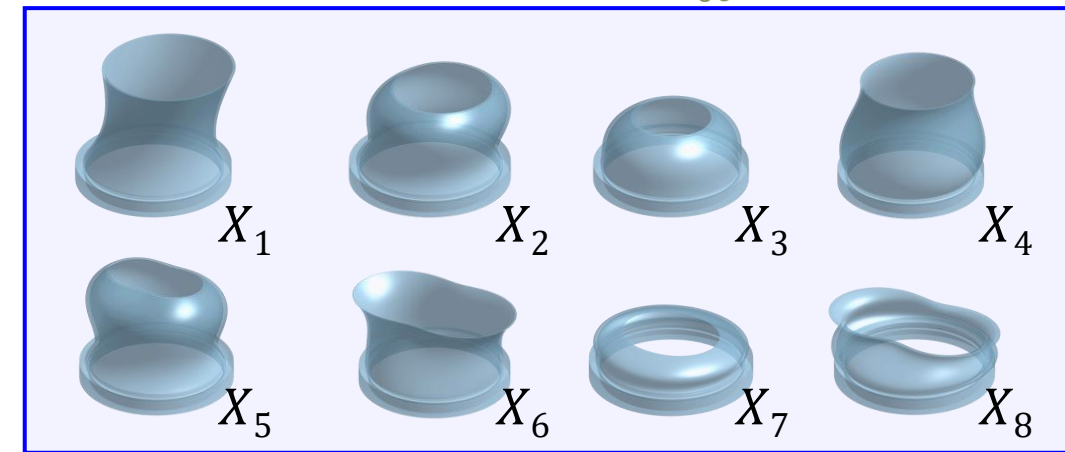
2nd generation



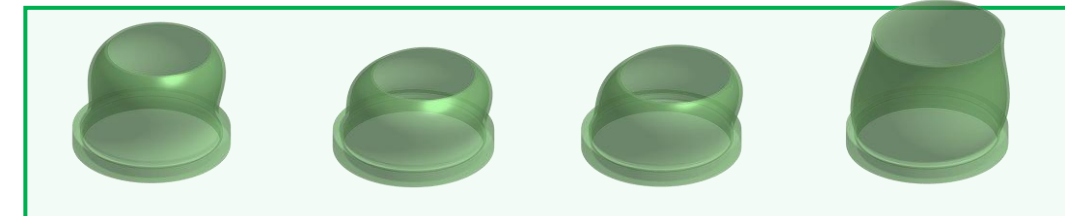
# Bayesian Optimization



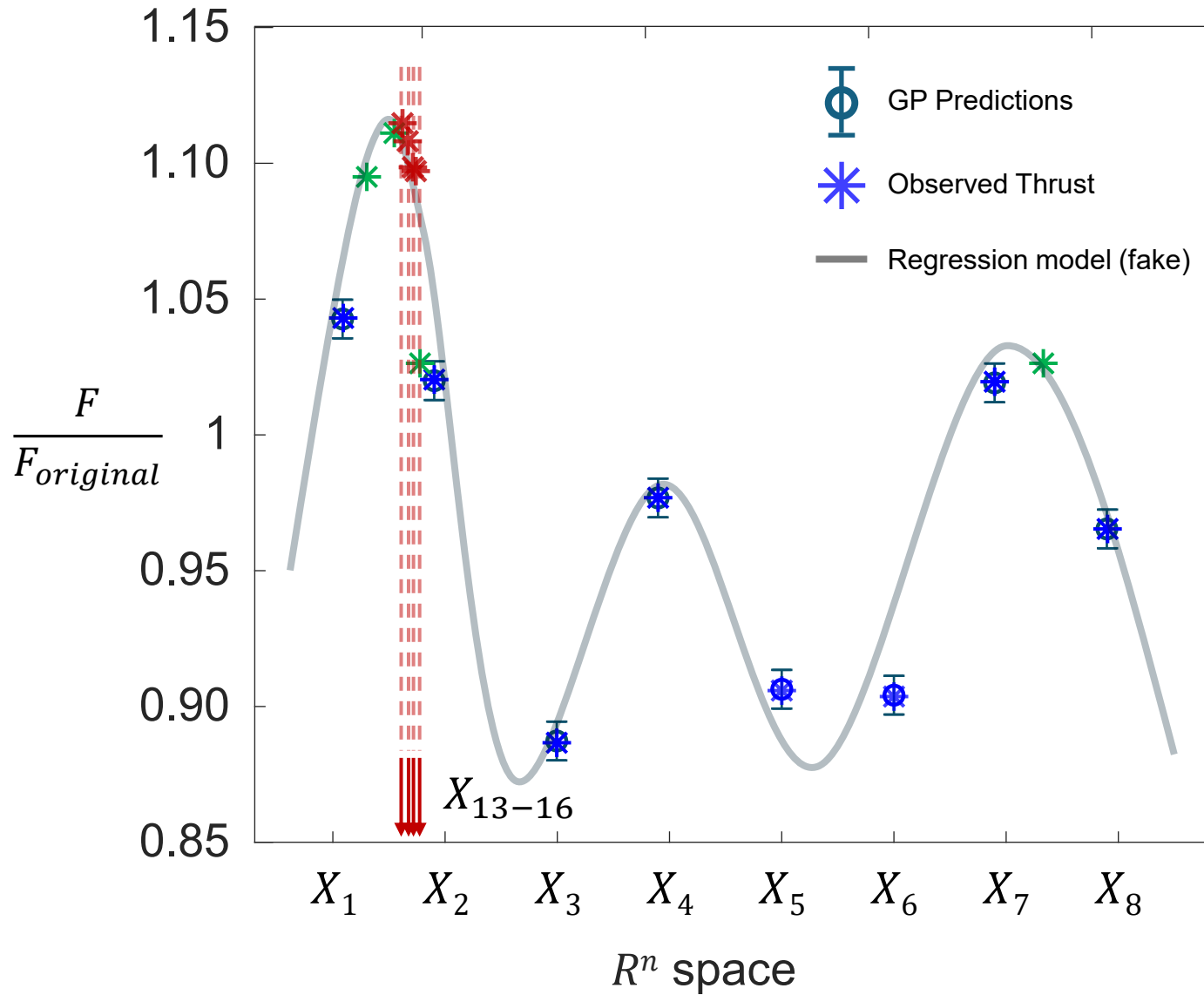
1st generation



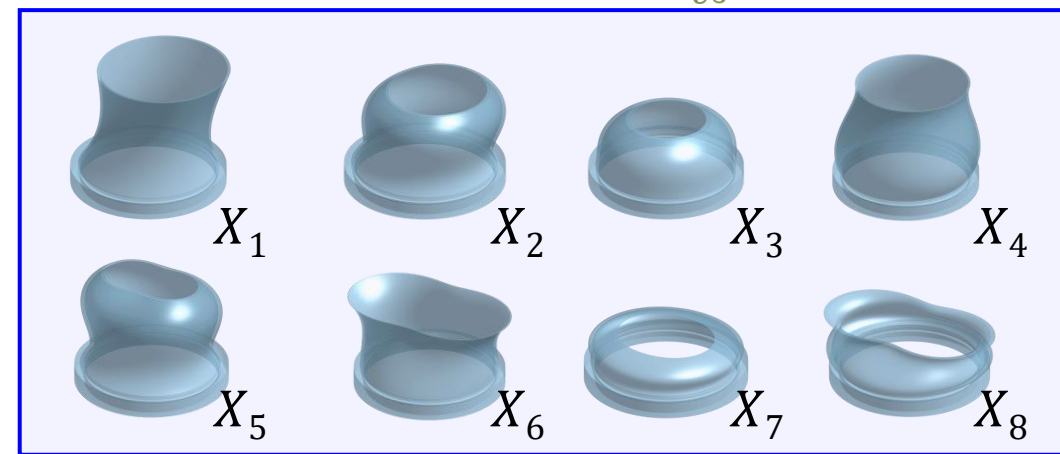
2nd generation



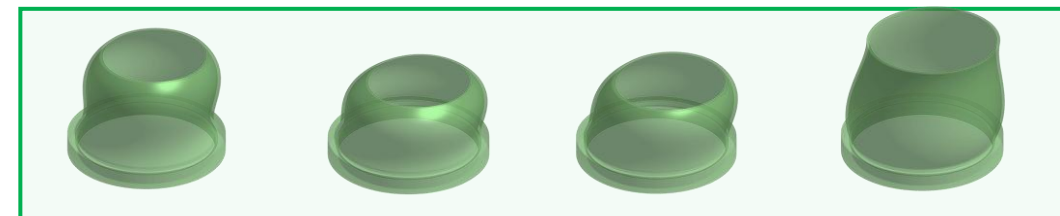
# Bayesian Optimization



1st generation



2nd generation



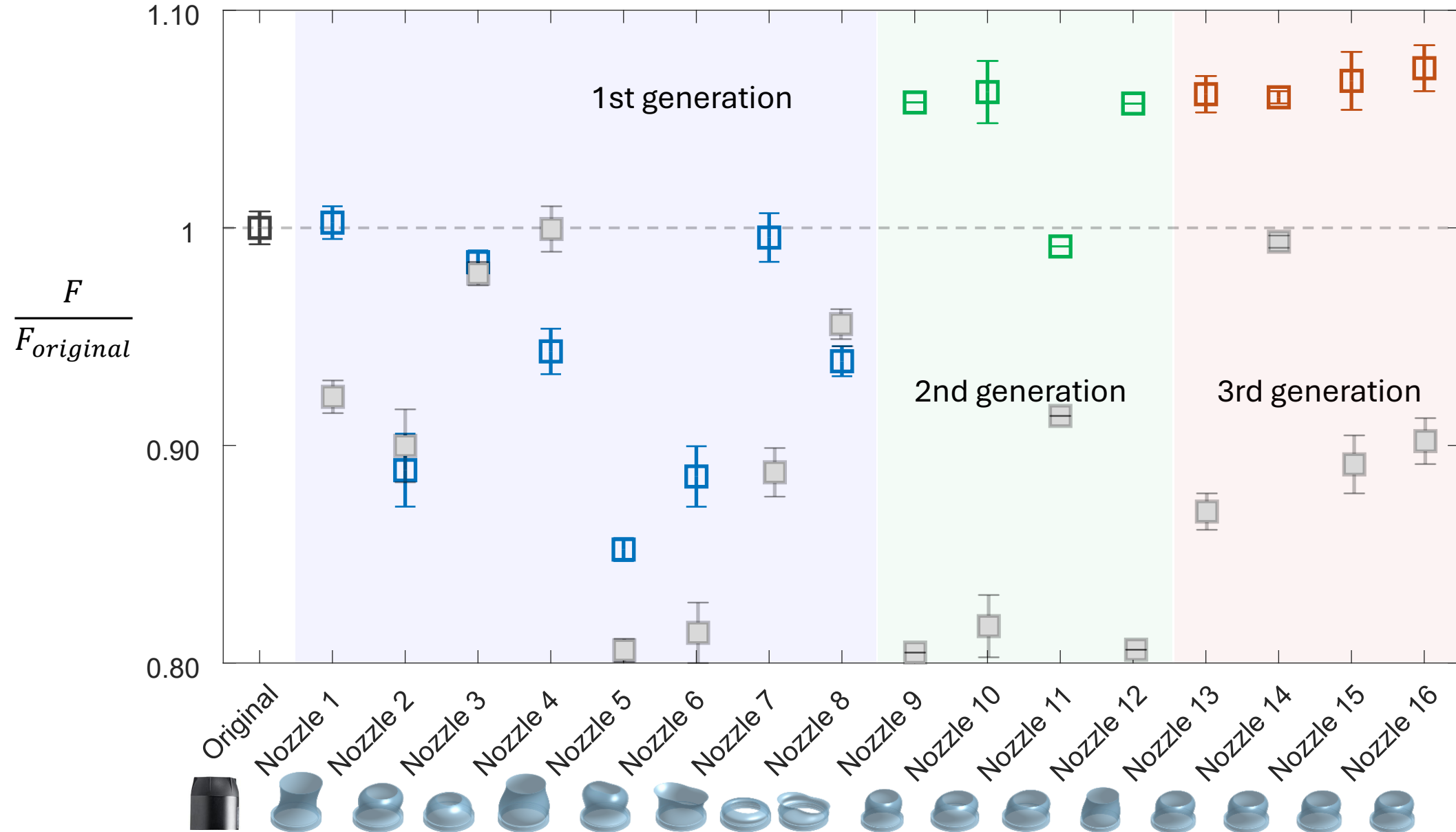
3rd generation



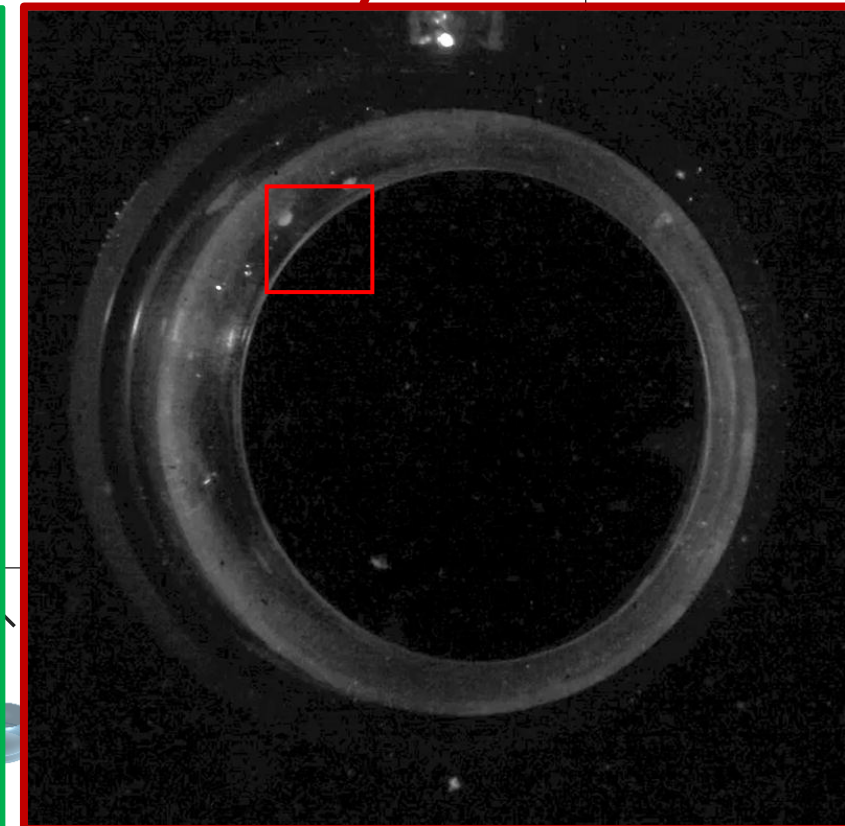
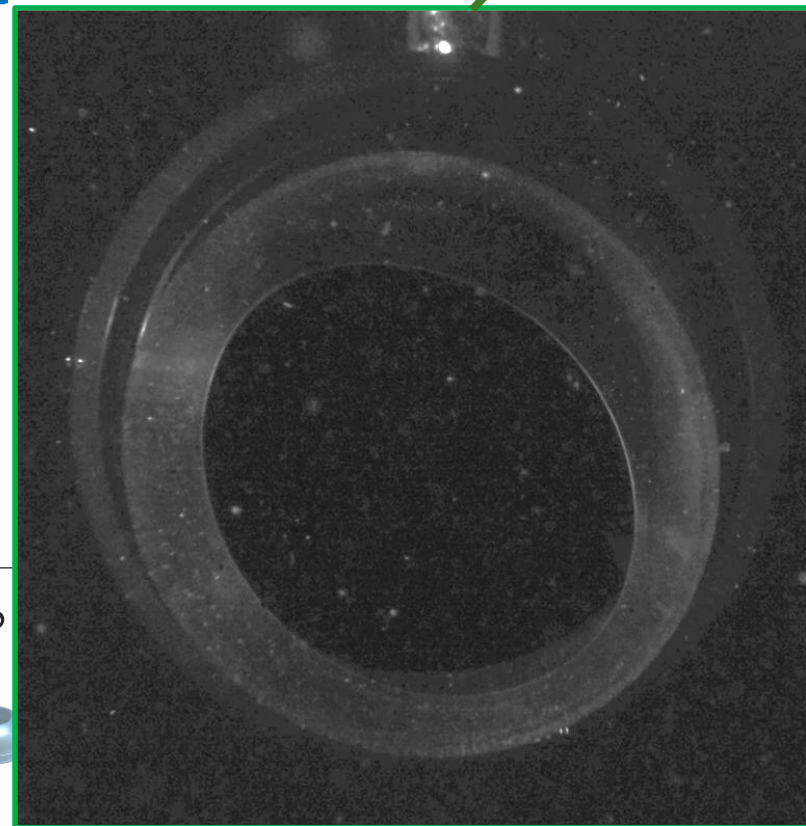
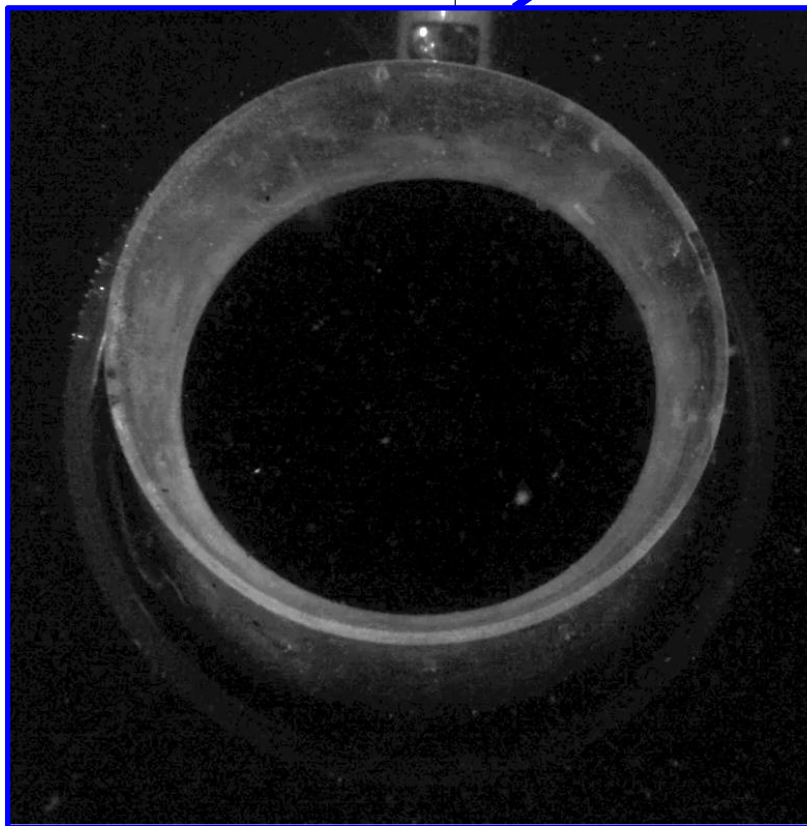
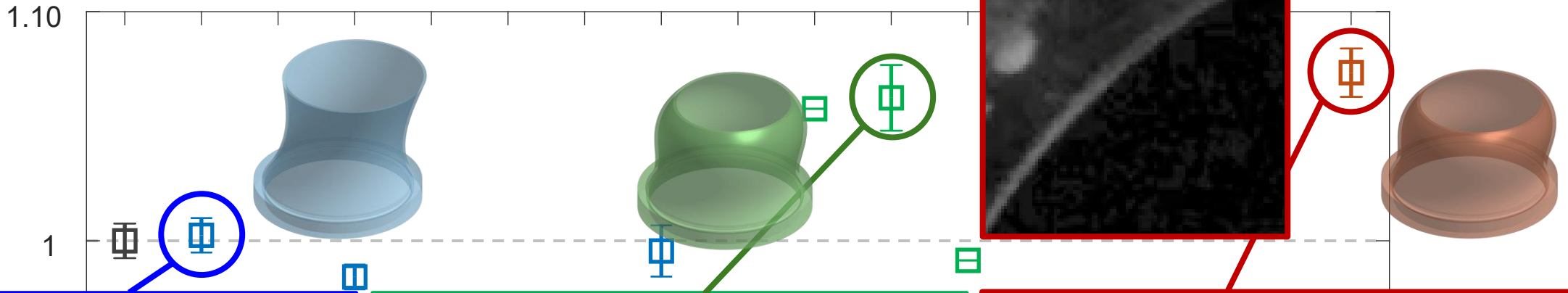
# Thrust improvement

Flexible  
Rigid

Halley  
Wallace

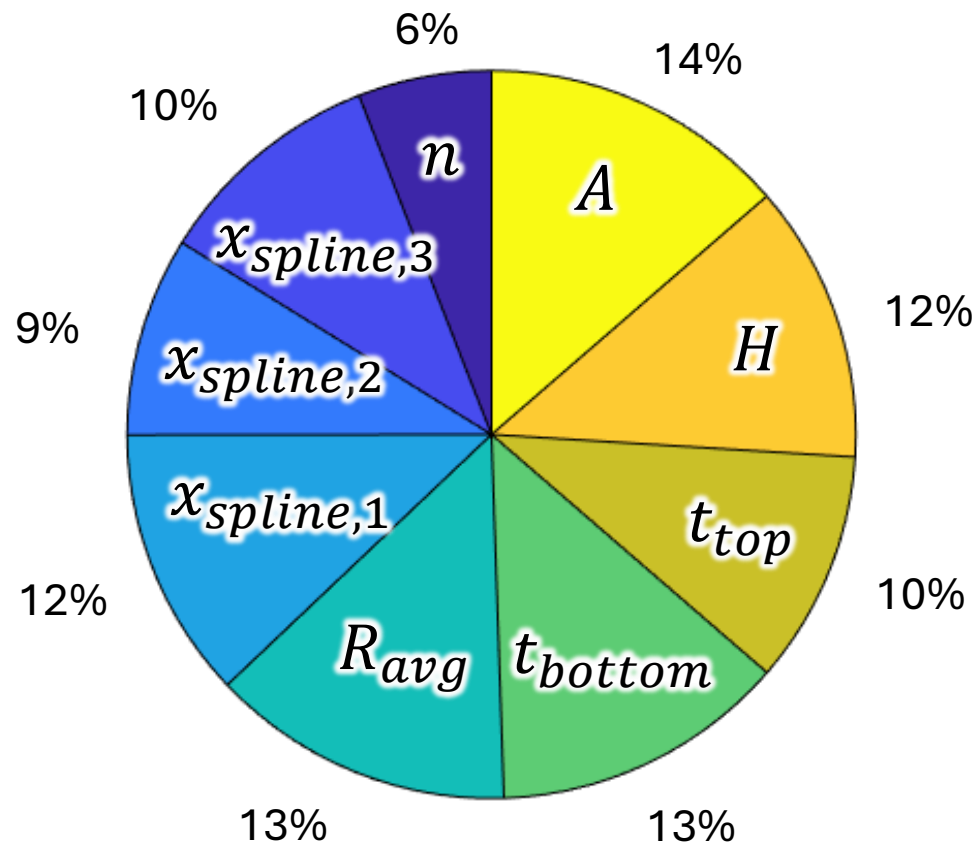


# Thrust improvement

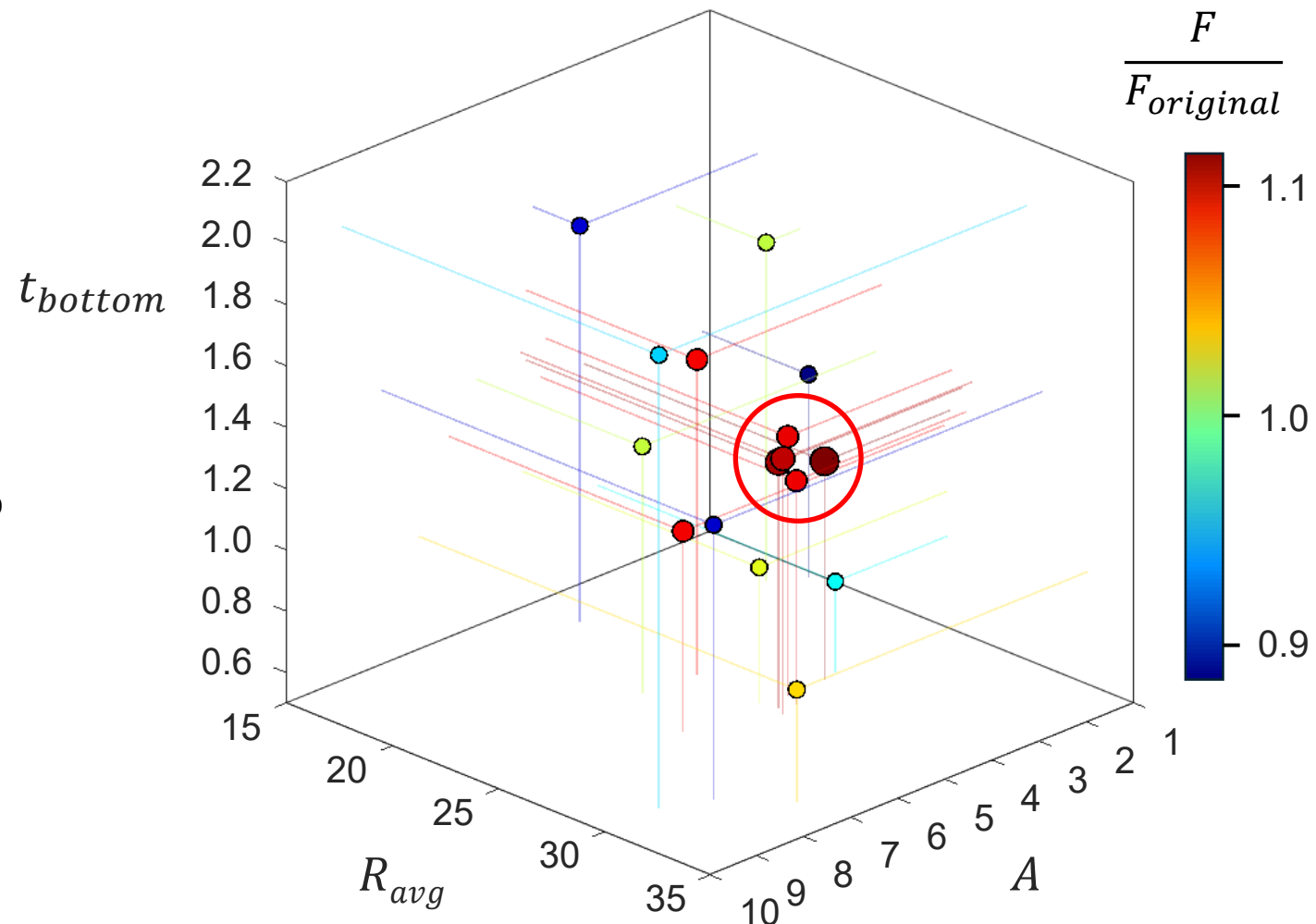


# Variable sensitivity

$$S_{T_i} = 1 - \frac{\mathbb{E}\left[f(A)\left(f\left(B_A^{(i)}\right) - f(A)\right)\right]}{Var[f(X)]}$$

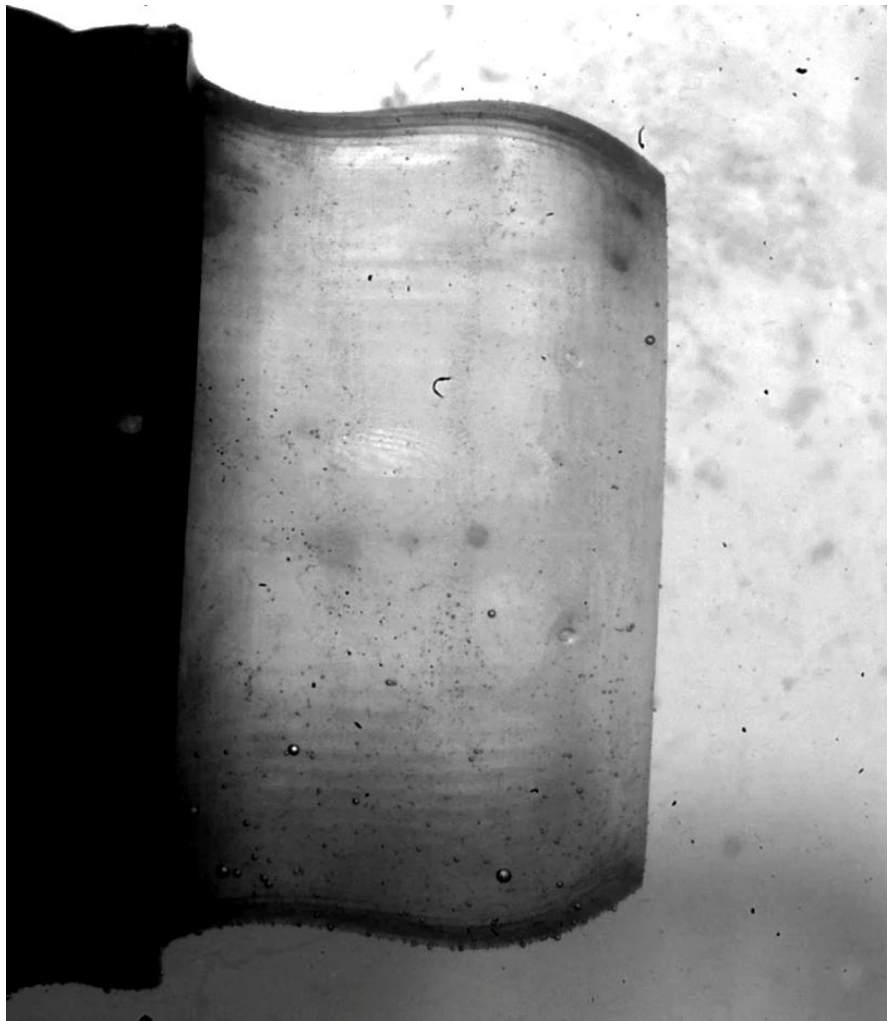


Parameters are equally sensitive



Parameters converged via Bayesian optimization

# Deformation



Side view



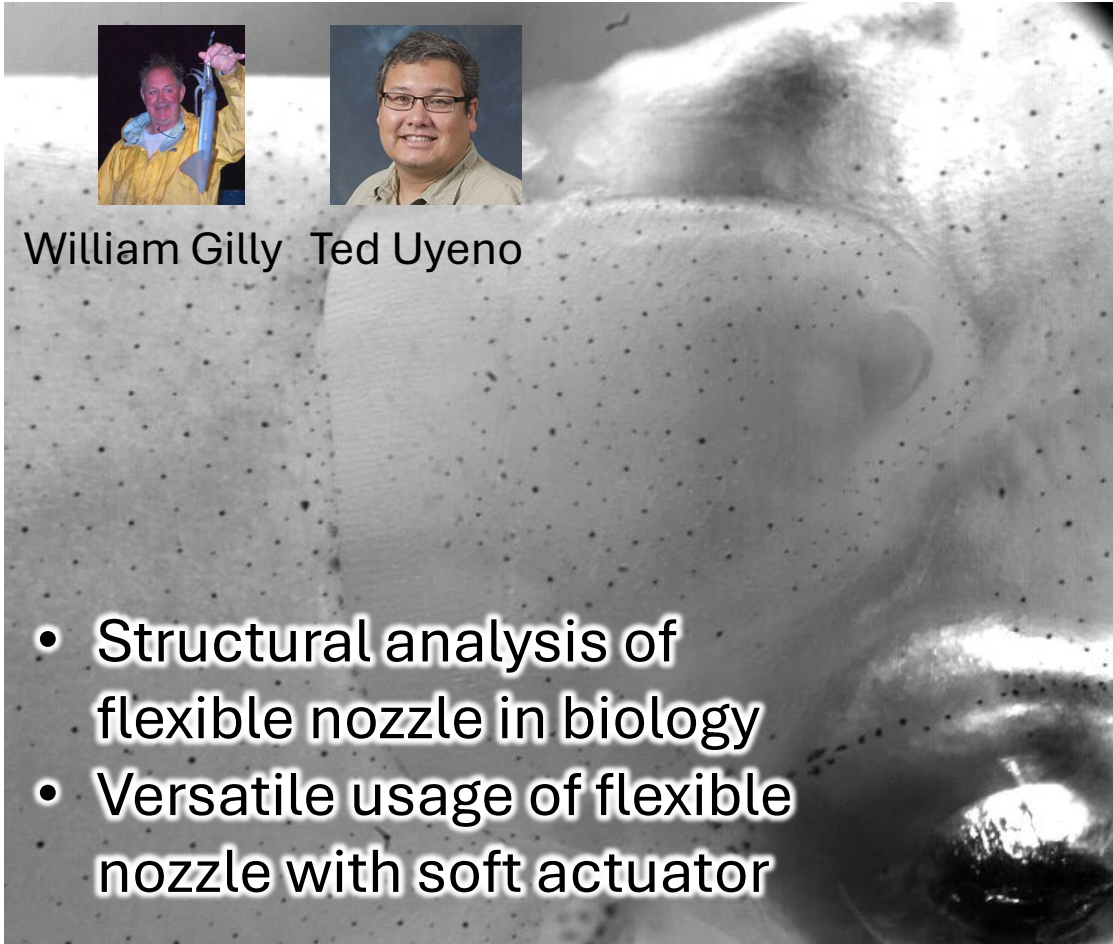
Rear vi



© Shawn M Miller 2014

# On-going work

## Active soft nozzle



William Gilly Ted Uyeno

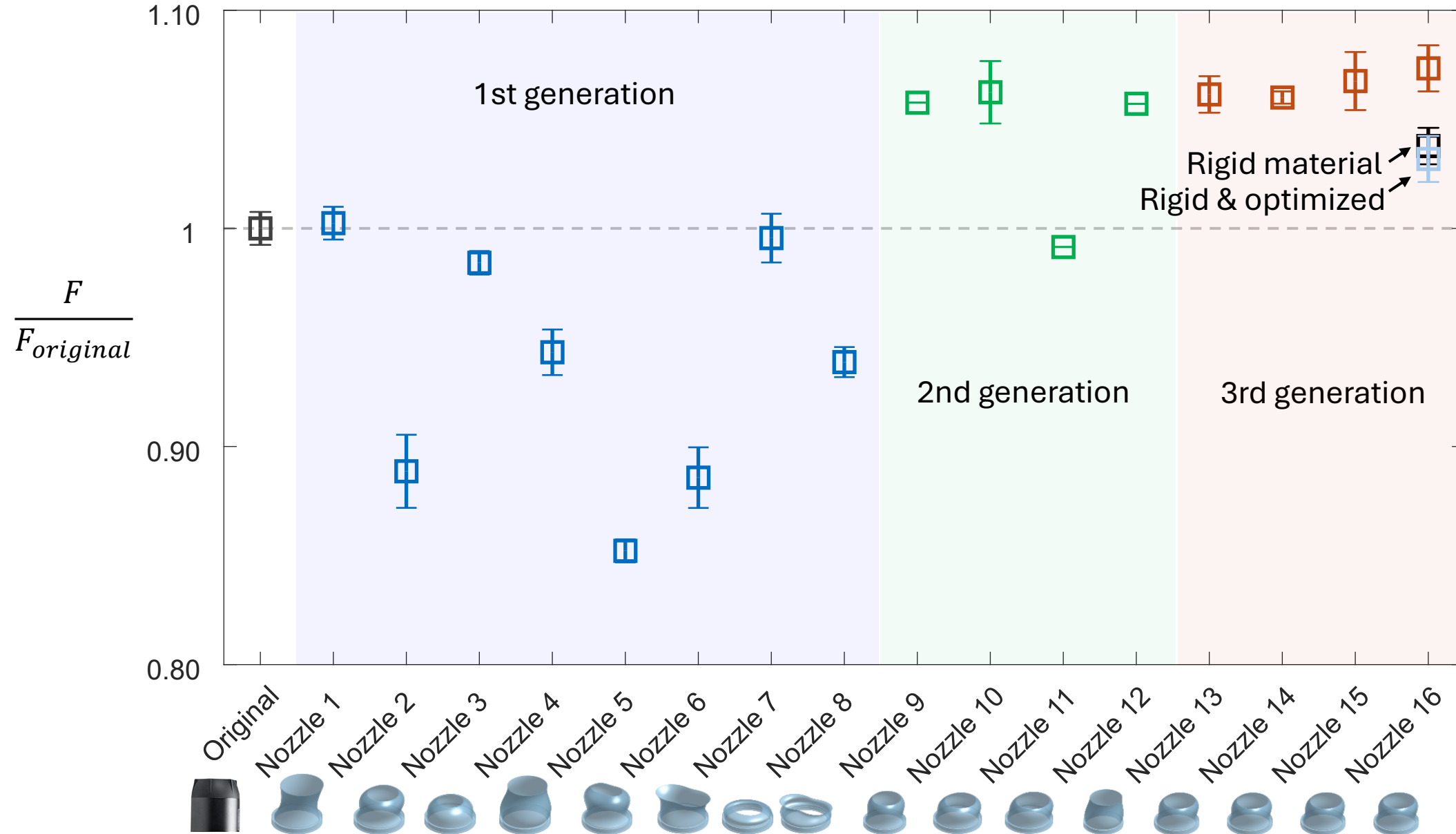
- Structural analysis of flexible nozzle in biology
- Versatile usage of flexible nozzle with soft actuator

## Multi-fidelity optimization

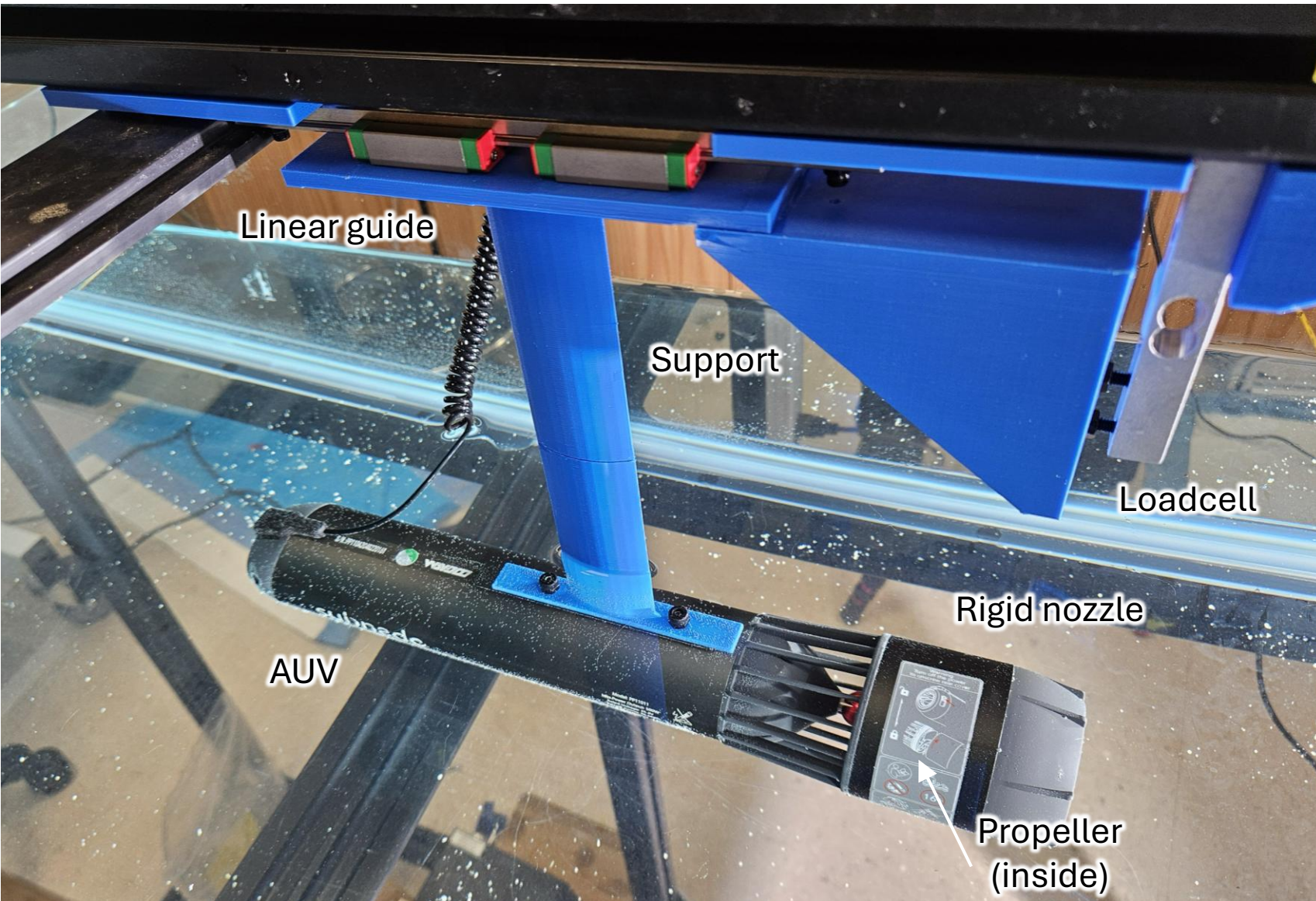


# Thrust improvement

Halley  
Wallace

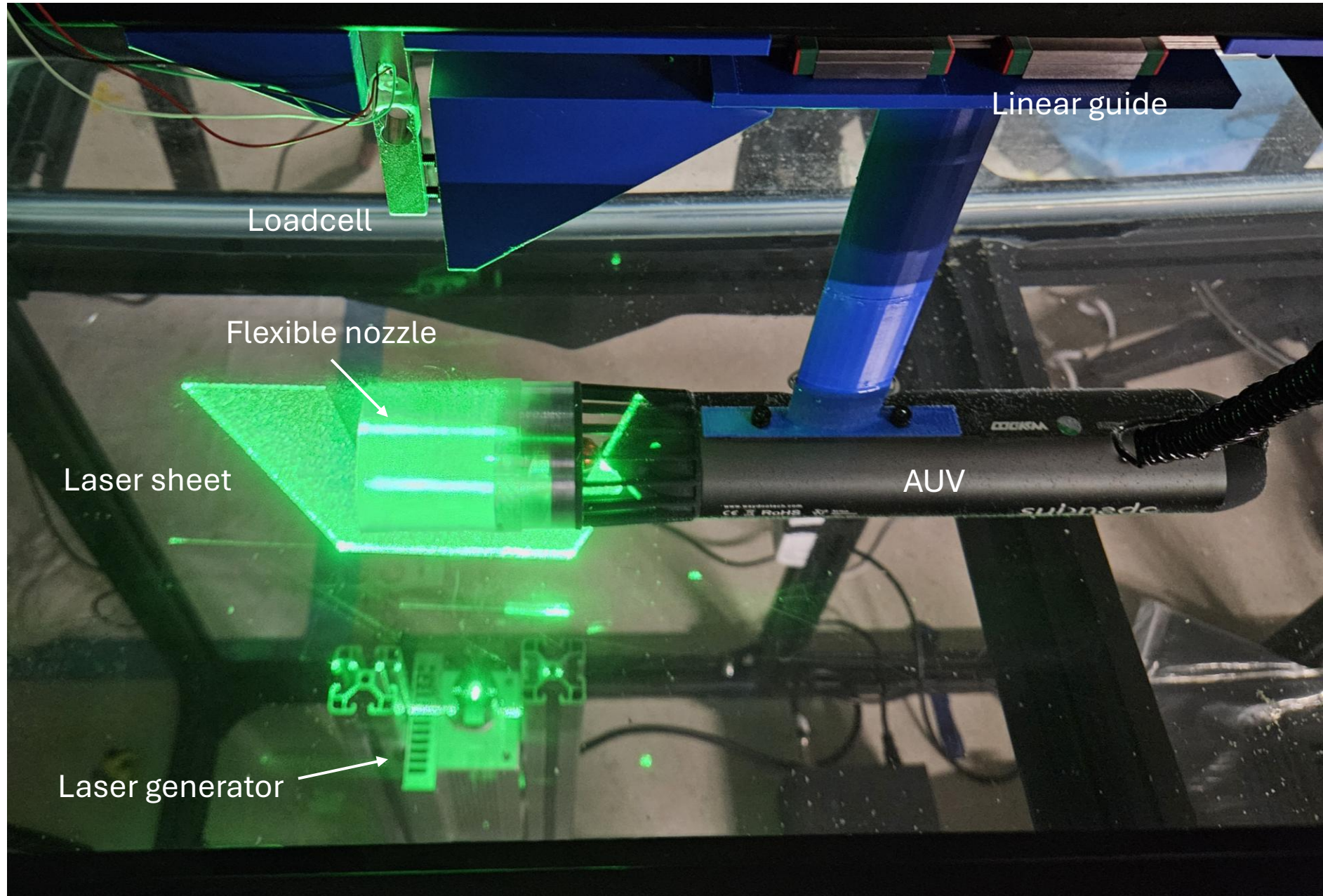


# Thrust measurement setup for AUV

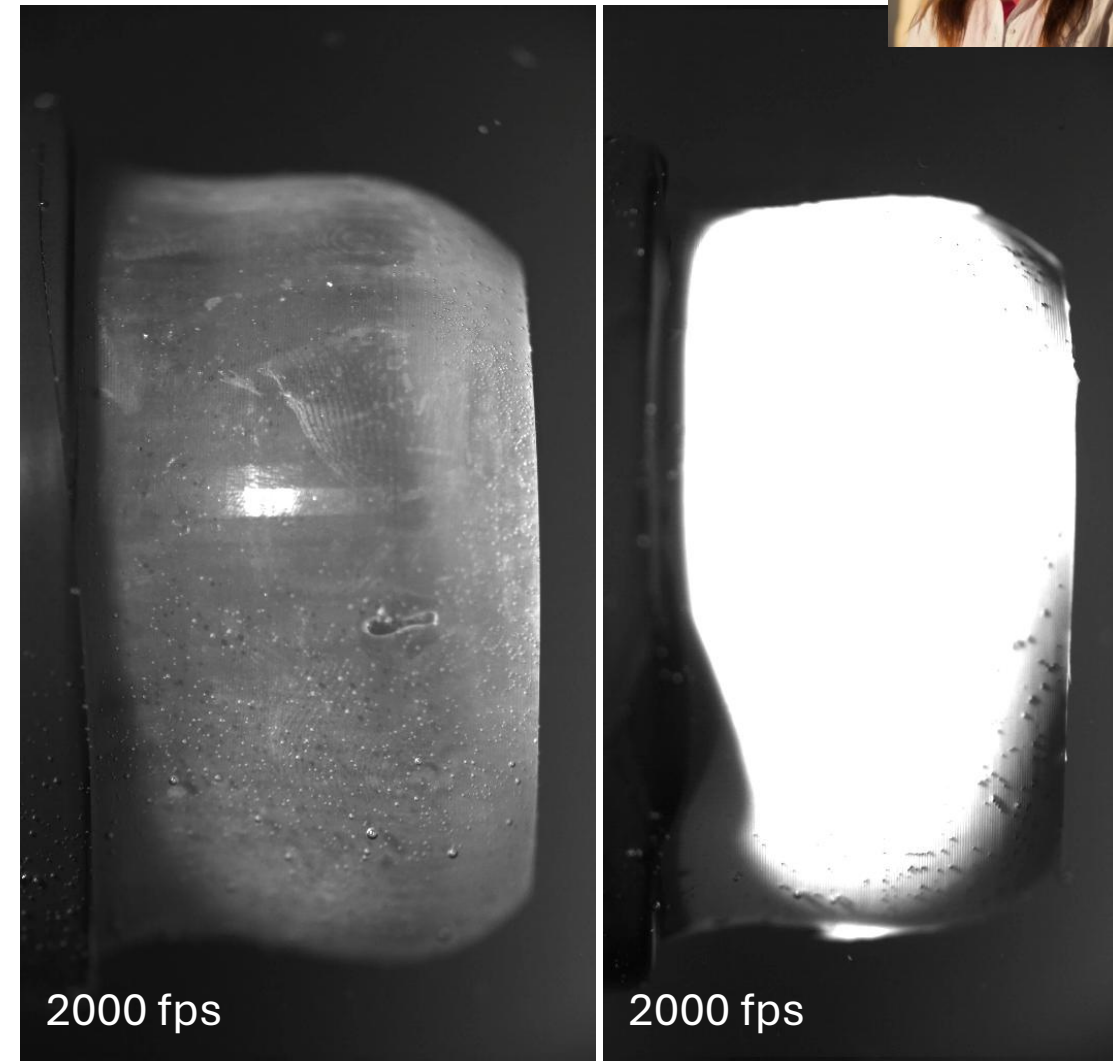
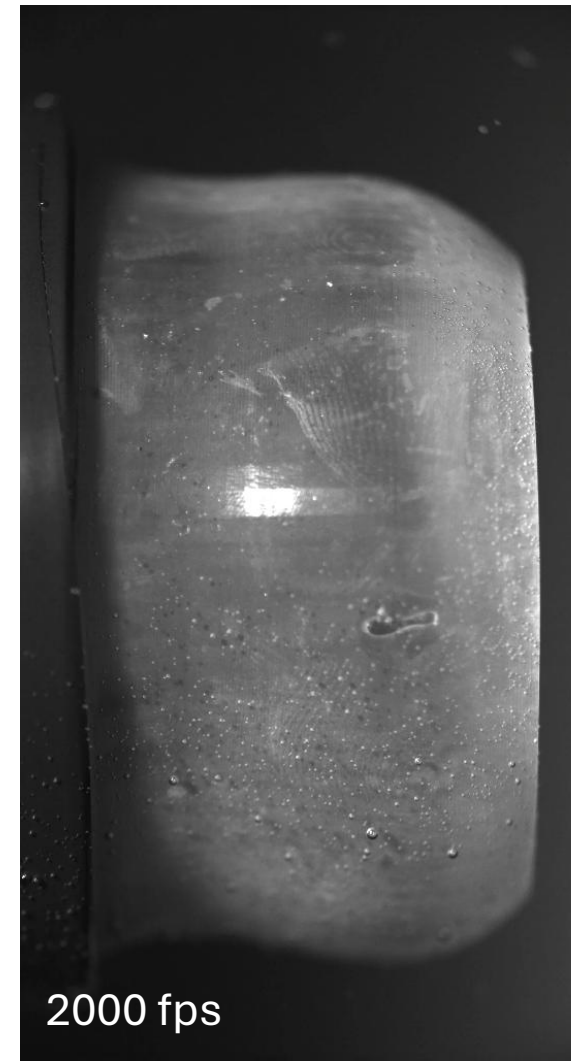
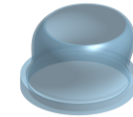
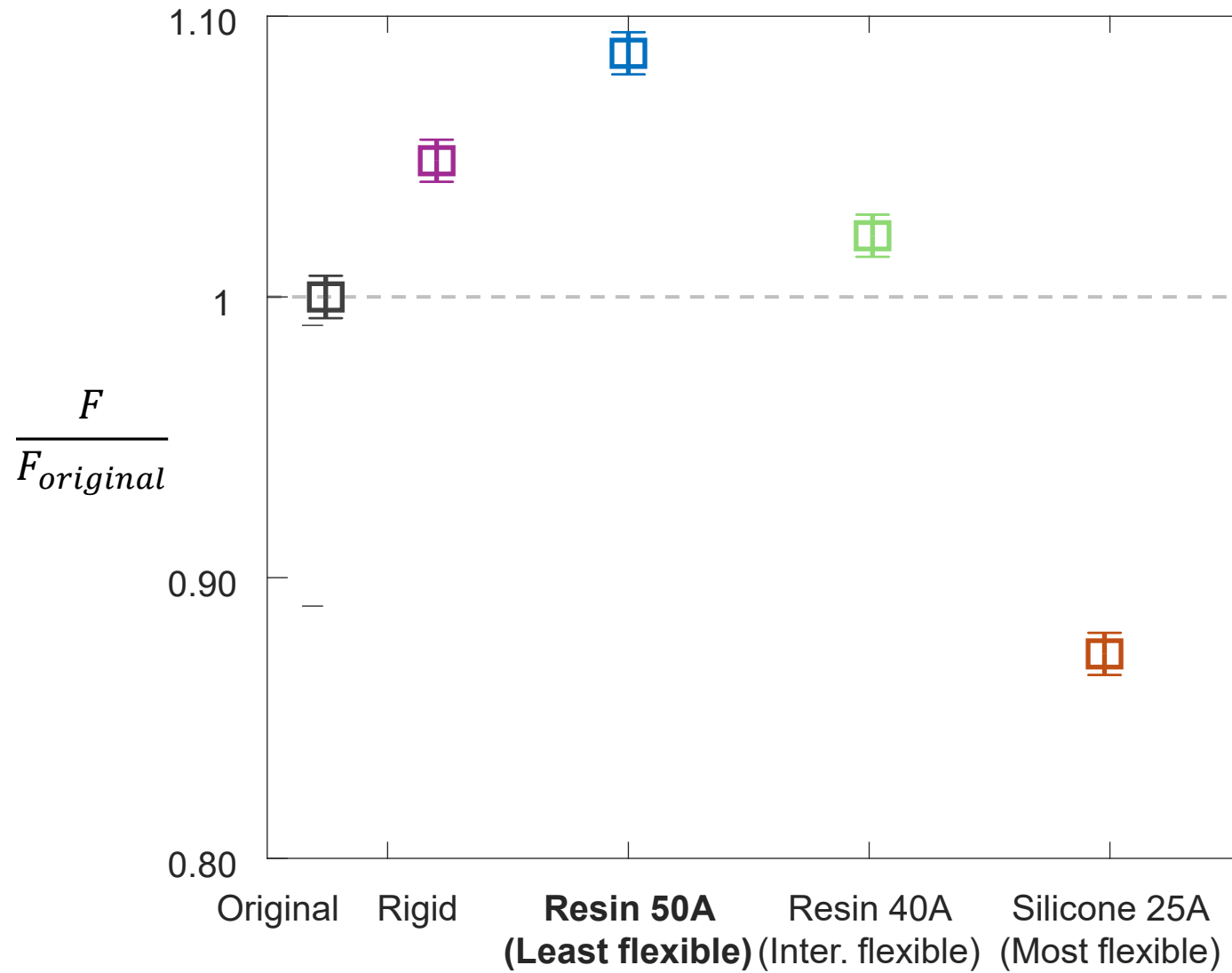


# PIV setup

- Photron Mini-X 1,000-10,000 fps
- 2.5W laser sheet
- Glass particles (50  $\mu\text{m}$ )



# Thrust Improvement – Material Comparison

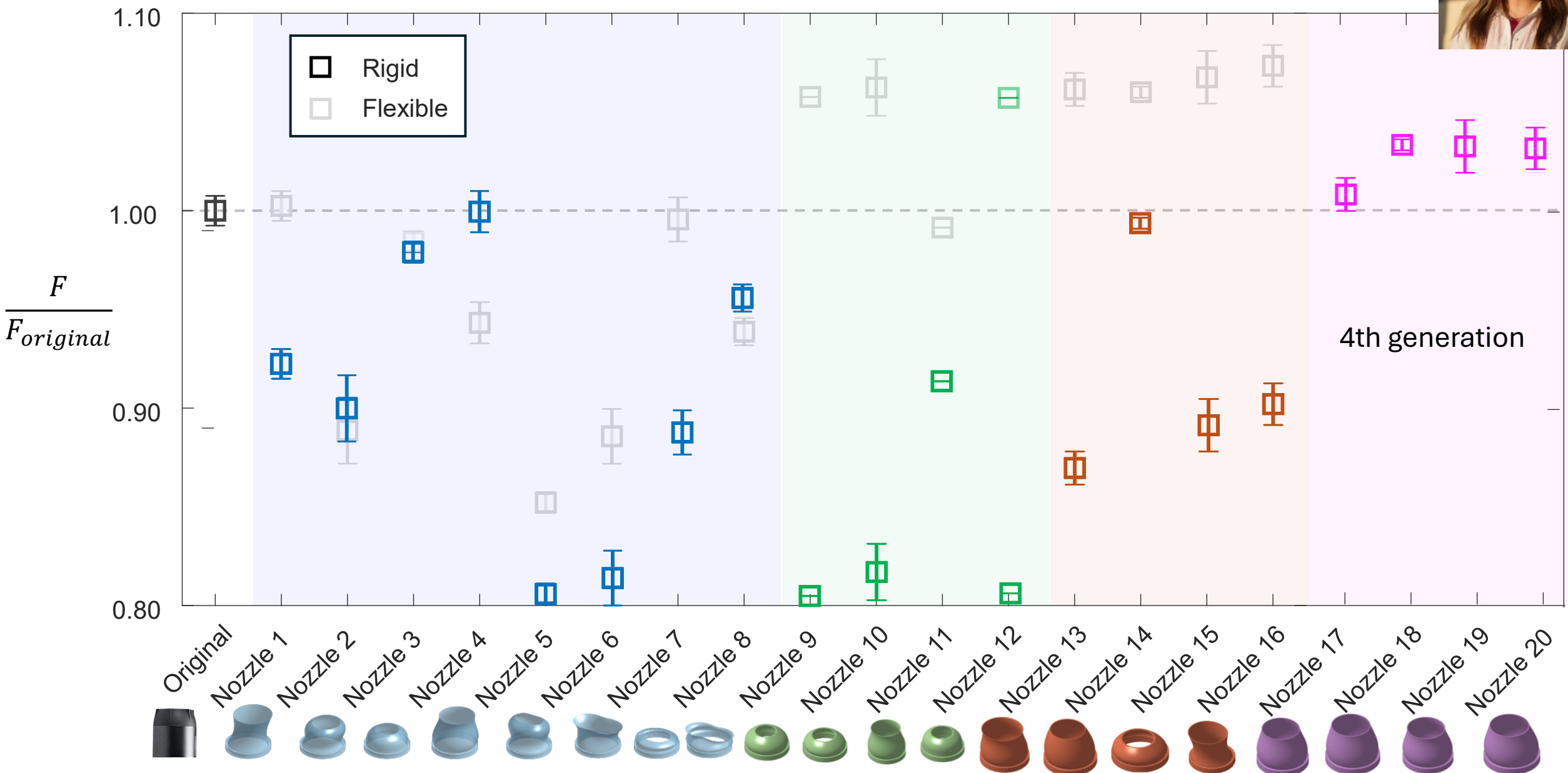


**Resin 50A**  
**(Least flexible)**



Silicone 25A  
(Most flexible)

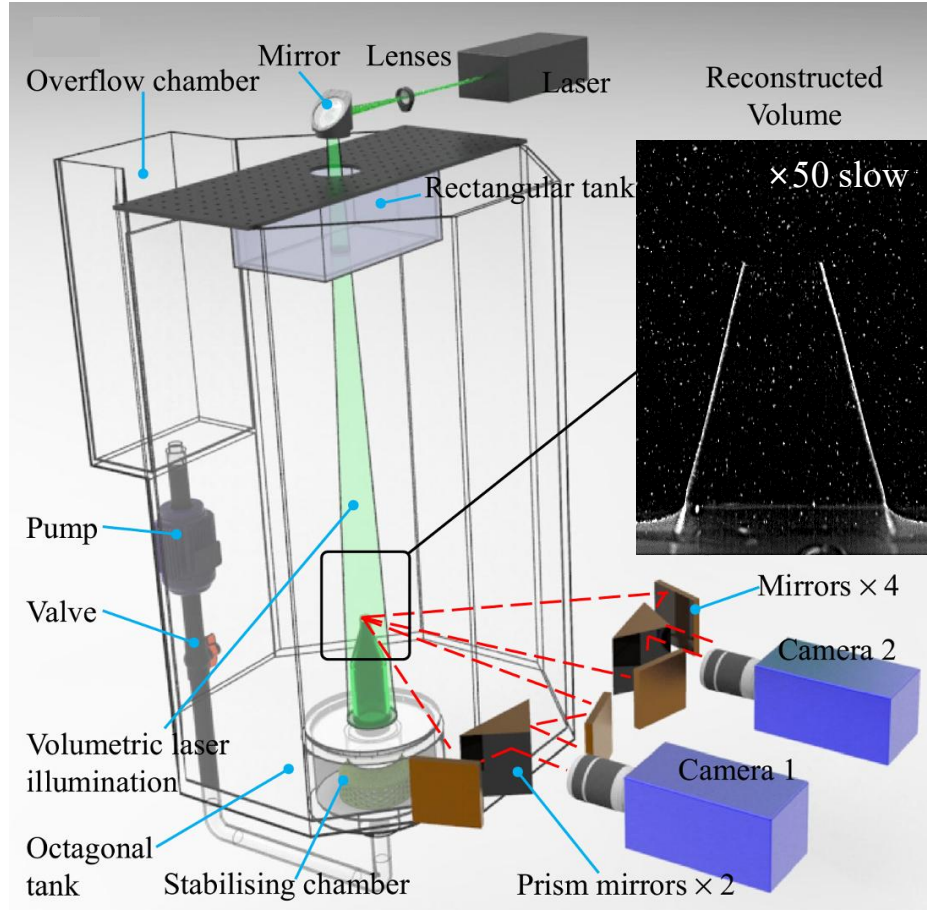
# Optimization test for rigid material



# 2D-PIV/3D-DIC measurement for $Re < 10^4$

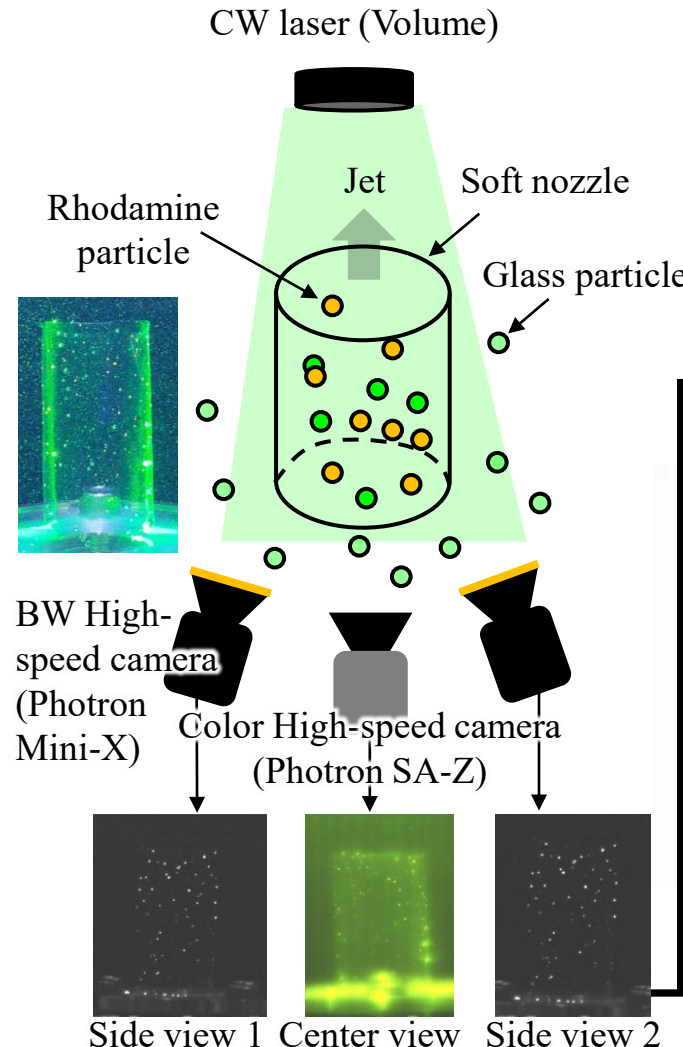


Gourav Samal

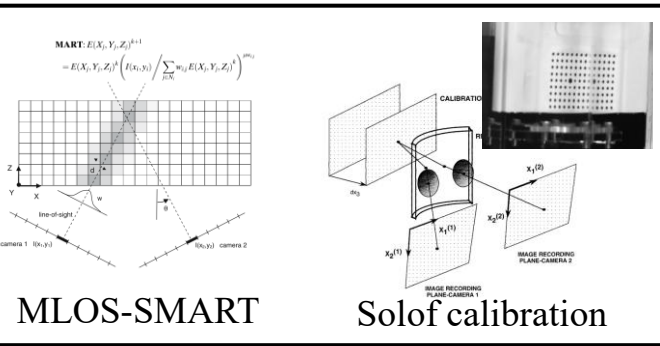


3D-DIC & 2D-PIV measurement plan

Zeng et al. 2023 EiF



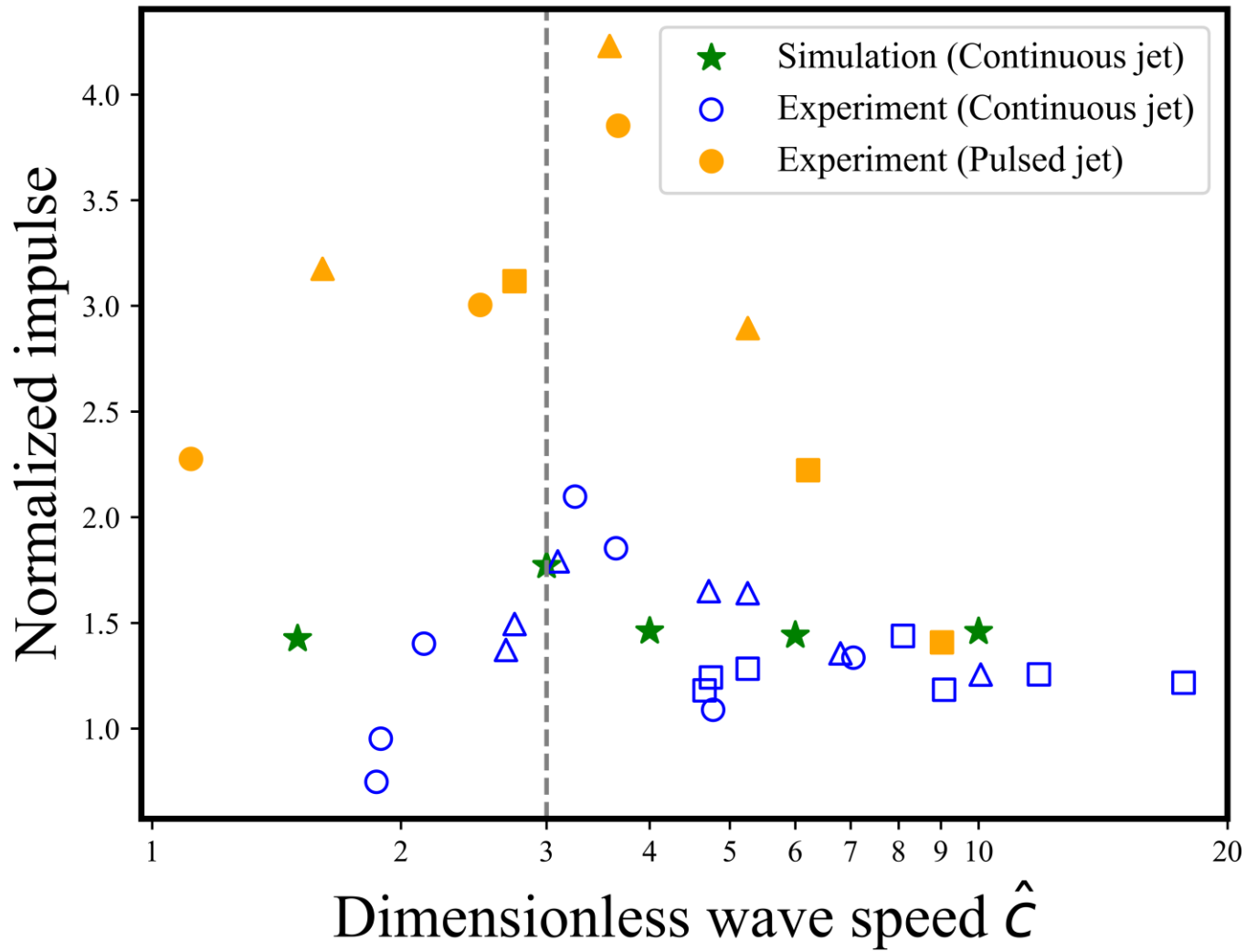
3D-DIC & 2D-PIV algorithm



Fluid-structure dynamics in soft nozzle

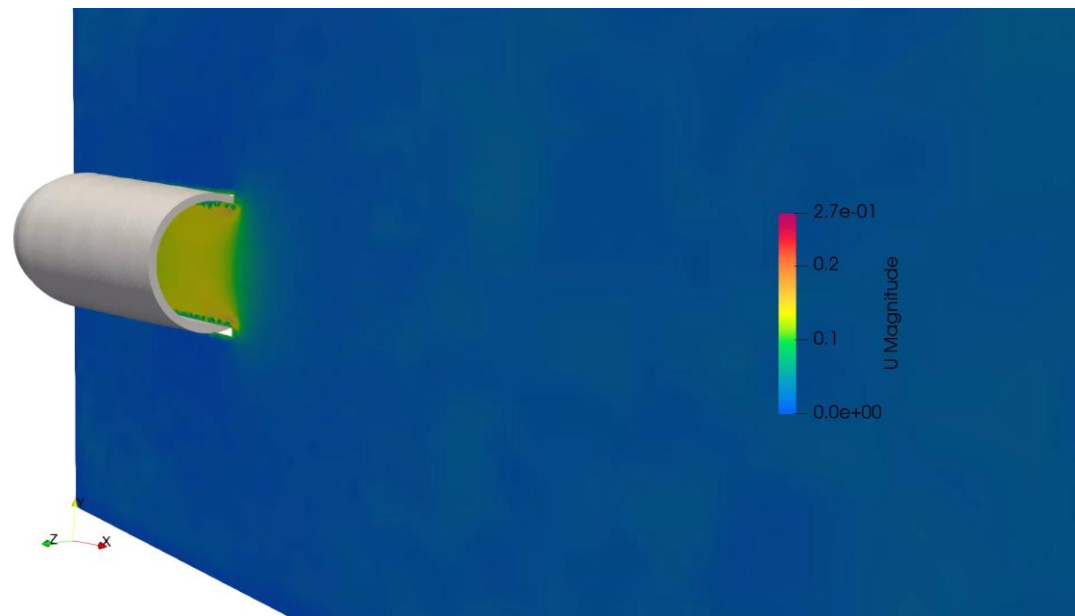
Choi. PhD Thesis 2021

# Validation of wave propagation hypothesis

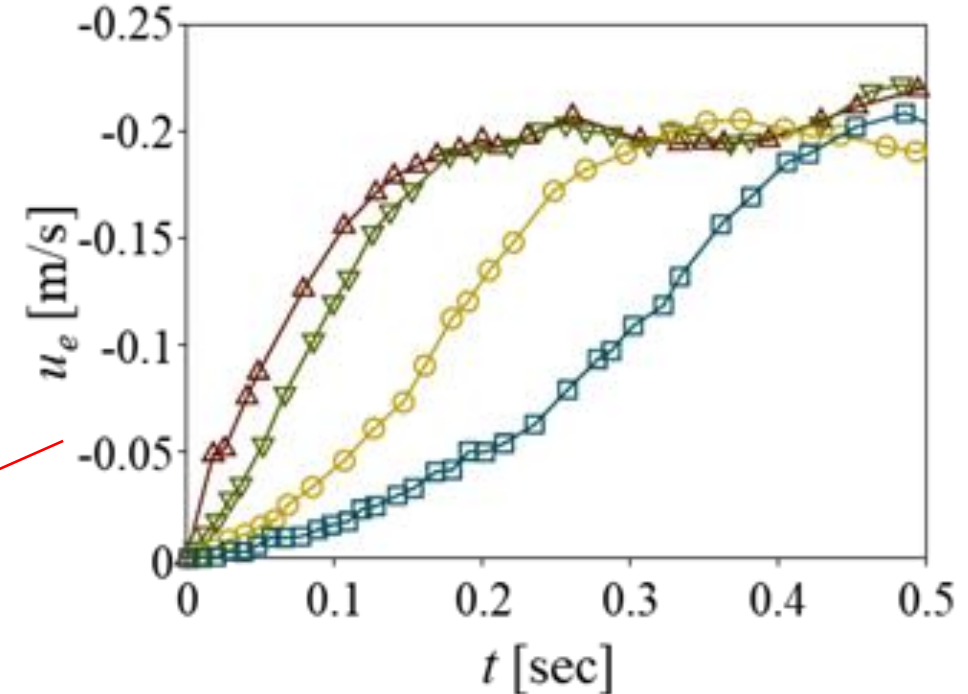
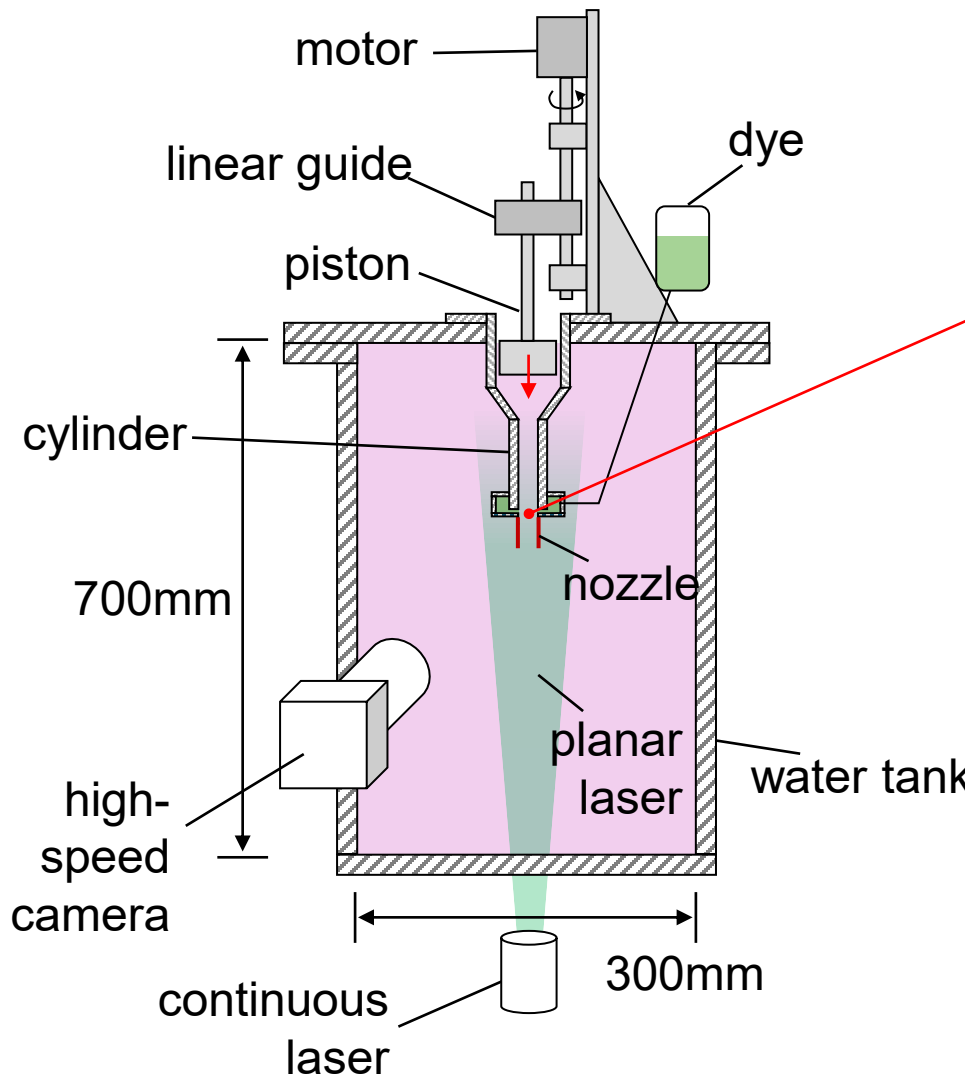


Paras Singh

Wave speed 3.0

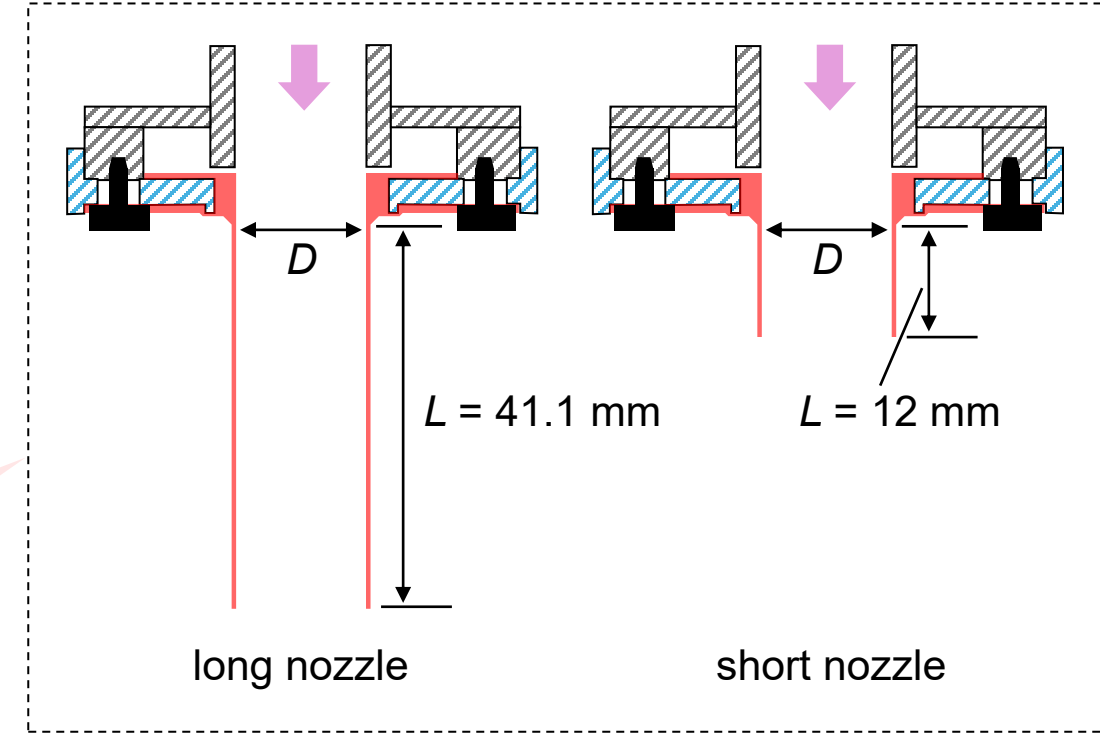
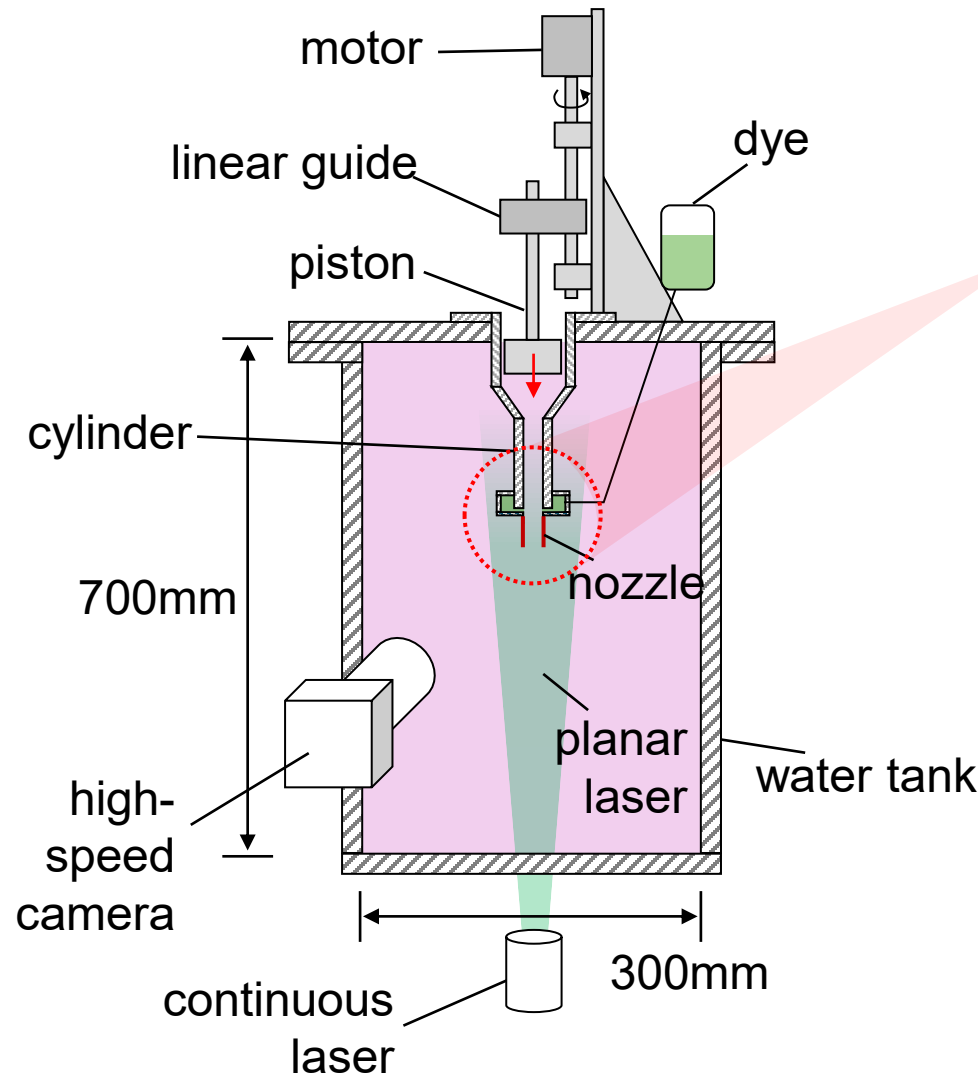


# Jet generator



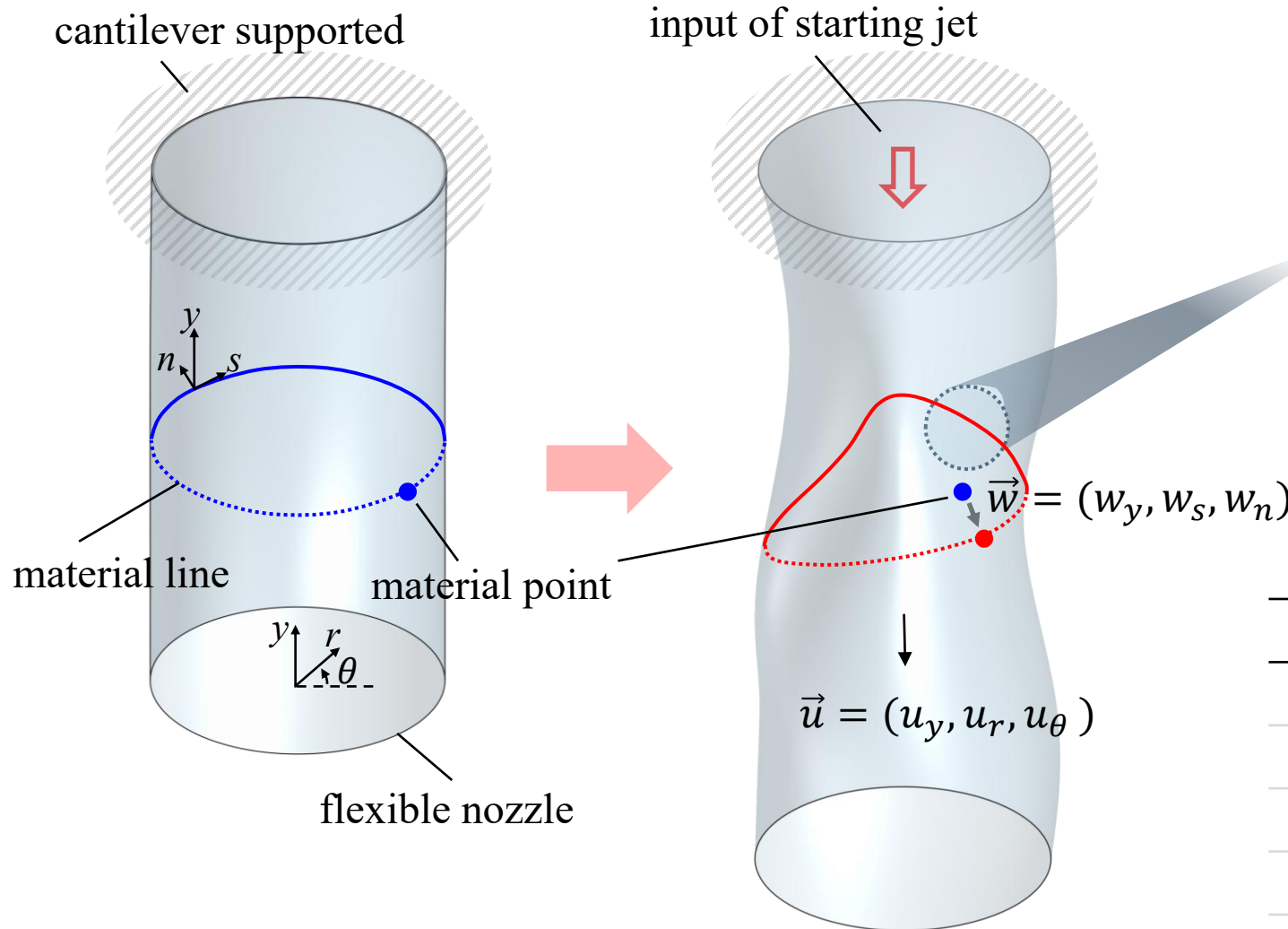
parameters	values
maximum velocity, $u_m$	0.08 - 0.24 m/s
acceleration time, $T_{acc}$	0.08 - 0.23 s
Reynolds number, $Re_j$	1,200 - 3,250
formation number, $F = L_p / D$	1.1 – 37
# of jets	4 long jets ( $F=37$ ) + 12 short jets ( $F=1.1-8.9$ )

# Flexible nozzle



parameters	values
nozzle length, $L$	12, 41 mm
nozzle diameter, $D$	15 mm
Structural stiffness, $Eh$	7.0, 14.4, 43.2 N m <sup>-1</sup>
# of nozzles	6 flexible nozzles + 2 rigid nozzles

# Governing equations for the FSI



parameters	symbol
displacement	$\vec{w}$
velocity	$\vec{u}$
shear stresses	$N$
surface stresses	$q$

# Governing equations for the FSI

- Equation of motion for the infinitesimal element
  - Flügge's shell equation (Krause 1968)

$$\frac{\partial N_{yy}}{\partial y} + \frac{\partial N_{ys}}{\partial s} + q_y = \rho_n h \frac{\partial^2 w_y}{\partial t^2}$$

$$\frac{\partial N_{yn}}{\partial y} + \frac{\partial N_{sn}}{\partial s} - \frac{N_{ss}}{R} - \textcolor{red}{q}_n = \rho_n h \frac{\partial^2 w_n}{\partial t^2}$$

parameters	symbols
surface stresses	$q$
shear stresses	$N$
displacement	$\vec{w} = (w_y, w_s, w_n)$
velocity	$\vec{u} = (u_y, u_r, u_\theta)$
nozzle density	$\rho_n$

- Mass-momentum conservation inside the tube
  - Tube law (Shapiro 1977)

$$\frac{\partial A}{\partial t} + \frac{\partial Q}{\partial y} = 0$$

$$\frac{\partial Q}{\partial t} + \frac{\partial (uQ)}{\partial y} + \frac{A}{\rho_f} \frac{\partial \textcolor{red}{q}_n}{\partial y} = -C_R u$$

parameters	symbols
cross-sectional area	$A$
volume flux	$Q$
bulk velocity	$u$
pressure	$q_n$
liquid density	$\rho_f$

# Governing equations for the FSI

- Governing equation
  - Dimensionless form

$$\frac{1}{\Pi_0} \frac{\partial \hat{w}_y}{\partial \hat{t}} + \hat{u} \frac{\partial \hat{w}_n}{\partial \hat{y}} + \frac{1 + \hat{w}_n}{2} \frac{\partial \hat{u}}{\partial \hat{y}} = 0$$

$$\frac{1}{\Pi_0} \frac{\partial \hat{u}}{\partial \hat{t}} + \hat{u} \frac{\partial \hat{u}}{\partial \hat{y}} + \Pi_1 \frac{\partial \hat{w}_n}{\partial \hat{y}} = 0$$

- Dimensionless parameters

$$\Pi_0 = \frac{u_m T_{acc}}{L} \quad \Pi_1 = \frac{Eh}{2\rho_f u_m^2 R}$$

Assumptions :

- 1) axisymmetric and
- 2) small deformation

parameters	symbols
displacement	$w$
velocity	$u$
nozzle length	$L$
nozzle radius	$R$
Young's modulus	$E$
liquid density	$\rho_f$
maximum velocity	$u_m$
acceleration time	$T_{acc}$

: effective acceleration time

$\sim St_L^{-1} \rightarrow$  Strouhal number  
(Kang et al. 2011)

: effective nozzle stiffness

$\sim \frac{\text{material stiffness}}{\text{liquid momentum}} \rightarrow$  aerodynamic stiffness  
(Siviglia & Toffolon 2014)

# Governing equations for the FSI

- Governing equation
  - Dimensionless form

$$\frac{1}{\Pi_0} \frac{\partial \hat{w}_y}{\partial \hat{t}} + \hat{u} \frac{\partial \hat{w}_n}{\partial \hat{y}} + \frac{1 + \hat{w}_n}{2} \frac{\partial \hat{u}}{\partial \hat{y}} = 0$$

$$\frac{1}{\Pi_0} \frac{\partial \hat{u}}{\partial \hat{t}} + \hat{u} \frac{\partial \hat{u}}{\partial \hat{y}} + \Pi_1 \frac{\partial \hat{w}_n}{\partial \hat{y}} = 0$$

Assumptions :  
at the initial state of acceleration  
( $t \ll T_{acc}$ ),  
1) small deformation ( $\hat{w}_n \ll 1$ )  
2) small bulk velocity ( $\hat{u} \ll 1$ )

- Dimensionless parameters

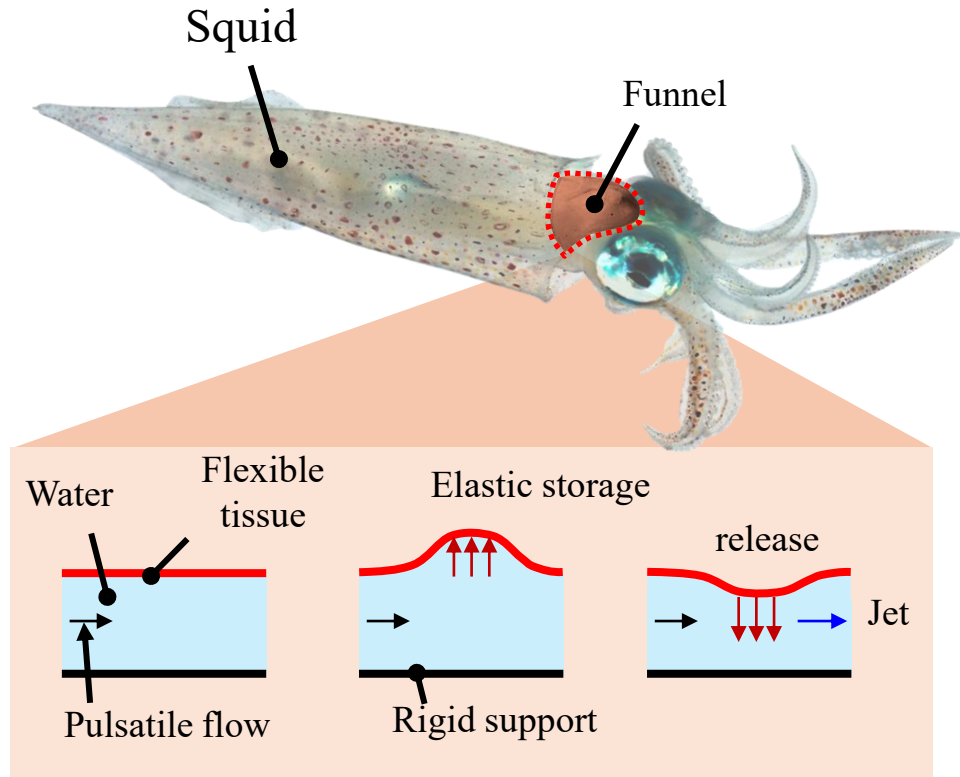
$$\Pi_0 = \frac{u_m T_{acc}}{L} \quad \Pi_1 = \frac{Eh}{2 \rho_f u_m^2 R}$$

$$\frac{\partial^2 \hat{w}_n}{\partial \hat{t}^2} - \hat{c}^2 \frac{\partial^2 \hat{w}_n}{\partial \hat{y}^2} = 0$$

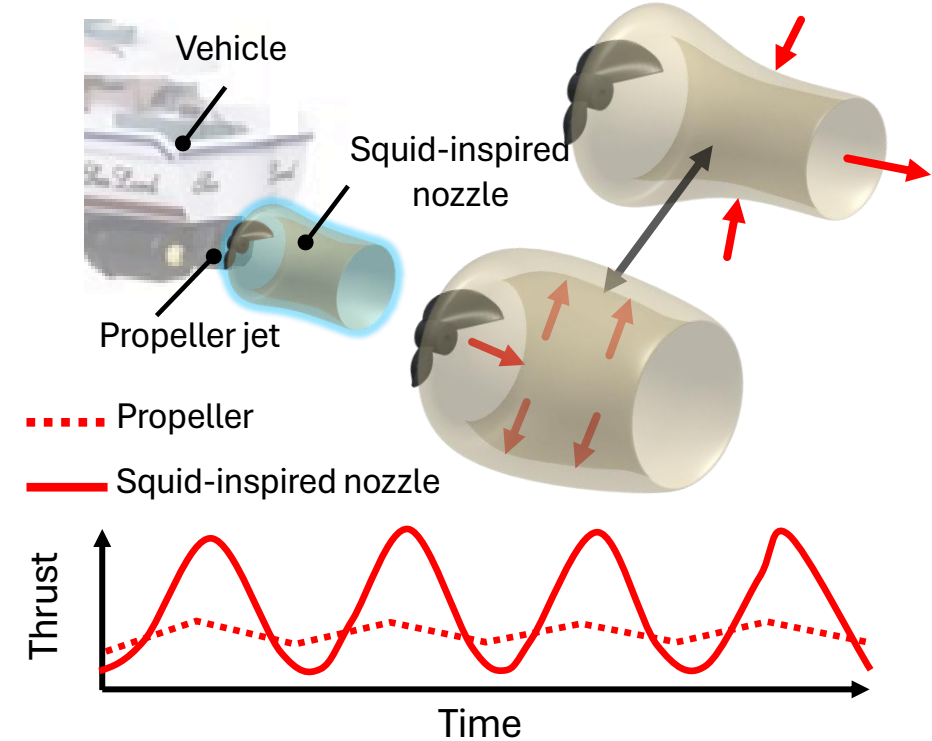
$$\text{where } \hat{c} = \left( \Pi_0^2 \Pi_1 / 2 \right)^{0.5}$$

wave equation for nozzle deformation

# Objectives



**Squid-inspired power redistribution** from hydrodynamic instability.

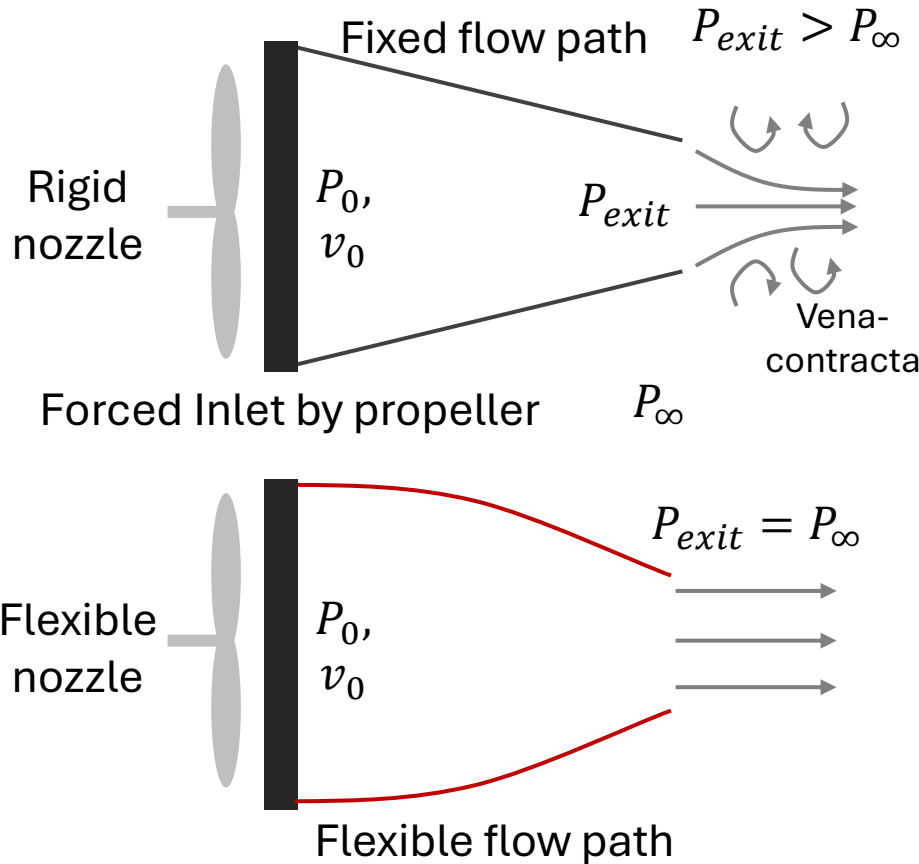


The highest vehicle efficiency of 80% and reducing fuel consumption.

# Hypothesis

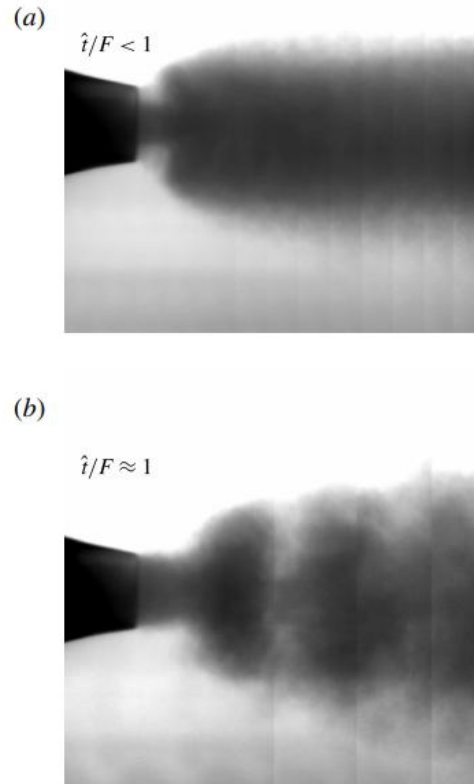
(Needs to be obtained by 3D measurement and CFD)

## 1. Shape optimization



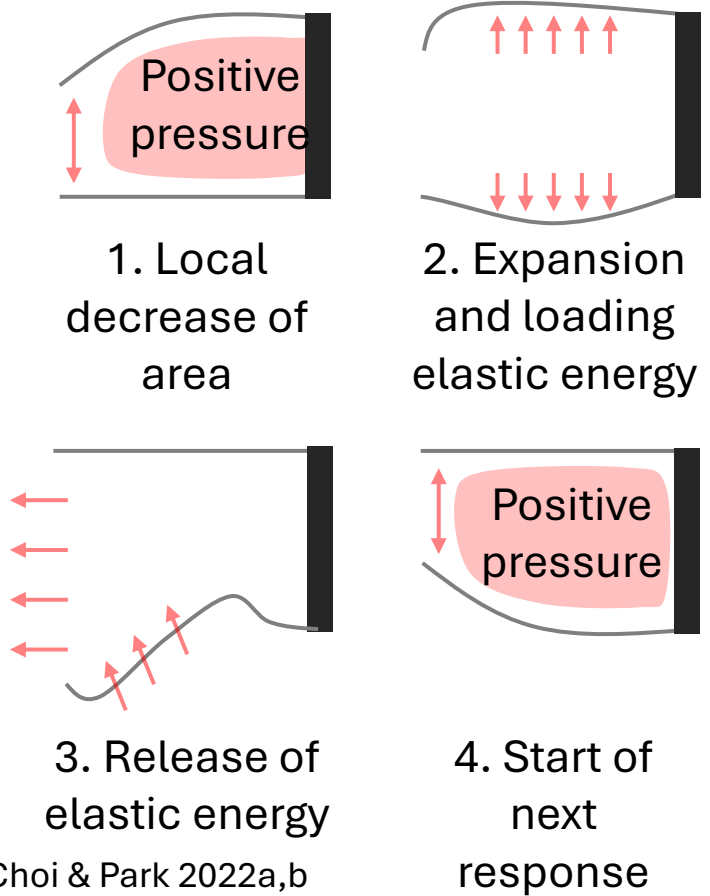
Nozzle can adapt according to the propeller condition

## 2. Pulsed jet effect



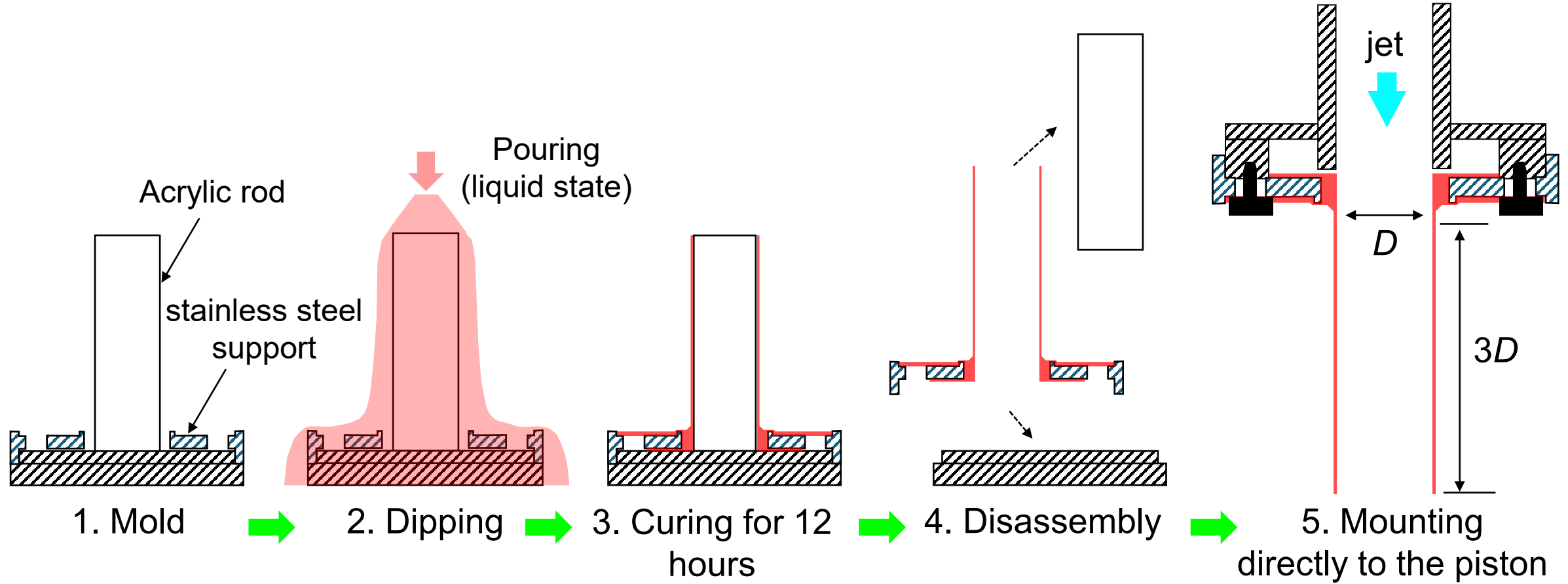
Whittlesey & Dabari 2013  
Pulsed jet is more efficient than continuous jet

## 3. Power amplification

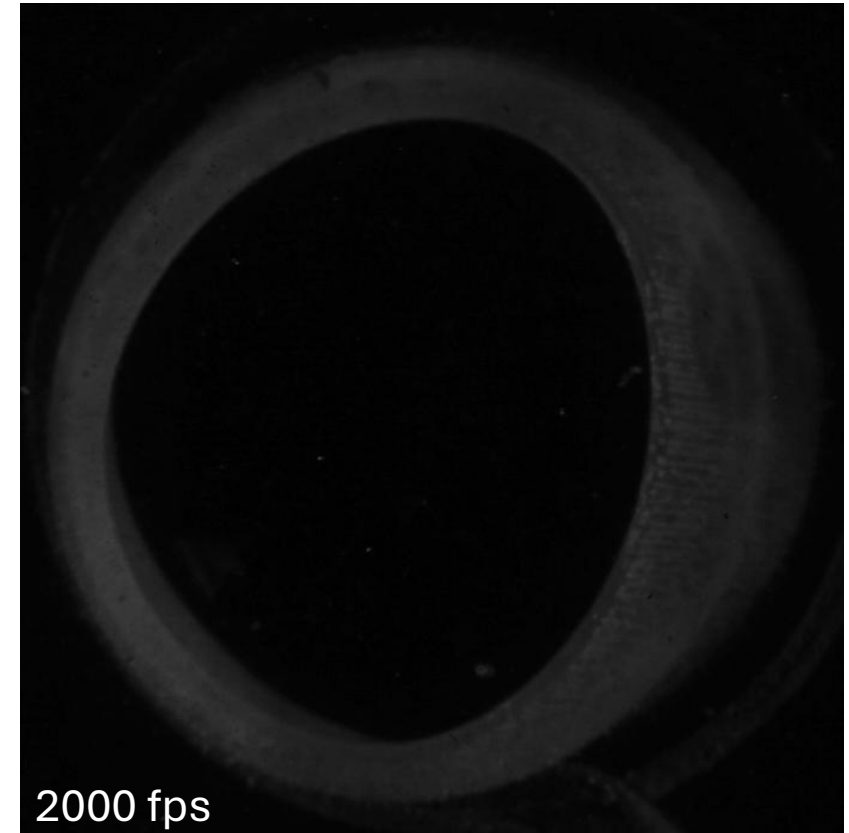


Choi & Park 2022a,b  
Flexible nozzle can amplify the pulsed jet

# Nozzle manufacturing



# FSI – Rear View



2000 fps

Printed Flexible 50A  
(Least Flexible)



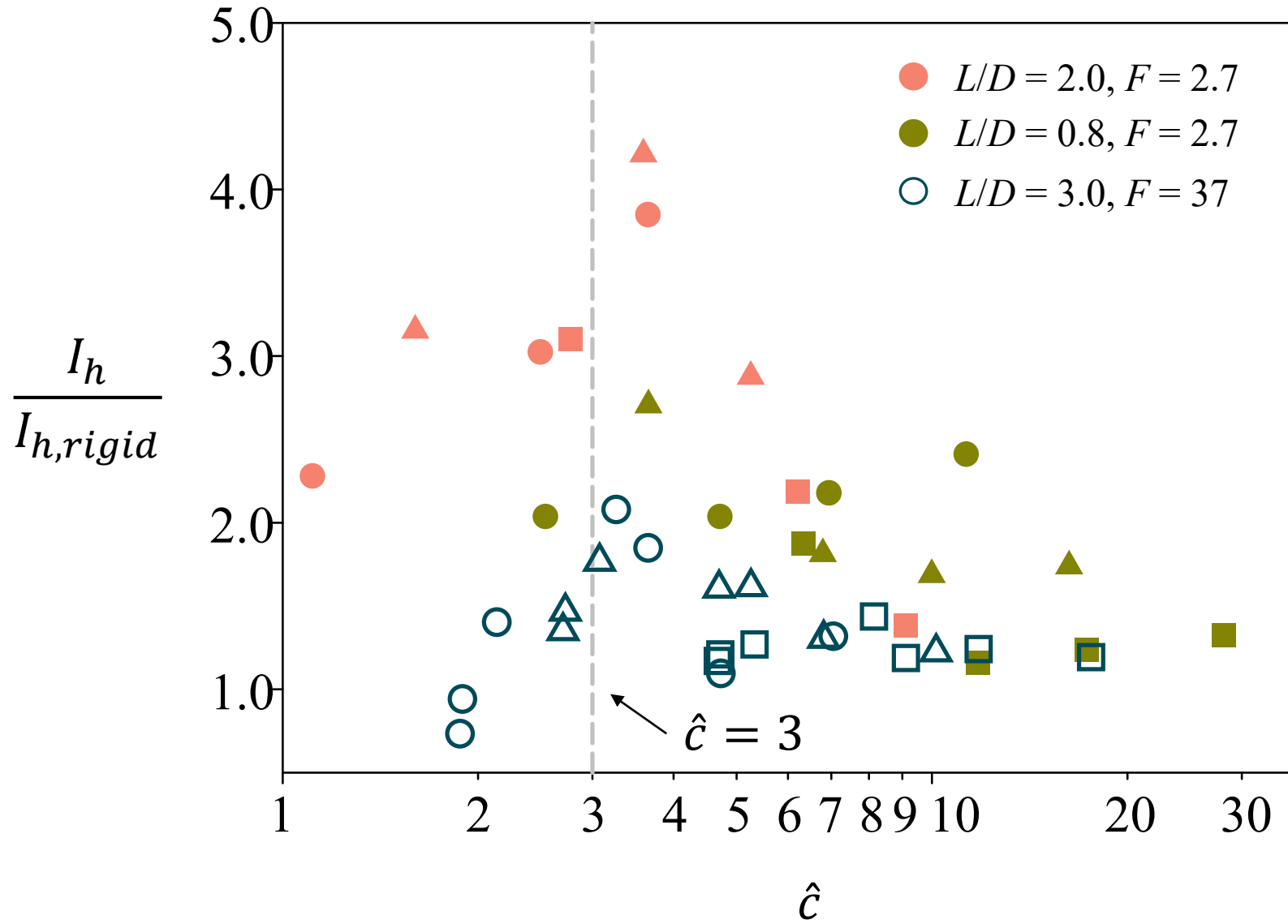
240 fps

Printed Silicone 40A  
(Intermediate Flexible)



240 fps

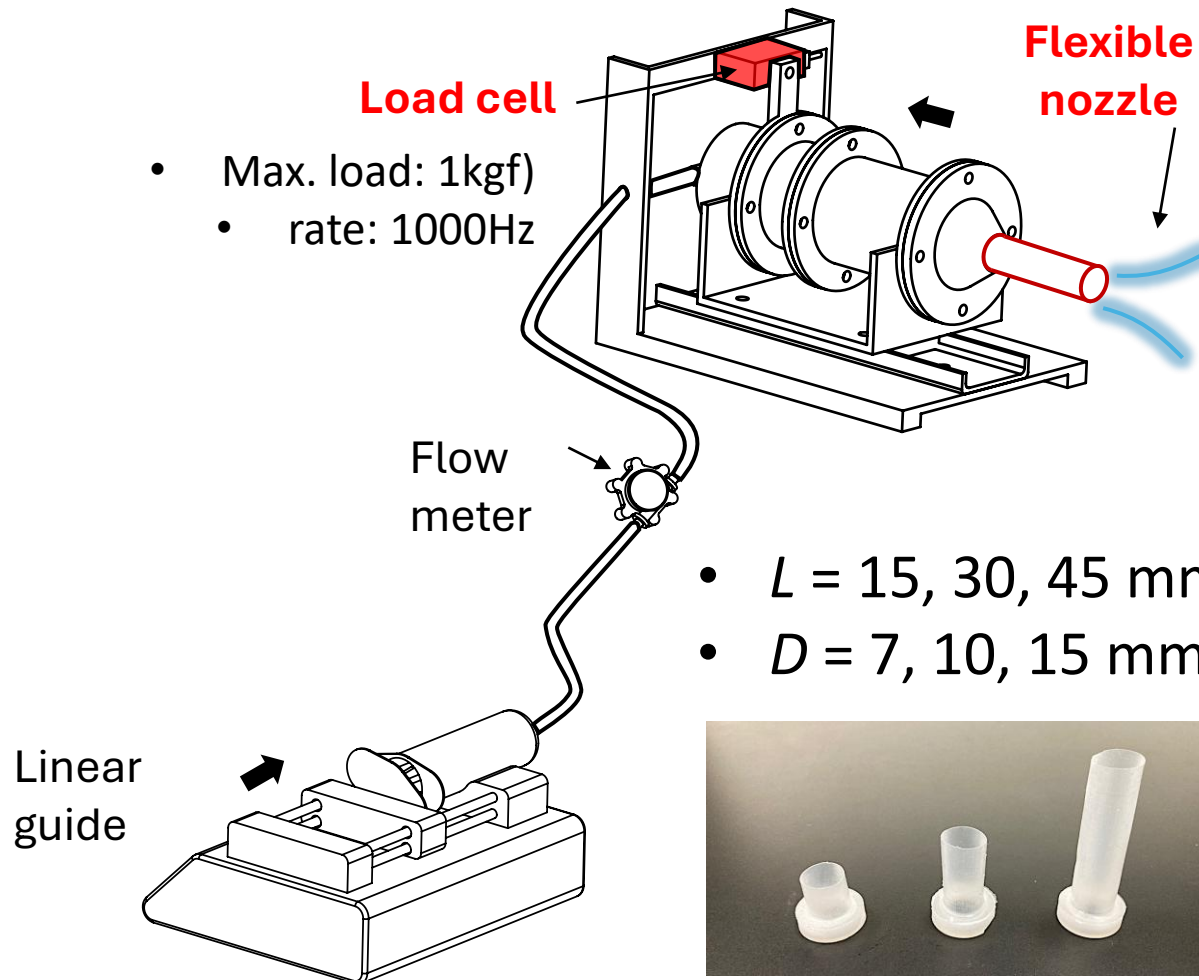
Silicone Molded 25A  
(Most Flexible)



- less flexible ( $\Pi_1 = 120$ )
  - moderate flexible ( $\Pi_1 = 40$ )
  - most flexible ( $\Pi_1 = 19$ )
- $L/D = 2.7, \text{continuous}$
  - $L/D = 1.0, \text{pulsed}$
  - $L/D = 2.0, \text{pulsed}$

# Thrust generation

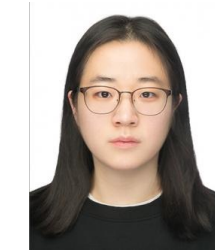
- Jet generator



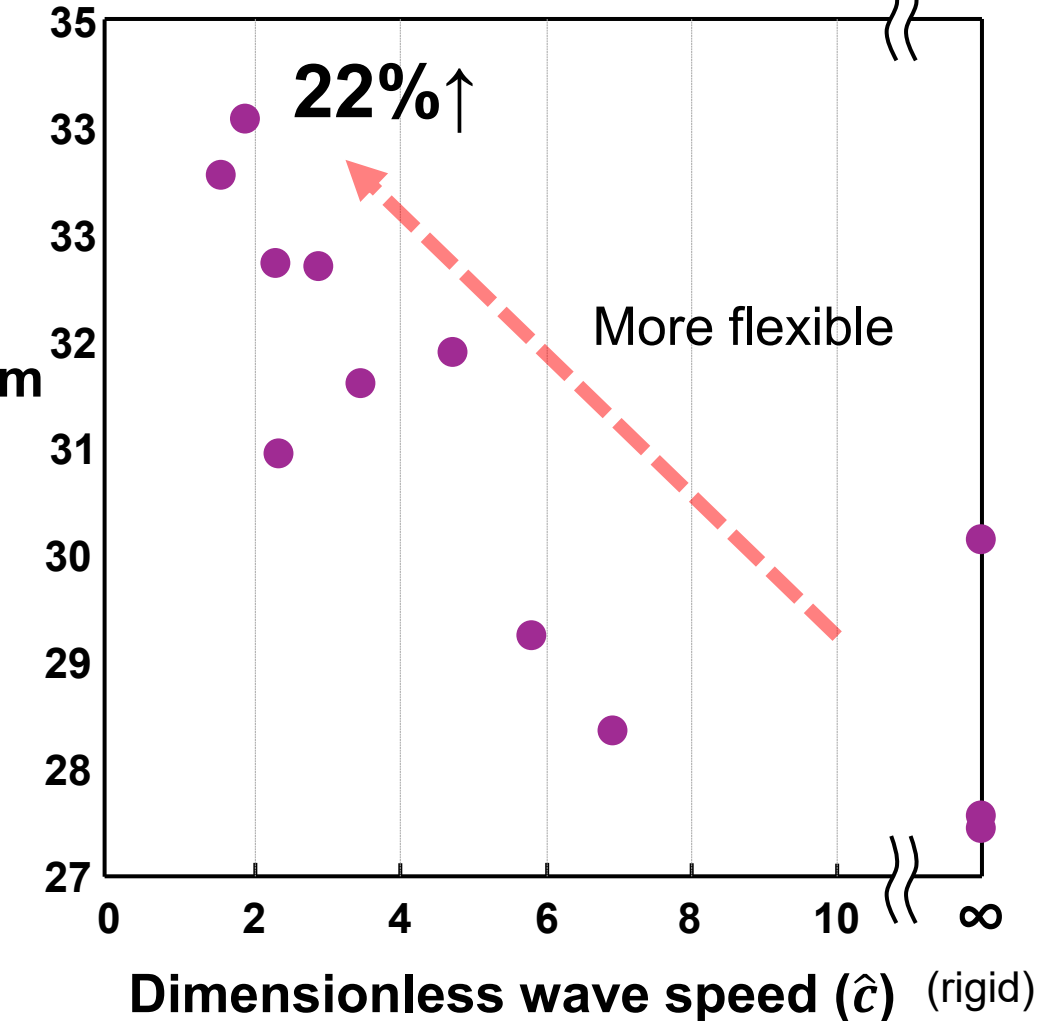
$$\hat{c} = \sqrt{\frac{EhT_{acc}^2}{2\rho_f D L^2}}$$



Minho Kim



Jieun Park

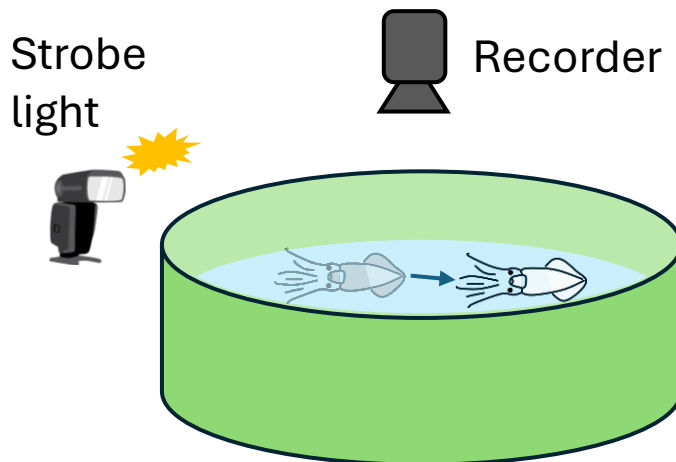


# Pool test

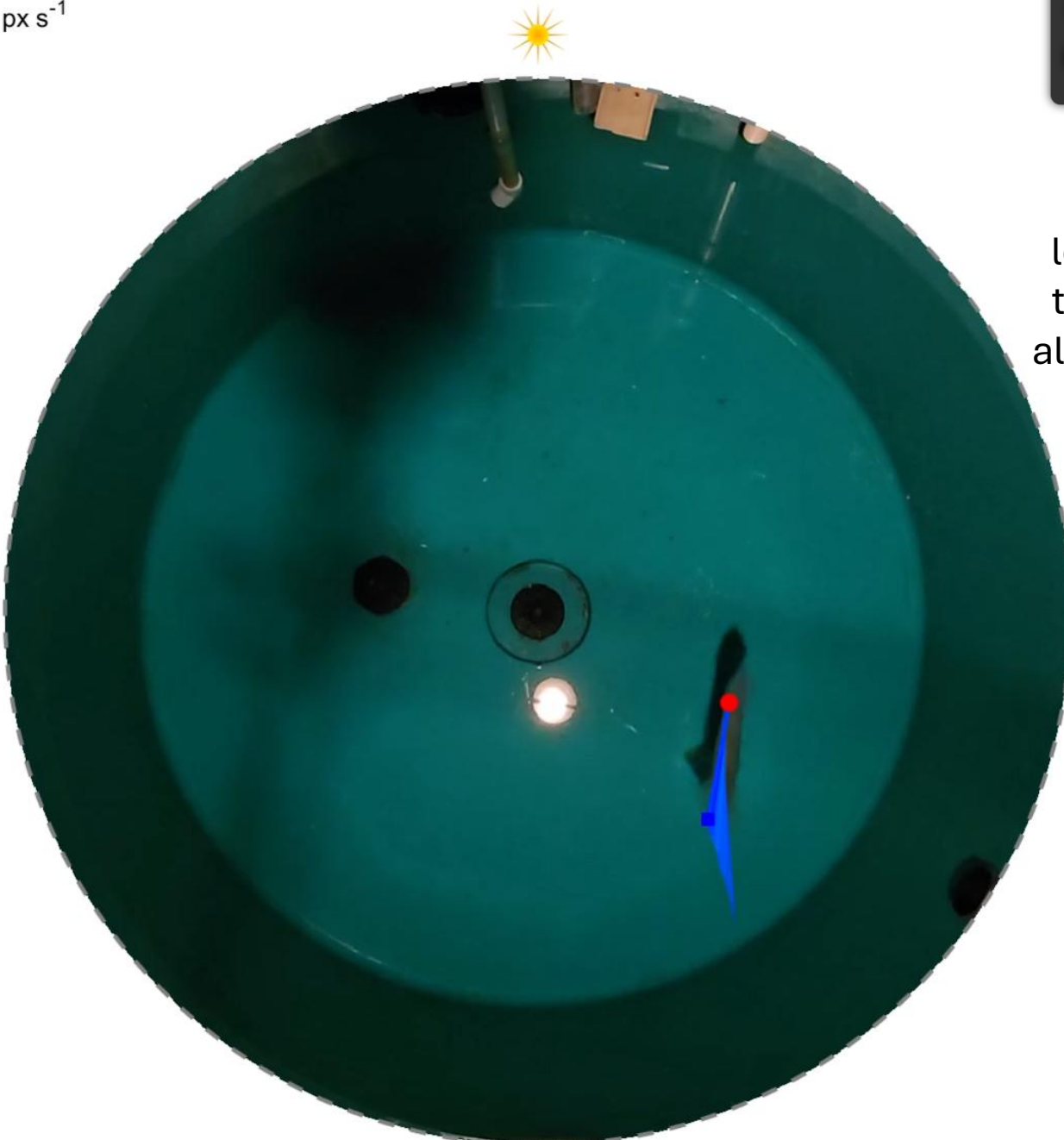
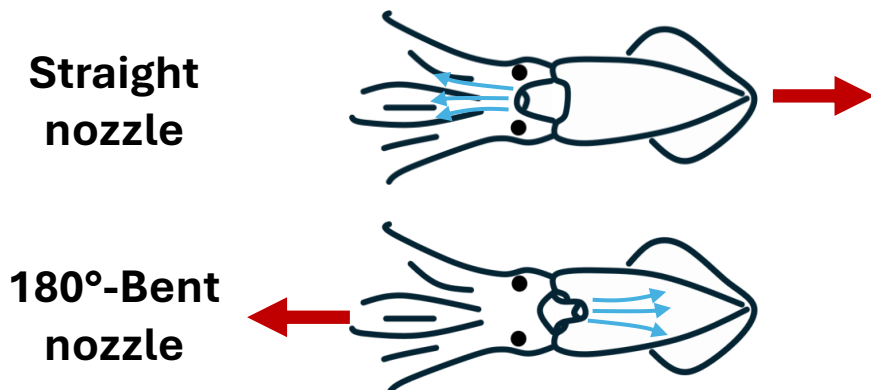
Frame 2127  
Time 70.87 s  
Speed 87.5 px s<sup>-1</sup>



SLEAP  
(Deep  
learning  
tracking  
algorithm)



**Pool test for  
strobe reflex**

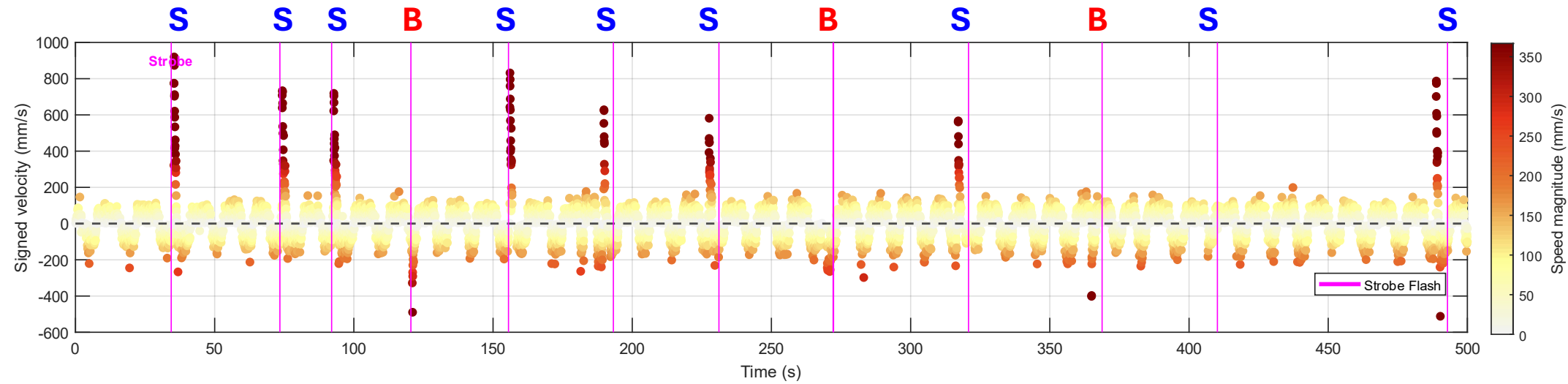


# Squid #2 (Velocity)

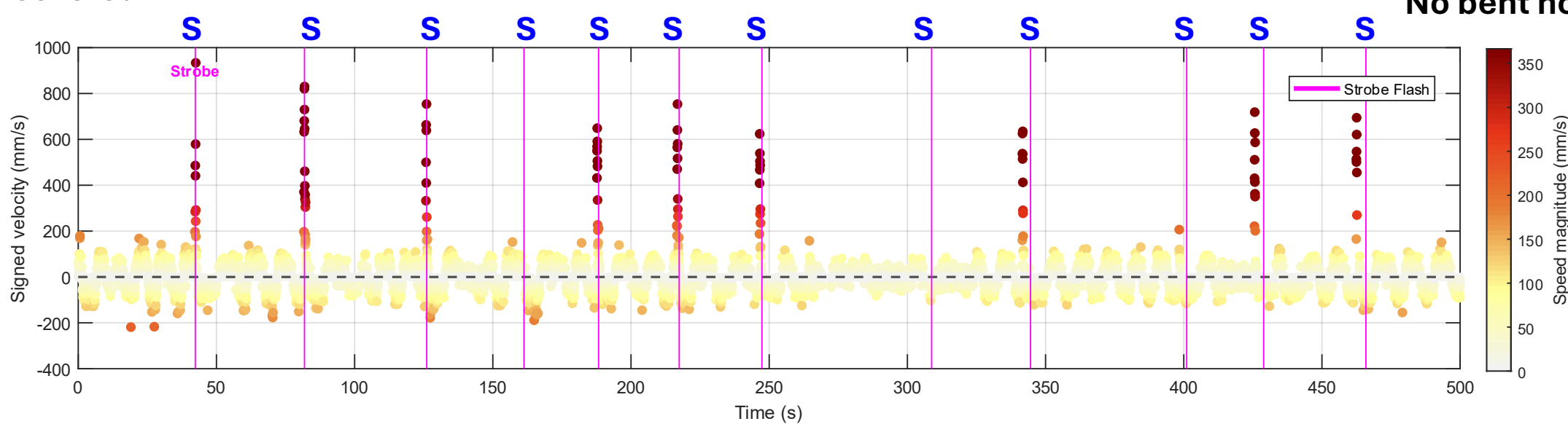
**S: straight nozzle**

**B: bent nozzle**

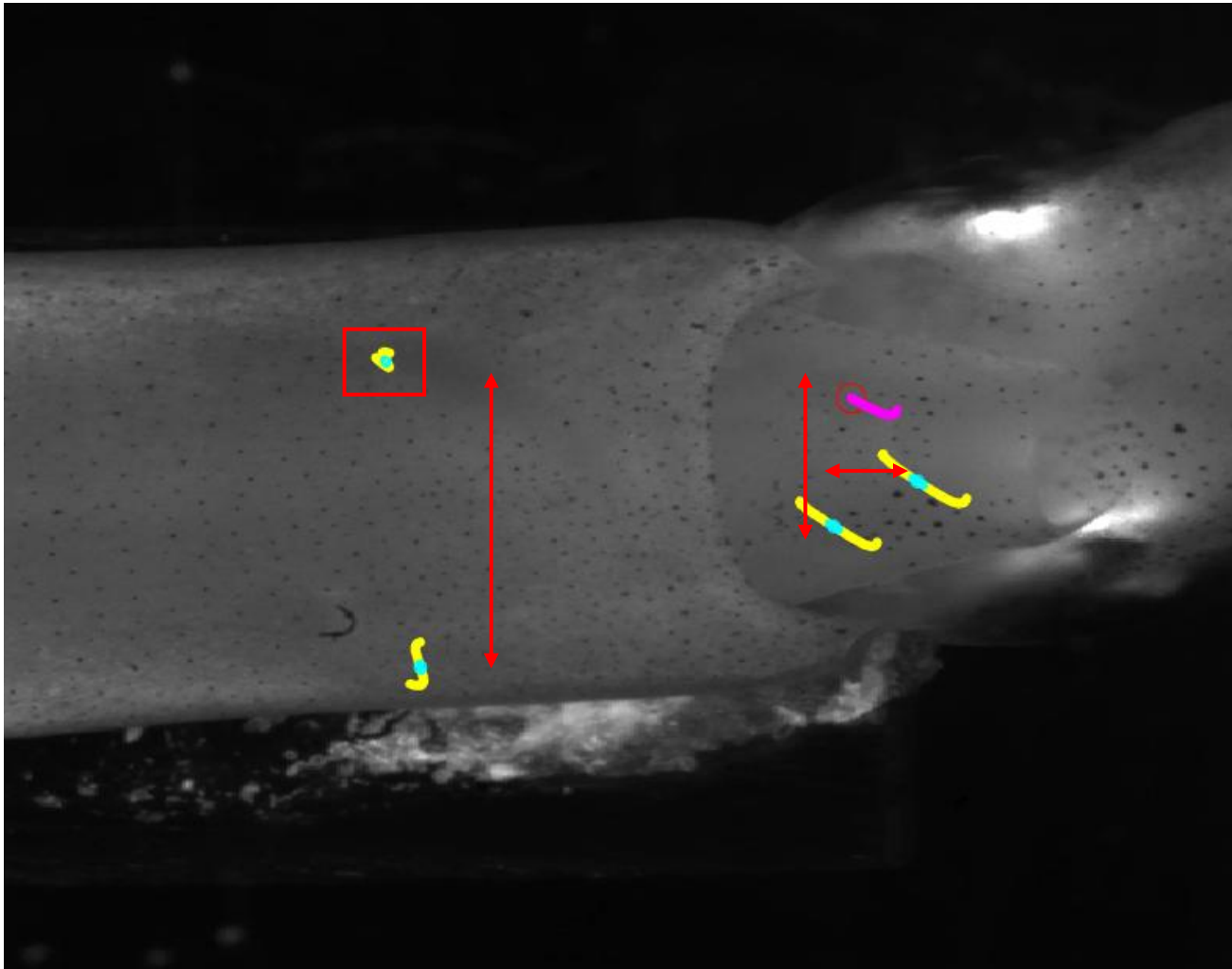
## Normal



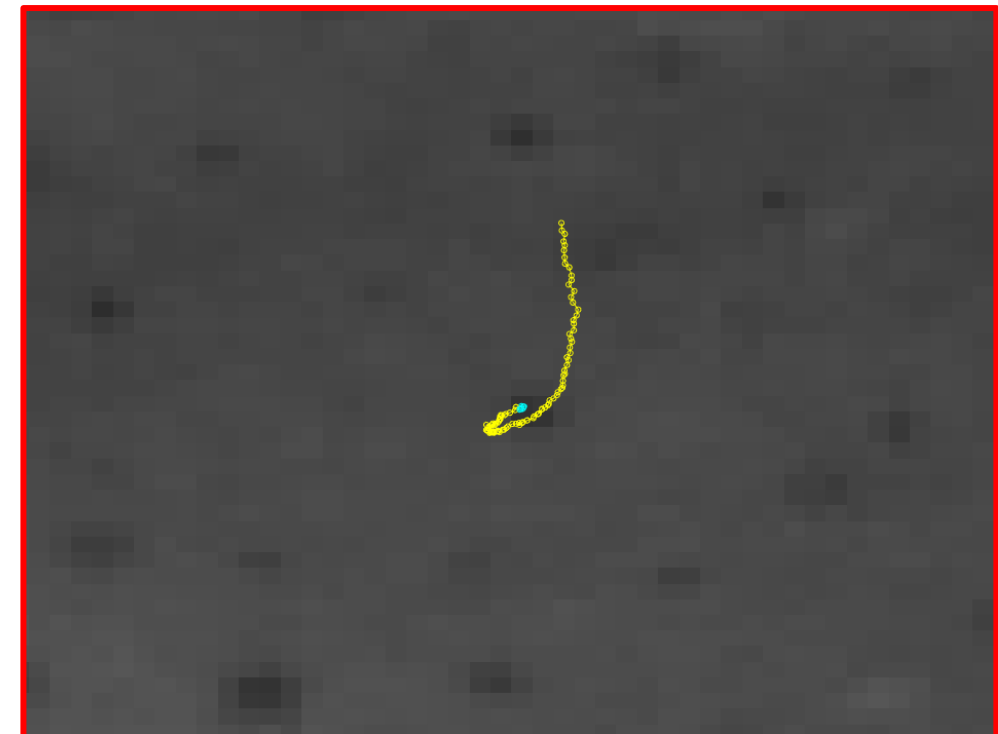
## Nerve-severed



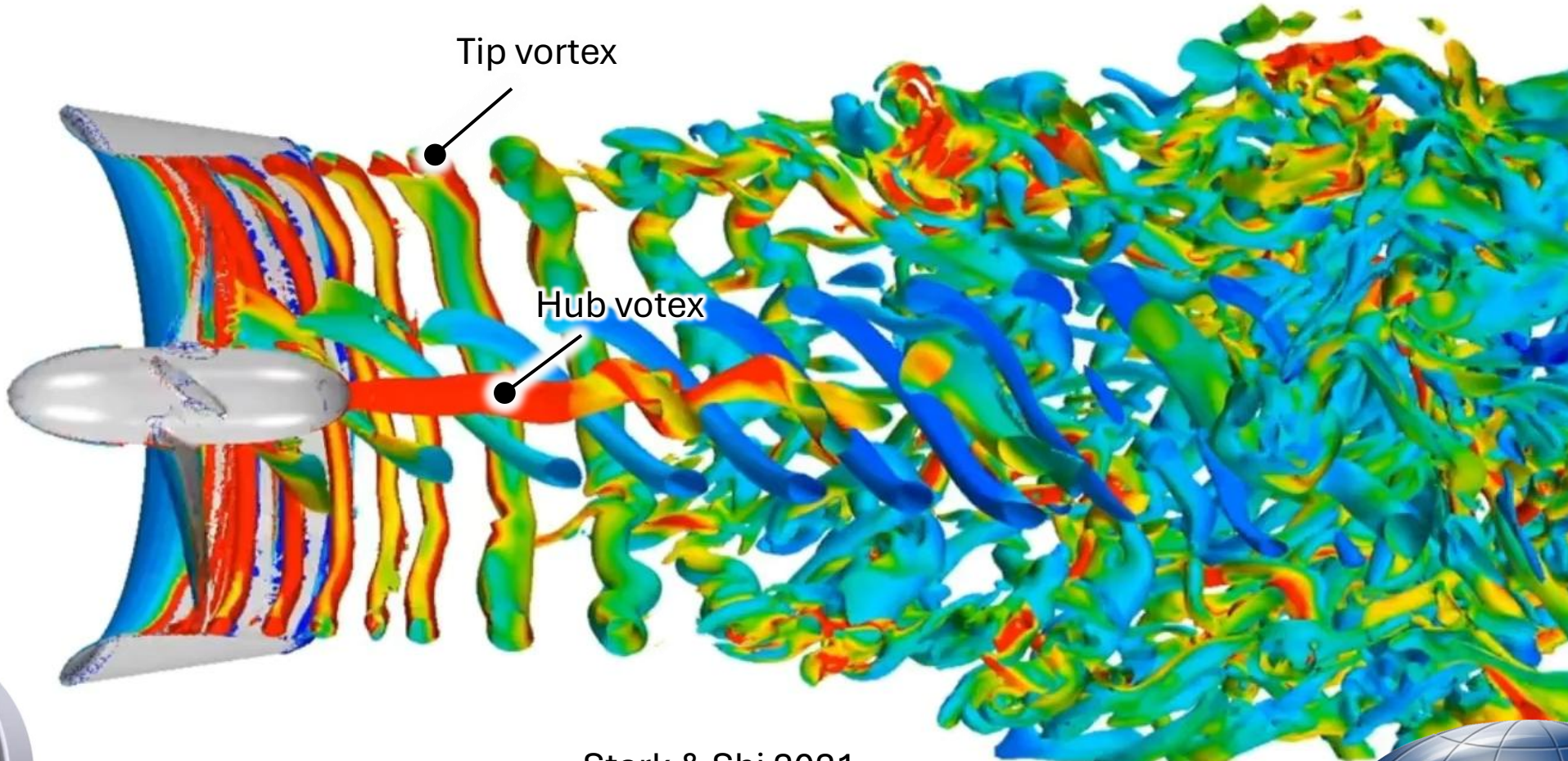
# Tracking chromatophores



- 2 points @ mantle
- 3 points @ funnel



# Application to propeller jet



Stark & Shi 2021

